To the Graduate Council:

I am submitting herewith a dissertation written by Michael P. McCann entitled "Two-Photon Spectroscopy of Atoms and Molecules." I have examined the final copy of this dissertation for form and content and recommend that it be accepted in partial fulfillment of the requirements for the degree of Doctor of Philosophy, with a major in Chemistry.

F. A. Grimm, Major Professor

We have read this dissertation
and recommend its acceptance

Accepted for the Council:

Vice Provost
and Dean of The Graduate School

TWO-PHOTON SPECTROSCOPY OF ATOMS AND MOLECULES

A Dissertation

Presented for the

Doctor of Philosophy

Degree

The University of Tennessee, Knoxville

Michael P. McCann

December 1987

DEDICATION

There are many people who have contributed to this work. A list of names would run on for a few pages. Rather than risk the omission of anyone, I have decided to simply dedicate this work to those people without enumeration. There were contributions large and small, but as I know and each person who contributed to this work knows, each contribution was important and vital to the successful completion of this work.

ACKNOWLEDGEMENTS

This research was sponsored in part by the Office of Health and Environmental Research, U.S. Department of Energy under contract DE-AC05-84OR21400 with Martin Marietta Energy Systems, Inc.

ABSTRACT

Two-photon spectroscopy has become an important scientific technique. In order for two-photon spectroscopy to become more fully utilized, parameters, such as the two-photon rate constant, need to be measured so that researchers will know how large their two-photon signal will be. In this work, the target species was excited by a photon of fixed wavelength and a visible photon of tunable wavelength to a two-photon allowed transition state. The excited species was then completely ionized by an additional photon. The ion pair was detected. Not only was the two-photon rate constant measured but also the spectra were recorded by tuning the visible photon wavelength.

Argon, krypton, and molecular hydrogen (H_2) were studied in a high pressure cell using parallel plate detection of the photoelectrons. Nitric oxide (NO) and the van der Waals molecule ArNO were studied using a molecular beam from a pulsed nozzle and detection of the parent ion with a quadrapole mass spectrometer. The fixed wavelength photon used with NO and ArNO was the third harmonic (355 nm) of a Nd:YAG laser. In the experiments with Ar, Kr, and H_2, the third harmonic of the Nd:YAG laser was tripled in xenon to yield a vacuum ultraviolet fixed wavelength photon (118 nm).

TABLE OF CONTENTS

LIST OF TABLES

LIST OF FIGURES

CHAPTER I

INTRODUCTION

Two-photon absorption was first discussed by Maria Göppert-Mayer[1] using time-dependent perturbation theory. The experiment had to await a light source of sufficient intensity to yield an observable two-photon signal. Soon after the laser was invented, two-photon absorption was observed.[2] Since that time, two-photon processes have been observed in gases,[3] liquids,[4] and solids.[5]

Two-photon spectroscopy has several advantages over conventional one-photon spectroscopy. In atoms and molecules with a center of symmetry, two-photon spectroscopy can excite states which are not allowed by a one-photon

---

[1]Maria Göppert-Mayer, "Über Elementarakte mit zwie Quantensprüngen," Annalen der Physik, Series 5, Volume 5, (1931), pp. 273-294.

[2]W. Kaiser and C. G. B. Garrett, "Two-Photon Excitation in CaF_2:Eu^{2+}", Physical Review Letters, Volume 7, Number 6, (September 15, 1961), pp. 229-231.

[3]L. A. Chewter, M. Sander, K. Müller-Dethlefs, and E. W. Schlag, "High resolution zero kinetic energy photoelectron spectroscopy of benzene and determination of the ionization potential," The Journal of Chemical Physics, Volume 86, Number 9, (1 May 1987), pp. 4737-4744.

[4]C. H. Chen and M. P. McCann, "Measurements of Two-Photon Cross Sections for Liquid Benzene, Toluene, and Xylene," (submitted to Chemical Physics Letters).

[5]S. K. Nikumb, V. Hari, A. S. Inamdar and Neela Mehendale, "Two Photon absorption in anthracene crystal with a nitrogen laser pumped dye laser," Indian Journal of Physics, Volume 54B, (1980), pp. 100-105.

transition. Thus information can be gathered on these two-photon allowed transition states, such as the potential energy curve, vibrational and rotational constants (in the case of molecules) which has been difficult if not impossible to do in the past. Two-photon spectroscopy can be used to examine the bulk properties of condensed matter. In one-photon spectroscopy, the absorption cross sections are so large that the impinging light is usually absorbed within the first few Ångströms. Therefore the resultant information yields more information about the surface of the sample than the properties of the bulk material. Two-photon absorption rate constants are typically 10^{-50}cm^4 sec molecule^{-1} photon^{-2}, therefore only a small portion of the light is absorbed by the surface layers. Two different color lasers could also be intersected in such a way as to probe selected volumes of the bulk material. This can not be done by one-photon absorption. Two counter-propagating laser beams with sufficiently narrow bandwidth can be used to produce spectra of a gas in a high pressure cell that is free of Doppler broadening. This makes the spectra much easier to utilize and interpret, and again this is not possible with one-photon spectroscopy.

Many spectroscopic studies are limited by the media through which they transmit. For example, air will start to absorb wavelengths that are shorter than 200 nm and high quality lithium fluoride or magnesium fluoride windows will completely absorb any light with wavelenghts shorter than 100 nm. This puts a limit on the energy that can be used to study transitions in atoms or molecules. Two-photon spectroscopy can go beyond these limits. Two photons can be used

to study a transition which would have required one photon which would have been absorbed in air or by the window. Finally, two-photon spectroscopy yields information about the symmetry of the excited state or molecule in randomly oriented samples. This is done by using two polarized laser beams whose polarity can be varied with respect to each other. To obtain molecular symmetry information using one-photon spectroscopy required the growth of a single crystal whose orientation was varied with respect the to incident light.

There are some disadvantages in using two-photon spectroscopy. Since the two-photon absorption rate constant (or two-photon absorption cross section) is so small, an intense light source is required. This means that an expensive laser must be used to obtain an adequate signal. At these high-photon fluences, other processes can occur such as multiphoton absorption or laser-induced breakdown.

With the great interest in two-photon spectroscopy, it would be useful to measure the two-photon absorption rate constant. This quantity would be helpful to theorists in the determination of fundamental atomic and molecular parameters. Alternatively, the two-photon absorption rate constant could be used to quantitatively measure a particular species. For example, the amount of impurities in various regions of a crystal could be nondestructively determined using two-photon spectroscopy.

This study has undertaken the task of measuring the two-photon absorption rate constant, which is of fundamental importance, and to demonstrate some novel methods of employing two-photon spectroscopy. In all cases, the two-photon ex-

citation is followed by the absorption of an additional photon which ionizes the species of interest. This ionization step is easily saturated so that the signal becomes independent of the ionizing laser energy.

To study Ar, Kr, and H_2, one of the two photons used for excitation was a vacuum ultraviolet (VUV) photon at a fixed wavelength of 118 nm. The VUV photon was produced by third harmonic generation of the third harmonic of a Nd:YAG laser (355 nm). The VUV generation occurred in a gas cell filled with xenon. The other photon used in the two-photon excitation was a visible photon from a tunable dye laser. Utilizing various dyes, the wavelength of the visible photon was varied from 400 nm to 700 nm. Then transitions of 11.9 eV to 13.7 eV may be studied. By frequency doubling the output of the dye laser, this range could easily be extended to 16.4 eV. The first excited state of all of the elements, except He and Ne, lie below 13.7 eV.

In the experiments with Ar, Kr, and H_2, the electrons that resulted from photoionization were collected in a cell with parallel plates. The plate which collected the signal was surrounded by a guard plate which helped to reduce the background. In the experiments with NO and ArNO the parent cation resulting from photoionization was detected by a quadrupole mass spectrometer. The mass spectrometer allowed the study of minority components (e.g. ArNO) and also helped to discriminate against incidental photoionization that occurs when ultraviolet light hits other species or metal surfaces inside the chamber.

These experimental arrangements offered several useful features. Using com-

mercially available lasers, transition energies could be determined to within 0.11 cm^{-1}, which rivals even the longest VUV monochromators.[6] Obviously, these experiments were designed to measure the two-photon absorption rate constant, which will be of fundamental importance to future applications of two-photon spectroscopy. Also the pulsed molecular beam and quadrupole mass spectrometer arrangement allows the examination of transition energies and two-photon absorption rate constants of rotationally cooled molecules and other species, such as van der Waals molecules, that are difficult to examine by other means.

[6]M. P. McCann, C. H. Chen, and M. G. Payne, "Energy Level Determination Using Two-Photon (Vacuum Ultraviolet and Visible) Resonance Spectroscopy," Applied Spectroscopy, Volume 41, Number 3, (1987), pp. 399-401.

CHAPTER II

EXPERIMENTAL DESIGN

A. Overall Arrangement

The apparatus used in this work went through three stages of development. The first stage is shown in Figure 1. It was comprised of a Nd:YAG laser with a harmonic generator (HG), a harmonic separator (HS), and a dye laser. The coherent vacuum ultraviolet (VUV) light was formed in the generation cell and the photoelectrons were collected by a proportional counter in the detection cell.

The Nd:YAG laser was an upgraded Quanta-Ray DCR-1A. The laser employed an unstable resonator which produced a characteristic "donut" shaped laser beam. The beam diameter was 6.5 millimeters and it had a divergence of less than 0.5 milliradians. The spectral bandwidth of the 1064 nm beam was less than 2 cm^{-1}. With the intra-cavity etalon the bandwidth of the fundamental was less than 0.2 cm^{-1}. The laser operated at a pulse rate of 10 Hz. The second harmonic (532 nm), had a pulse width of 6-7 nanoseconds and output up to 480 millijoules per pulse. The third harmonic (355 nm), had a pulse width of 5-6 nanoseconds and output up to 192 millijoules per pulse. The fourth harmonic (266 nm) had a pulse width of 4-5 nanoseconds and could produce up to 90 millijoules per pulse but this energy was not stable at room temperature. The dye laser had a spectral

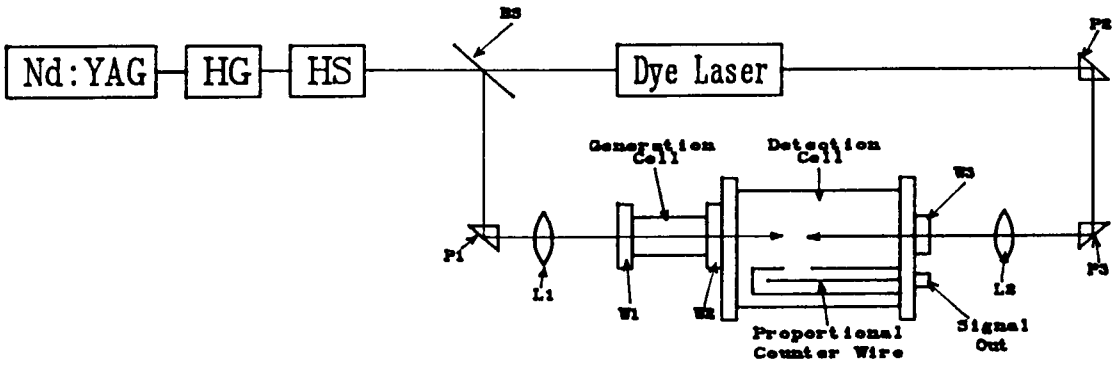

Figure 1. Experimental Apparatus, First Stage.

bandwidth of 0.2 cm^{-1}. The output of both the Nd:YAG and the dye laser had vertical polarization. The dye laser beam characteristics depend on whether end-pumping or side-pumping is employed. The more efficient dyes use end-pumping and the less efficient dyes use side-pumping.

The generation cell was a standard $2\frac{3}{4}$-inch stainless steel nipple with lithium fluoride (LiF) windows at both ends. The generation cell was attached to a stainless steel chamber which contained a proportional counter. The proportional counter had an opening of 1 cm to the inside of the detection cell. This was done to help the proportional counter detect only the photoelectrons from the three-photon ionization volume. The small opening in the proportional counter helped to minimize the detection of photoelectrons that were produced by the UV and VUV light hitting metallic surfaces. The proportional counter wire was biased from +50 volts to +200 volts which means that there was little if any gain from the proportional counter.

The apparatus operated in the following manner. Third harmonic light (355 nm) was produced by the Nd:YAG laser system. The laser beam went to a beam splitter (BS), which was composed of a quartz slide. Fifty percent of the light went to pump the dye laser and fifty percent went through a UV-grade prism (P1) to the generation cell. The output from the dye laser went through two prisms (P2,P3) to the detection cell. The UV laser beam was focused in the generation cell by a UV-grade lens (L1) which had a focal length of 15 cm. The UV beam focused in the center of the generation cell. The dye laser beam was focused with

a 25 cm lens (L2). The dye laser beam focused adjacent to the opening in the proportional counter. The proportional counter collected the photoelectrons of each laser pulse and produced a signal that was proportional to the number of target atoms or molecules that were ionized. The generation cell was typically filled with 30 torr of xenon for third harmonic generation of coherent VUV (118 nm) light. The detection cell was typically filled with <60 torr of Ar, Kr, or H_2.

The second stage of development is shown in Figure 2. The main difference in this apparatus was that the proportional counter had been replaced by a parallel plate detector. This was done so that the number of ion pairs that were produced by three-photon ionization could be more definitely determined. The plates were large enough (2.54 cm in diameter) to collect all of the electrons from the three-photon ionization volume without any gain. This apparatus was also used to measure the amount of VUV that was produced in the generation cell. The plates did have guard rings which minimized the background due to the ultraviolet laser light ejecting photoelectrons from metal surfaces inside the detection cell.

The third stage of development is shown in Figure 3. This apparatus allowed the application of two-photon spectroscopy to more than noble gas atoms. The high pressure gas chamber that was used as a detection cell is now a vacuum chamber. The target species was introduced through a pulsed nozzle. The gas jet passed in front of a quadrupole mass spectrometer which was used to detect the parent cation from the three-photon ionization. The apparatus had several advantages. In general, molecular spectra cannot be studied in a high pressure

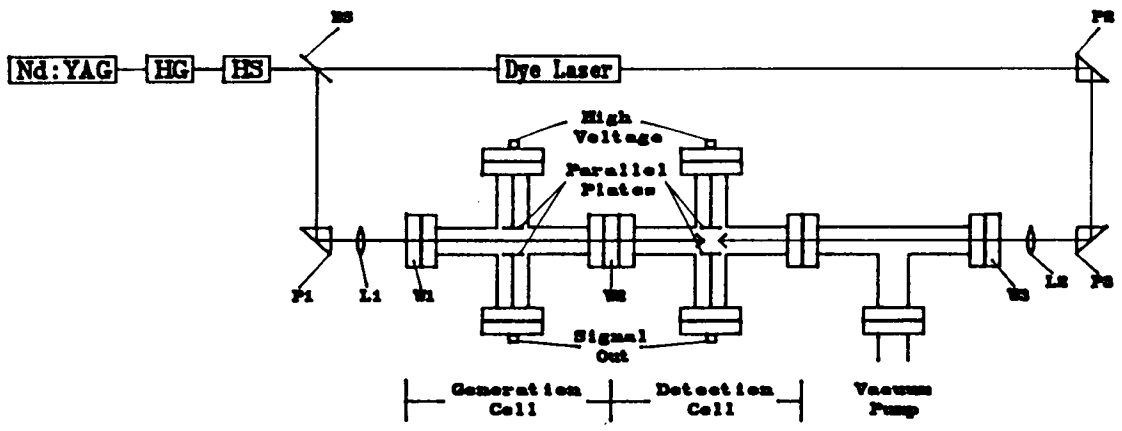

Figure 2. Experimental Apparatus, Second Stage.

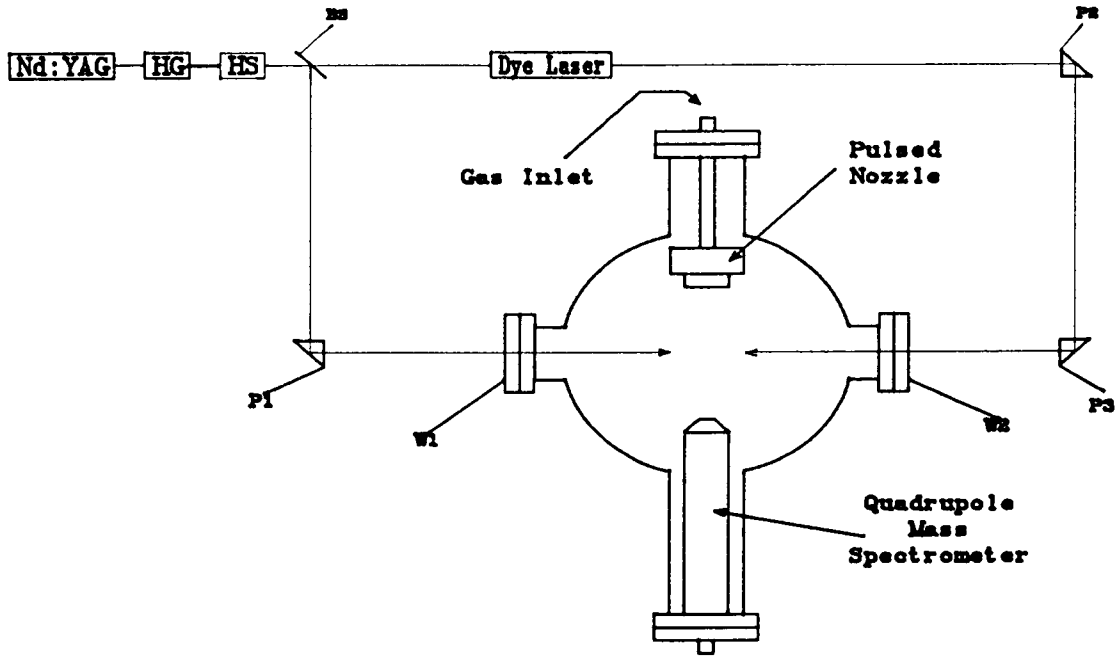

Figure 3. Experimental Apparatus, Third Stage.

cell because the vibrational and rotational states tend to overlap each other. The obvious exception is H_2, whose mass is small enough that the rotational states do not overlap at high pressure and room temperature. The supersonic gas expansion into a vacuum provided rotational cooling of a molecule. Only the lowest rotational states were populated and the overlap problem was greatly reduced or even eliminated. Minority components could be studied since the mass spectrometer could be set to detect species of one particular mass. The pulsed nozzle worked well with a pulsed laser because the nozzle could be synchronized with the laser. Using a pulsed nozzle greatly reduced the pumping requirements compared to a nozzle that was continuously opened. This also meant that the number density in front of the mass spectrometer was higher than compared to a continuous jet expansion because the pulsed nozzle was open for only a short time. This meant that, the overall number of atoms or molecules that were pumped away per unit time was small.

The pulsed nozzle was a Lasertechnics Model LPV with a Lasertechnics Model 203 Pulsed Valve Driver. The pulsed nozzle utilized a piezoelectric crystal for opening and closing the valve. The remainder of the valve body was made of stainless steel. The valve could not be moved once it was inside the chamber and it operated only at room temperature. The pulsed valve was typically operated at +170 volts (open) with a pulse width of 102 microseconds. The nozzle back pressure was typically 1-3 atmospheres of 10% nitric oxide (NO) in argon. The quadrupole mass spectrometer was a EAI QUAD 1110A from CVC Products Inc.

It had a mass range of 1 to 300 amu. The original ionizer was removed so that the pulsed nozzle and laser ionization could be used. In place of the original ionizer, two plates were used. Both plates were 6.7 cm in diameter. One plate was put in place of the ionizer and the other plate was parallel and 5.1 cm away. The detector was a Model 4830G channeltron from Galileo Electro-Optics Corp. The gain curve was measured. It is shown in Figure 4. The overall detection sensitivity of the mass spectrometer could be easily measured. The outer two plates of the mass spectrometer were used as a parallel plate detector. The outer plate was biased -100 V and the inner plate was at ground potential. Nitric oxide from the pulsed nozzle was ionized using a three-photon laser scheme. The number of ions pairs was measured using the parallel plate mode. Then the mass spectrometer was operated in its normal manner and it was tuned to detect NO^+. The channeltron was biased to -800 V at the front end and ground at the collection electrode. Under these conditions, with unit resolution, the sensitivity was 0.07% of the NO^+ cations that were generated by laser photoionization. This number is consistent with the original specification for the mass spectrometer. The channeltron gain at 800 V was very low and the large plates used to extract the cations into the mass spectrometer could not be nearly as efficient as the original ionizer. Obviously the mass spectrometer sensitivity could be influenced by several factors. As the particle density in between the parallel plates increased, the sensitivity could be expected to decrease due to decreasing extraction and throughput efficiencies. Also the sensitivity was a function of the bias voltages used on the parallel plates to

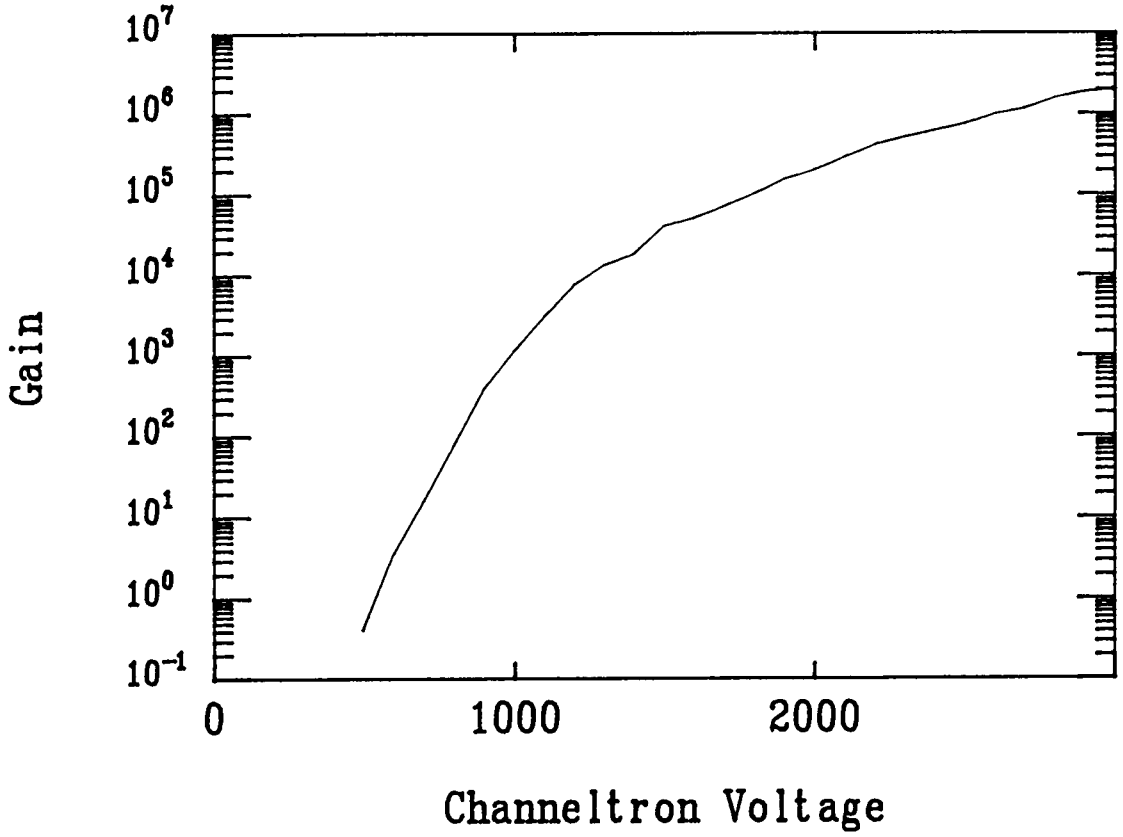

Figure 4. Channeltron Gain Curve.

extract the cations into the mass spectrometer. The optimum conditions were +38 V on the outer plate and +10 V on the inner plate. Position of the ions with respect to the entrance hole also affected the sensitivity. The quadrupole mass spectrometers typically had a small acceptance angle, so the position of the laser beam with respect to the mass spectrometer was also critical. It was found that positioning the laser beam about 0.5 cm above the entrance hole (toward the pulsed nozzle) of the mass spectrometer gave the best signal in terms of magnitude and rotational cooling.

The pulsed nozzle - mass specrometer apparatus worked in the following manner. The mass spectrometer was tuned to the appropriate mass. A trigger pulse was obtained from the laser. Some set delay time after this trigger pulse, the pulsed nozzle was fired. After the pulsed nozzle was fired, the laser fired. The laser was free-running and the pulsed nozzle was synchronized with the laser, since the laser worked best at 10 Hertz. Some time after the laser fired, the signal was detected. The timing diagram is shown in Figure 5. The signal pulse could be viewed on an oscilloscope, put into a sample-and-hold for output to a strip chart recorder or a computer. Spectra could be obtained by scanning the dye laser and recording the signal on a strip chart recorder or the computer.

B. Electronics Configuration

The electronics that were used for the observation of the two-photon signal evolved along with the apparatus. Initally the signal was observed through a

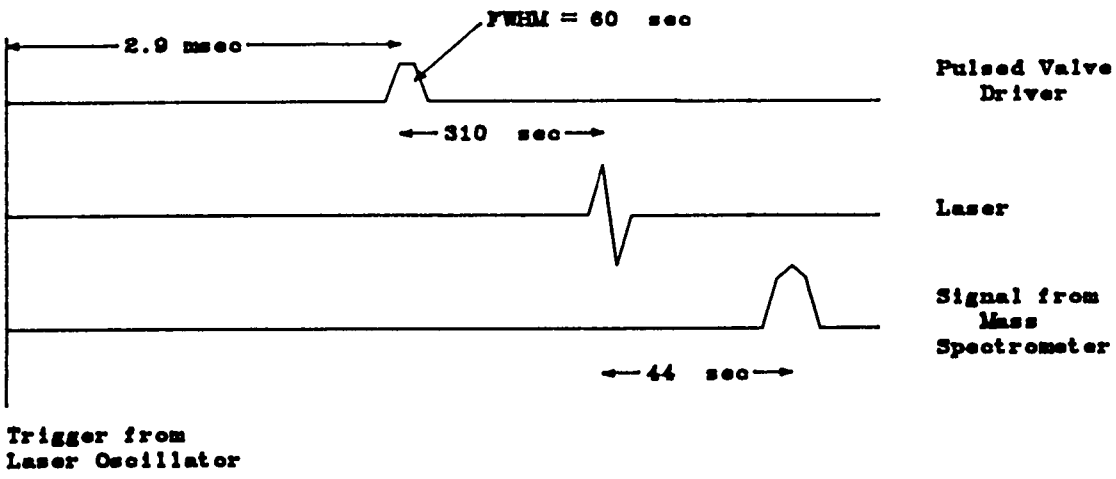

Figure 5. Timing Diagram.

preamplifier and amplifier on an oscilloscope. Thus there were no spectra recorded of the early data. The latest electronics configuration is shown in Figure 6. The entire sequence of events was triggered by an initial pulse from the Nd:YAG laser. This pulse from the oscillator output of the laser went to a single channel analyzer (Ortec 551) to eliminate some noise pulses from the laser. The trigger pulse from the single channel analyzer went to the pulsed valve driver (Lasertechnics Model 203). The pulsed valve driver had a delay adjustment of up to 4.1 milliseconds. The pulsed nozzle was opened 2.9 milliseconds after a trigger pulse from the oscillator output of the Nd:YAG laser. The pulse width was set to 102 microseconds. This was measured with the mass spectrometer using electron impact ionization. The repetition rate was synchronizated with the laser at 10 Hertz. A +170 V pulse from the pulsed valve driver was used to open the valve.

The signal typically came from the channeltron of the mass spectrometer. The high voltage to the channeltron could be varied to change the magnitude of the signal. The signal went through a preamplifier (Ortec 142PC) which had a gain of 6.5 volts per picocoulomb. The signal pulse went from the preamplifier to an amplifier (Ortec 571) which typically had a gain of 10. The signal pulse then went to the sample and hold module and at the same time could be viewed on an oscilloscope.

A photodiode (EG&G HUV-4000B) which picked up light from the laser was used to generate another trigger pulse. The pulse from the photodiode went to an amplifier (Ortec 571) and then to two gate and delay generators (Ortec 416A).

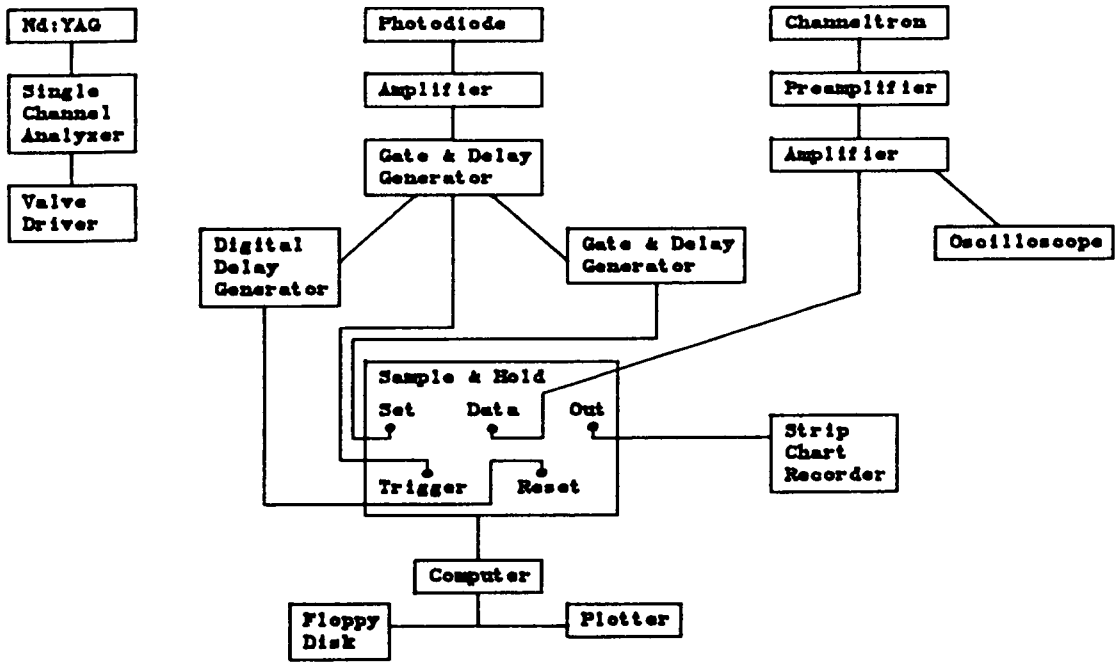

Figure 6. Electronics Configuration.

From the first gate and delay generator the trigger pulse went to the trigger input of the sample-and-hold module (built in the Photophysics Group at Oak Ridge National Laboratory). This prepared the sample-and-hold to take a datum. The trigger pulse from the second gate and delay generator went to the set input of the sample-and-hold module, and to a digital delay generator (Berkeley Nucleonics Corp., Model 7010). When the sample-and-hold module received a set pulse it then held the voltage from the signal pulse. The held signal voltage could then be sent to a strip chart recorder or it could be read and recorded by a computer. The digital delay generator had a delay setting of 90 milliseconds. The trigger used to set the sample-and-hold module coincided with the peak of the signal pulse as seen on an oscilloscope. The trigger pulse from the digital delay generator, which was delayed 90 milliseconds, went to the reset input of the sample-and-hold module. This cleared the voltage from the signal pulse and enabled the sample-and-hold module to take another datum.

The sample-and-hold module is necessary because this is a pulsed experiment. In order to see a spectrum on a strip chart recorder, the voltage from the signal pulse must be held long enough for the recorder to respond. The computer can not be expected to read a signal pulse of such short time duration. The computer operates at its own clock rate and so the signal must still be present when the computer goes to read the signal. The sample-and-hold had eight channels. So eight sets of data, such as signal, laser energy, gas pressure, ect., could be recorded with each laser shot. Each channel requires a set pulse.

The computer was a Zenith Model ZF-151-52. It is IBM XT compatible and uses MS-DOS. The computer also had a C.Itoh Model 8510 printer and a Hewlett Packard 7470A plotter. Data were taken from the sample-and-hold module using a MetraByte DASH-16 multifunctional I/O expansion board which was intalled in the computer. Data aquisition was performed using various programs that were written in Assembler, PASCAL, or C. Once the data were acquired, it could be displayed on the monitor, the printer, or the plotter and it could be stored on floppy disks. The data could also be manipulated by various programs for analysis. To record a spectrum, the scan drive on the dye laser was set for a particular speed in terms of nanometers per second. The scan drive and the data acquisition program were started simultaneously. Once the scan was over, a program, which required information about the starting wavelength and the scan speed, would convert the raw data into a spectrum where averaging, the vacuum wavelength correction and the photon energy in terms of wavenumbers had all been included.

C. Laser Schemes

There were two groups of lasers schemes employed in this work. The first group employed a fixed wavelength photon in the VUV region at 118 nm. In the second group the fixed wavelength photon was in the UV region at 355 nm.

The VUV photon was used in two-photon transitions in Ar, Kr and H_2. A photon of high energy was required to reach even the lowest excited states in these species. A typical laser scheme for ionizing argon is shown in Figure 7. The third

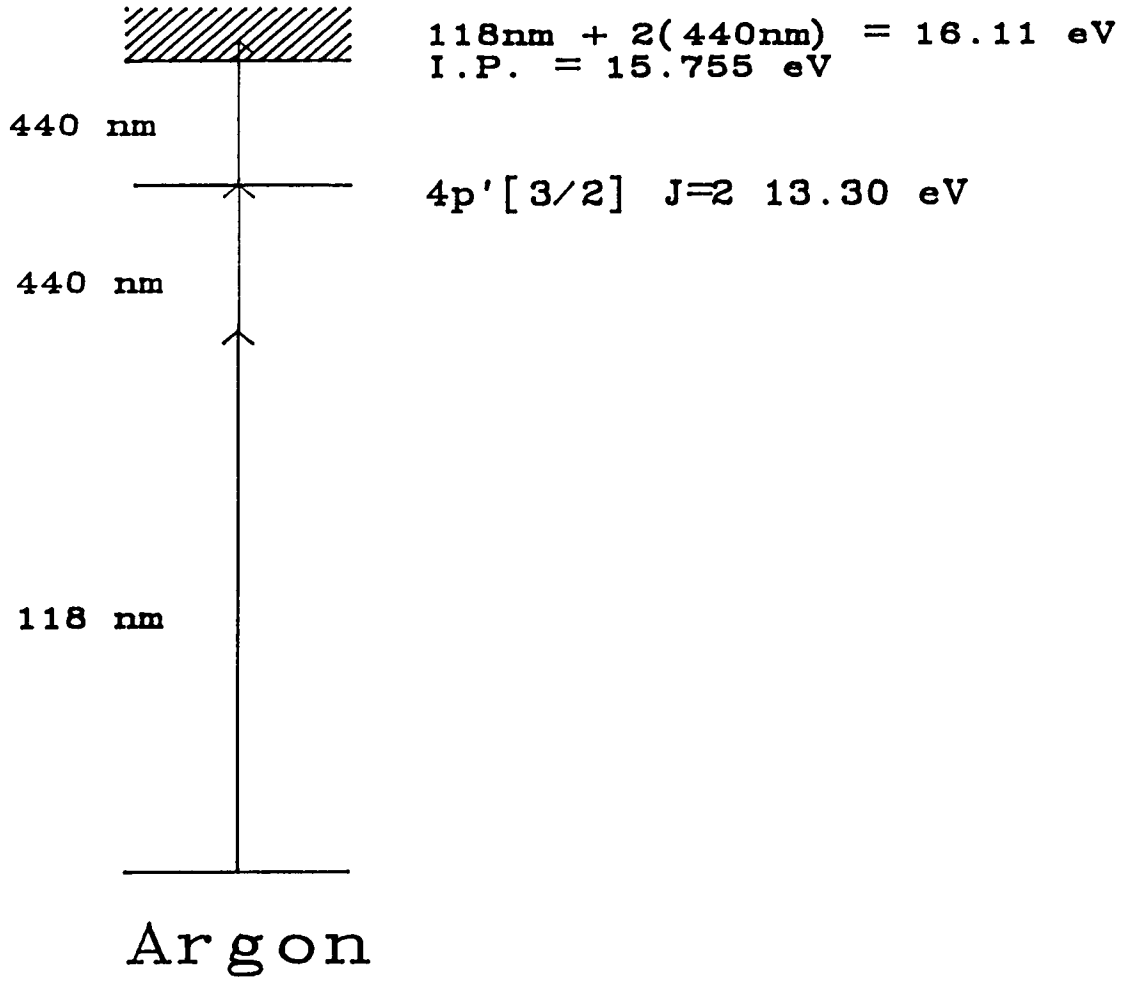

Figure 7. Laser Scheme for Argon.

harmonic (355 nm) from the Nd:YAG laser was focused into the generation cell filled with xenon gas. Third harmonic generation occurs in xenon. The resultant VUV photon and the original UV photon go into the detection cell. The VUV photon and the visible photon which came from the dye laser through the opposite end of the detection cell, combined to bring the argon atom to an excited electronic state. An additional visible photon ionized the excited argon atom. In other cases, the UV photon ionized the atom or molecule. The photoelectron was then detected by the proportional counter or the parallel plate detector. The signal disappeared when the xenon was pumped from the generation cell, confirming the fact that the transition to the excited state utilized a VUV photon in a two-photon absorption process (rather than three UV photons and one visible photon used in a four-photon absorption process).

As the sum of the photon energies had to match the energy of the two-photon transition, a UV-visible laser scheme was employed with NO and ArNO. A typical process for NO is shown in Figure 8.[7] The third harmonic from the Nd:YAG laser and visible light from the dye laser were focused between the parallel plates of the mass spectrometer. The rotationally cooled NO molecules from the pulsed nozzle were excited by the simultaneous absorption of the UV and visible photons. The excited NO molecule was then ionized by the absorption of an additional UV photon. The NO^+ cation was then detected by the mass spectrometer. In

[7]Wan Yee Cheung and Steven D. Colson, "Optical-Optical Double Resonance-Multiphoton Ionization Spectroscopy," Adavances in Laser Spectroscopy, Volume 2, Edited by B. A. Garetz and J. R. Lombardi, (John Wiley & Sons Ltd., 1983) pp. 73-104.

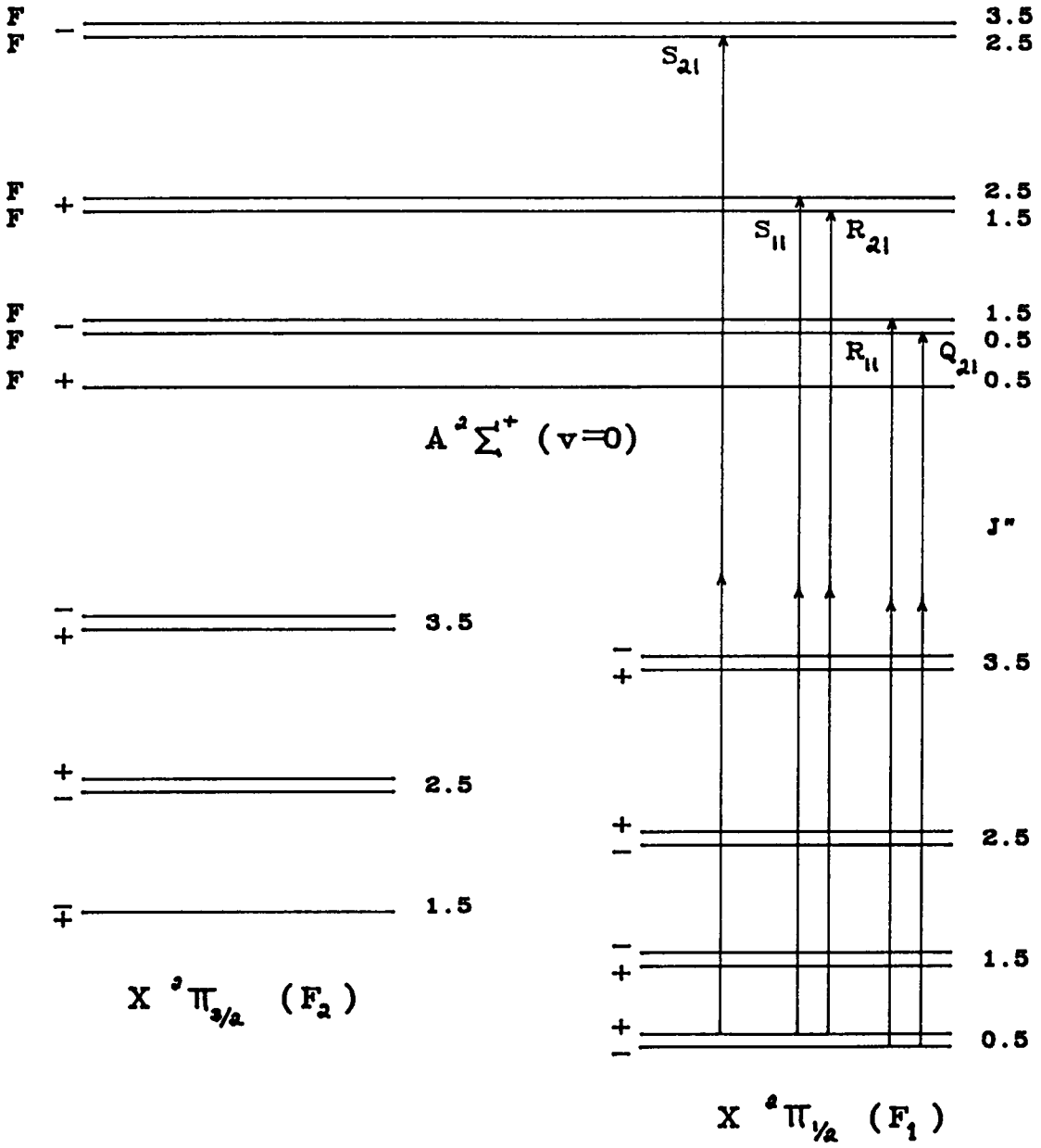

Figure 8. Laser Scheme for Nitric Oxide.

some cases, two visible photons could cause a two photon transition in NO and two additional visible photons would ionize the molecule. Care had to be taken to distingush the UV-visible two-photon transitions from the visible-visible two-photon transitions.

CHAPTER III

VACUUM ULTRAVIOLET GENERATION

A. Overall Process

In order to do two-photon spectroscopy on Ar, Kr, and H_2, at least one photon needed to have high energy. To use two equal photons would have meant using a photon in the region of 185 nm. Though this was not impossible, it would involve some expensive equipment (e.g. doubling and mixing crystals, Raman cell, dichroics, etc.) and there would not be a wide range of tunability. A simpler approach would be to do third harmonic generation of the third harmonic of the Nd:YAG laser. This produces a photon of fixed wavelength in the VUV region. To produce the VUV photon, all that was required was some sort of inexpensive cell to hold xenon gas, with a UV grade window at one end and a LiF window at the other end. This was extremely simple to obtain and use. The dye laser could then be used to produce a visible photon that was tunable over a wide range and required no changes in the optical arrangement. (Mixing and doubling crystals require an adjustment as the wavelength is varied. Dichroics are functional over a very narrow range of wavelengths and therefore a large number of dichroics would be needed for tunability over a large wavelength region.)

The third harmonic generation scheme is shown in Figure 9. There has been a great deal of work on four-wave mixing to produce VUV.[8] Focusing the UV with a 15 cm lens in 30 torr of xenon was found to produce the optimal quantity of VUV.[9] Phase matching with argon would enhance the magnitude of the VUV by a factor of two but usually phase matching with argon was not used. Phase matching in an unfocused beam produced a very dramatic enhancement,[10] but the focused beam produced a larger number of VUV photons.

In unfocused beams, the phase mismatch was due to the difference in the refractive index at the UV and VUV wavelengths. Since the refractive index subtracted from unity was directly proportional to the number density of the species present in the cell (in this case, xenon), then the phase mismatch could be minimized by using low pressures of the active medium. To use low pressures of xenon would also reduce the amount of VUV that was produced since the number of VUV photons was directly proportional to the square of the number density of xenon atoms. There was another solution to the problem. As shown in Figure 9, the third harmonic lies between the 5d and 7s level in xenon. The refractive index

---

[8]W. Jamroz and B. P. Stoicheff, Progress in Optics, Volume XX, edited by E. Wolf (New York: North-Holland), pp. 327-370.

[9]Gary C. Bjorklund, "Effects of Focusing on Third-Order Nonlinear Processes in Isotropic Media," IEEE Journal of Quantum Electronics, Volume QE-11, Number 6, (June 1975), pp. 287-296.

[10]Wanda R. Ferrell, "Determination of Optical Properties by Third-Harmonic Generation in Noble Gases in Unfocused Laser Beams," Doctoral Dissertation, The University of Tennessee, Knoxville, (March 1985).

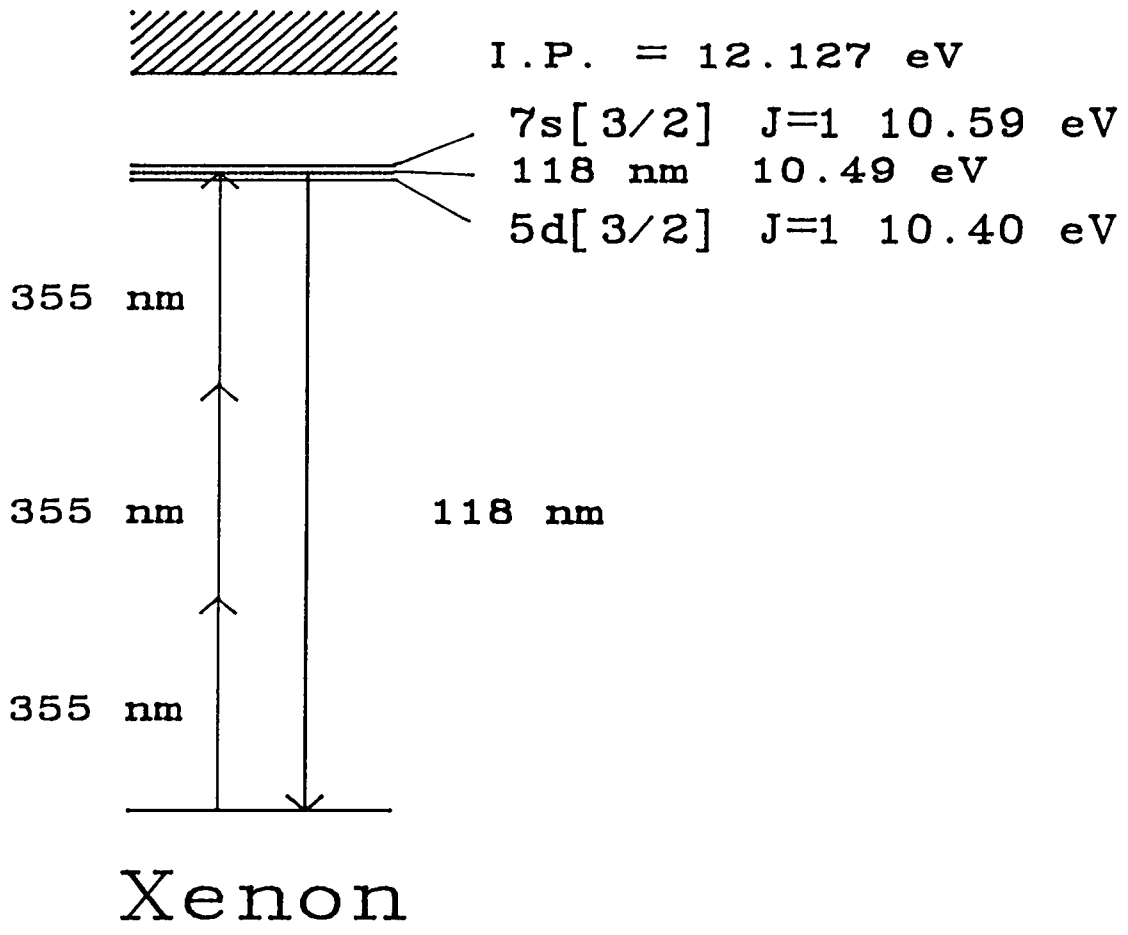

Figure 9. Third Harmonic Generation Scheme.

of any monoatomic gas becomes negatively dispersive (the refractive index is less than unity) for light that is to the high energy side of an optically allowed transition as can be seen in Figure 10. Since 118 nm lies in between two resonances, the refractive index is changing rapidly with wavelength and is difficult to predict.[11] Far from resonances, monoatomic gases are all positively dispersive, as can also be seen from Figure 10. If xenon is negatively dispersive at 118 nm then argon, which is positively dispersive at 118 nm, can be added to xenon so that

$$\Delta n = n(118 \text{ nm}) - n(355 \text{ nm}) = 0. \tag{1}$$

The two wave fronts will not be out of phase with each other and constructive interference will occur. Xenon is negatively dispersive at 118 nm and thus a gas, such as argon which has no resonances in that region, can be used for phase matching.

B. Estimate of Vacuum Ultraviolet Yield

It is useful to calculate how much VUV the third harmonic process will produce. Without sufficient VUV, the two-photon signal will be difficult if not impossible to see. The following expression[12] can be used to calculate the total generated

[11]Rita Mahon, Thomas J. McIlrath, Valerie P. Myerscough, and David W. Koopman, "Third-Harmonic Generation in Argon, Krypton, and Xenon: Bandwidth Limitations in the Vicinity of Lyman-α ," IEEE Journal of Quantum Electronics, Volume QE-15, Number 6, (June 1979), pp. 444-451.

[12]Gary C. Bjorklund, op. cit. pg. 290.

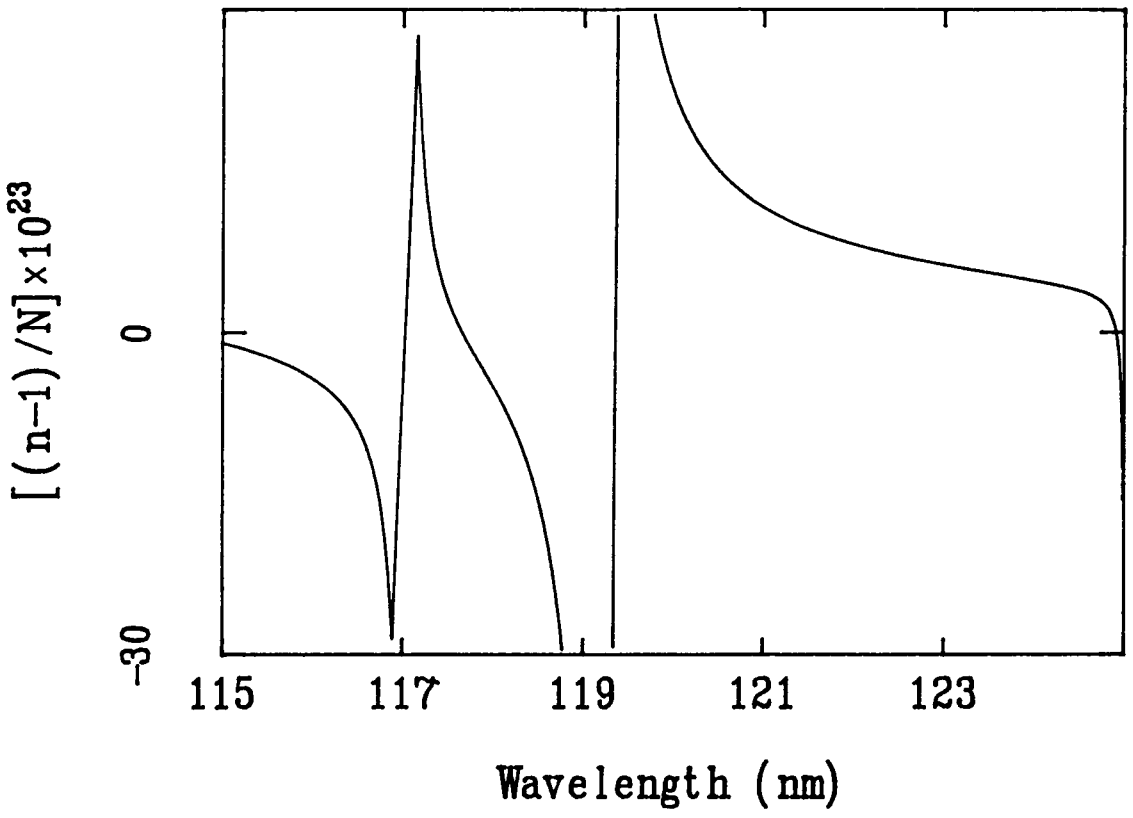

Figure 10. Refractive Index of Xenon.

power P_4 of VUV

$$P_4 = (1.755 \times 10^{-5}) \frac{k_0^4 k_3^2}{3k_4^2} \frac{N^2 \chi^2 P_3^3 F_1}{b^2} \tag{2}$$

where

P_4 = VUV power in watts

k_0 = wave vector of VUV in a vacuum = $2\pi/\lambda$

= 531572 cm^{-1}

k_3 = wave vector of UV in xenon = $n(355\ nm)2\pi/\lambda$

= 177146 cm^{-1}

k_4 = wave vector of VUV in xenon = $n(118\ nm)2\pi/\lambda$

= 531531 cm^{-1}

χ = third-order nonlinear susceptibility

= 5.6×10^{-35} esu

N = number density of xenon atoms = $9.39 \times 10^{17} cm^{-3}$

P_3 = power of UV beam

F_1 = geometric factor = $\pi^2 (b\Delta k)^2 e^{b\Delta k/2}$

where

b = confocal parameter of UV = $2n(355\ nm)\lambda f^2/(d^2\pi)$

$\Delta k = k_4 - 3k_3$

where

f = focal length of the lens = 15 cm

d = beam diameter = 0.6 cm.

The third-order nonlinear susceptibility is an experimentally determined quantity.[13] Using Equation 1, the amount of VUV generated can be determined for various experimental parameters. The maximum amount of VUV versus the focal length can be generated.[14] In the unfocused case, the function F_1 is equal to $4L^2/b^2$ where L is equal to the length of the cell (12.3 cm). Using a pulse duration of 6 nanoseconds, Table 1 was tabulated.

Table 1

Calculated VUV Energies and Conversion Efficiencies

Ultraviolet Energy	Xenon Pressure	Lens Focal Length (cm)	VUV Energy	Conversion Efficiency
6.5 mJ/pulse	29 torr	15 cm	4.5 μJ/pulse	7×10^{-4}
56 mJ/pulse	71 torr	∞	625 pJ/pulse	1×10^{-8}

The energy per pulse conversion efficiencies agree well with previous calculations for third harmonic generation of 118 nm.[15,16] There are other methods of calcu-

[13]A. H. Kung, J. F. Young, and S. E. Harris,"Erratum: Generation of 1182-Å radiation in phase-matched mixtures of inert gases [Appl. Phys. Lett. 22, 301 (1973)]," Applied Physics Letters, Volume 28, Number 4, (15 February 1976), pg. 239.

[14]Gary C. Bjorklund, op. cit. pp. 291-295.

[15]Ibid. pg. 295

[16]A. H. Kung, "Third-harmonic generation in a pulsed supersonic jet of xenon," Optics Letters, Volume 8, Number 1, (January 1983) pp. 24-26.

lating how much third harmonic will be produced.[17,18,19] All of the calculations require two numbers which are not readily accessible, some measure of how the atom will respond to three-photon absorption and the refractive index at the third-harmonic wavelength. The first quantity, the three-photon Rabi frequency or the third-order nonlinear susceptibility can be calculated reasonably well. The refractive index at 118 nm is more difficult because the refractive index is changing so rapidly in that region. This makes calculation of third-harmonic generation difficult to do with a high degree of accuracy.

C. Experimental Results

The experimental apparatus shown in Figure 2 on page 10 was used to measure VUV production. The generation cell was filled with xenon gas and also occasionally argon gas was added to the generation cell for phase matching. The detection cell was filled with 140 torr of 1% nitric oxide in argon. The nitric oxide in the detection cell was photoionized by the absorption of a single VUV photon. The collection of photoelectrons by the parallel plates was a measure of the num-

[17]J. F. Ward and G. H. C. New, "Optical Third Harmonic Generation in Gases by a Focused Laser Beam," Physical Review, Volume 185, Number 1, (5 September 1969), pp. 57-72.

[18]M. G. Payne and W. R. Garrett, "Theory of the effect of third-harmonic generation on three-photon resonantly enhanced multiphoton ionization in focused beams," Physical Review A, Volume 28, Number 6, (December 1983), pp. 3409-3429.

[19]S. H. Lin, Y. Fujimura, H. J. Neusser, E. W. Schlag, Multiphoton Spectroscopy of Molecules, (Orlando: Academic Press, Inc., 1984), pg. 59.

ber of VUV photons that entered the detection cell. The following simple equation was used to measure the intensity of the VUV beam.

$$I = I_0 e^{-kx} \tag{3}$$

where

I = resultant light intensity

I_0 = original light intensity

k = absorption coefficient = 62.8 cm^{-1} at 0°C, 1 atm

x = distance through the absorbing medium

Using the above equation, the following equation can be used to relate the observed signal to the amount of VUV produced.

$$I_0 = \frac{S}{GY\left[e^{-kx_1p} - e^{-kx_2p}\right]} \tag{4}$$

where

S = observed signal (mV)

G = gain of electronics = 54 mV/10^6 electrons

Y = photoionization yield = 0.89

x_1 = distance from the generation cell window to the closest edge of the parallel plate = 5.73 cm

x_2 = distance from the generation cell window to the farthest edge of the parallel plate = 8.27 cm

p = pressure = 1.84×10^{-3} atm

This results in the following conversion

$$I_0 = 2.67 \times 10^{-13} \text{J/mV}. \tag{5}$$

The absorption coefficient[20] and the photoionization yield have been determined experimentally.[21] The absorption through the lithium fluoride window of the generation cell also had to be taken into account in order to calculate the amount of VUV produced in the generation cell. The lithium fluoride window was 5.0 mm thick. Using data for a window with a thickness of 2.09 mm, which had a transmittance of 52% ,[22] and Equation 3, the transmittance of the lithium fluoride window on the generation cell was found to be 21% . This was used to tabulate the experimental information in Table 2.

The data in Table 2 were taken with an unfocused UV beam. As shown in Figure 11, the experimental data agreed well with the calculated curve. The unfocused beam would have been difficult to use in an experiment because the VUV generation efficiency was very sensitive to the concentration and mixing of

[20]K. Watanabe, Frederick M. Matsunaga, and Hajime Sakai, "Absorption Coeffcient and Photoionization Yield of NO in the Region 580-1350 Å," Applied Optics, Volume 6, Number 3, (March 1967), pp. 391-396.

[21]Ibid. pg. 395, Note: Table IV on page 395 was not printed properly. At λ = 1140.0 in the first column, go to the top of the second column. At λ = 1184.4 in the second column, go to the top of the third column. At λ = 1223.5 in the third column, go to λ = 1225.6 in the middle of the first column (just after 1140.0) and so on.

[22]Donald F. Heath and Paul A. Sacher, "Effects of a Simulated High-Energy Space Environment on the Ultraviolet Transmittance of Optical Materials between 1050 Å and 3000 Å," Applied Optics, Volume 5, Number 6, (June 1966), pp. 937-943.

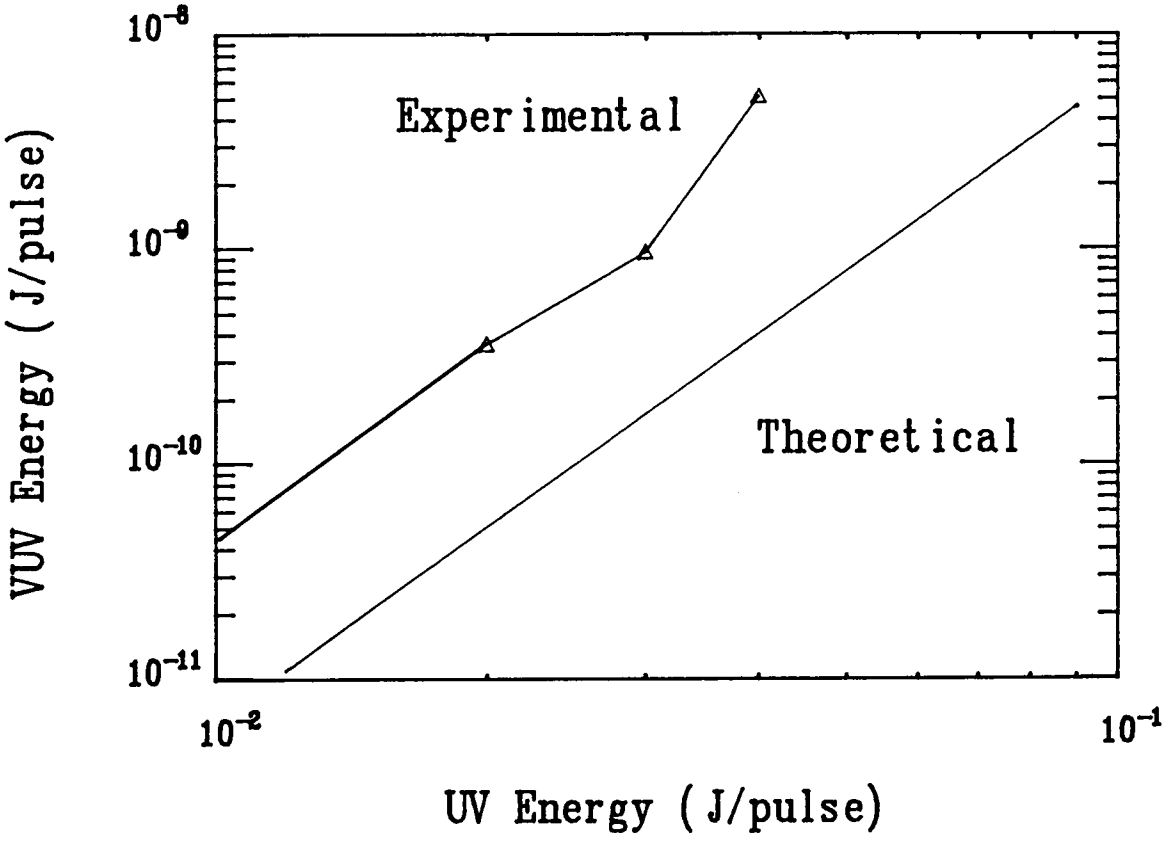

Figure 11. Conversion Efficiency of UV to VUV, Unfocused Geometry.

Table 2

Experimental VUV Energies and Efficiencies, Unfocused Geometry

Ultraviolet Energy	Xenon Pressure	Argon Pressure	VUV Energy	Conversion Efficiency
10 mJ/pulse	60 torr	645 torr	4.24 pJ/pulse	4.2×10^{-10}
20 mJ/pulse	60 torr	645 torr	36.3 pJ/pulse	1.8×10^{-9}
30 mJ/pulse	60 torr	645 torr	96.9 pJ/pulse	3.2×10^{-9}
45 mJ/pulse	60 torr	645 torr	515 pJ/pulse	1.1×10^{-8}

the phase-matching gas. It could have been difficult to obtain reproducible results if the VUV intensity was varying in an uncontrolled manner.

The focused data in Table 3 also agreed well with the calculated results as shown in Figure 12. The VUV conversion efficiency was consistent with previous calculations[23] and previous observations.[24] Obviously, the focused geometry was prefered because it yielded the greater amount of VUV. The focused geometry also allowed the use of pure xenon. This meant that there was no problem of mixing a precise amount of a positively dispersive gas for phase-matching.

An attenuation cell was used for the measurement of the VUV. This was done because the signal could have space charge problems and also exceed the limits of the electronics from which a saturated signal would be obtained. With the attenuation cell, the signal from the amplifier could be kept in a linear region. The attenuation cell was a standard $2\frac{3}{4}$-inch stainless steel nipple with two LiF

[23]A. H. Kung, "Third-harmonic generation in a pulsed supersonic jet of xenon," op. cit. pg. 26.

[24]Ibid.

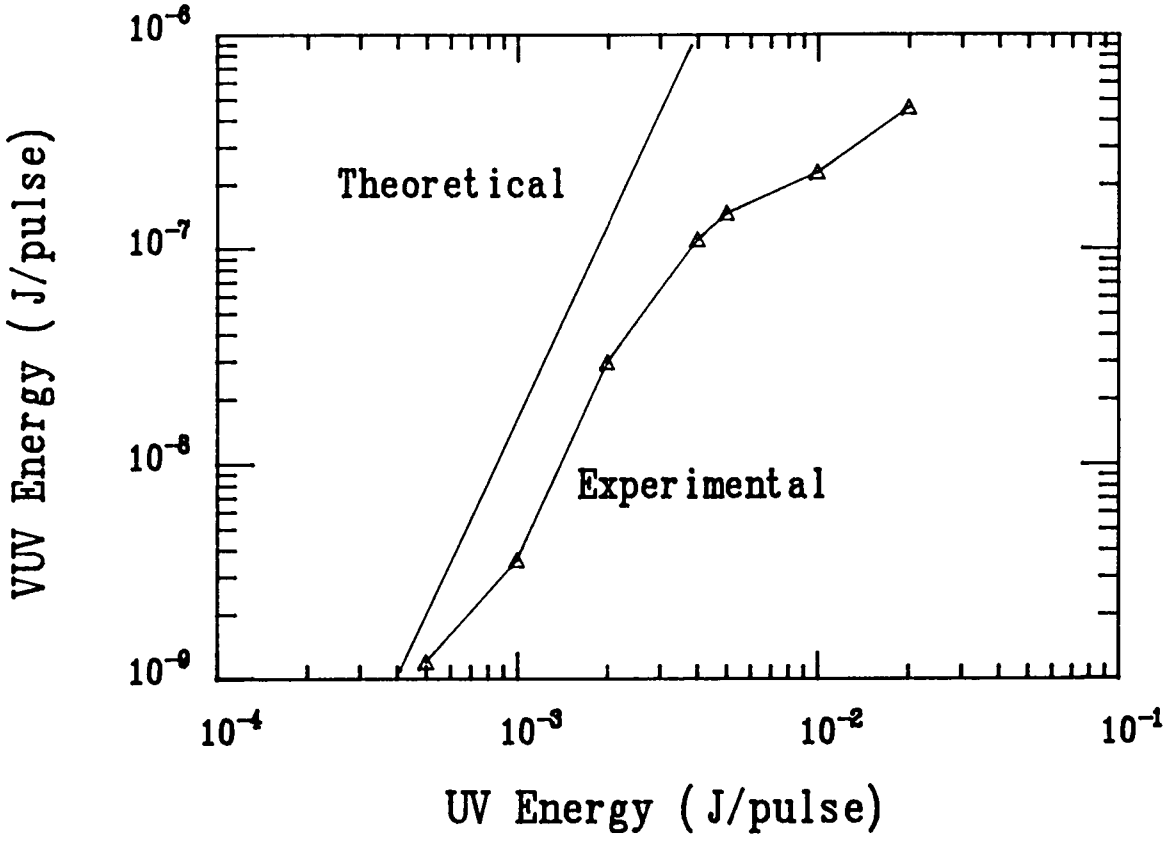

Figure 12. Conversion Efficiency of UV to VUV, Focused Geometry.

Table 3

Experimental VUV Energies and Efficiencies, Focused Geometry

Ultraviolet Energy	Xenon Pressure	Lens Focal Length (cm)	VUV Energy	Conversion Efficiency
0.5 mJ/pulse	29 torr	15 cm	1.21 nJ/pulse	2.4×10^{-6}
1.0 mJ/pulse	29 torr	15 cm	3.63 nJ/pulse	3.6×10^{-6}
2.0 mJ/pulse	29 torr	15 cm	30.0 nJ/pulse	1.5×10^{-5}
4.0 mJ/pulse	29 torr	15 cm	112 nJ/pulse	2.8×10^{-5}
5.0 mJ/pulse	29 torr	15 cm	149 nJ/pulse	2.9×10^{-5}
10.0 mJ/pulse	29 torr	15 cm	231 nJ/pulse	2.3×10^{-5}
20.0 mJ/pulse	29 torr	15 cm	462 nJ/pulse	2.3×10^{-5}

windows at each end. Therefore, the VUV had to go through two LiF windows before it entered the detection cell. The amount of attenuation could be calculated using Equation 4, and also the attenuation due to the two LiF windows.

Equation 2 indicates that the amount of VUV will continue to increase with increasing xenon pressure and UV power. Obviously this is not the case. At higher xenon pressures, absorption, especially by dimers (Xe_2 and XeAr), begins to diminish the VUV power. As the laser power is increased or the focal length of the lens decreased, breakdown can occur,[25] which could greatly reduce coherent VUV generation or eliminate it entirely. The slope of all but the highest two points in Figure 12 is 2.2. This deviation from a slope of 3 as shown in Equation 2, indicates that absorption may already be a problem with a xenon pressure of

[25]A. H. Kung, J. F. Young, and S. E. Harris, "Generation of 1182-Å radiation in phase-matched mixtures of inert gases," Applied Physics Letters, Volume 22, Number 6, (15 March 1973) pp. 301-302.

29 torr. The higher two points in Figure 12 deviate even further from a slope of 3 indicating that perhaps breakdown is starting to be a problem.

D. Phase Matching

As previously mentioned, the refractive index of xenon at 118 nm and 355 nm was not the same. In the plane wave, unfocused arrangement, this resulted in nearly complete destructive interference. When the UV beam was focused in pure xenon, the amount of VUV generated did not suffer much from destructive interference. Addition of appropriate amounts of argon for phase matching only increased the amount of VUV that was generated by a factor of two when a 15 cm focal length lens was used.

As indicated by Figure 10 and verified by experiment, xenon is negatively dispersive, which means that it has a refractive index just slightly less than unity at 118 nm. Also xenon is positively dispersive, with a refractive index just slightly greater than unity at 355 nm. This means that when VUV is generated in a xenon atom, as the VUV and the UV travels to the next atom, they get out of phase with each other due to the different wavefront velocities in xenon. The wavespeed is given by

$$v = \frac{c}{n} \tag{6}$$

where

v = wavespeed

c = speed of light

n = refractive index.

So the VUV generated at the next xenon atom is out of phase with the VUV generated at the previous atom, due to the difference in the wavespeeds of the the VUV to the UV. Depending on the phase difference, destructive interference could occur and VUV generation would be diminished. When the phase mismatch is π then complete destructive interference occurs and there isn't any VUV generation at all.

A two parameter fit can be made[26] to the Sellmeier formula[27] which yields the refractive indices of Xe and Ar at wavelengths longer than 110 nm. The results of this calculation are shown in Figures 13 and 14. It was this index that was used in the calculation of Equation 2.

Knowing the refractive index of argon and xenon at 355 nm and 118 nm, the ratio of argon to xenon can be chosen using Equation 1. The refractive index of the gas mixture at some wavelength λ is

$$n(\lambda) = 1 + N_{Xe} f_{Xe}(\lambda) + N_{Ar} f_{Ar}(\lambda) \tag{7}$$

where

N = number density of the atoms (Xe or Ar)

$f(\lambda)$ = dispersive term calculated from Sellmeier formula at wavelength λ

[26]M. G. Payne, private communication.

[27]M. Born and E. Wolf, Principles of Optics, (New York: Pergamon Press, 1959), pg. 95.

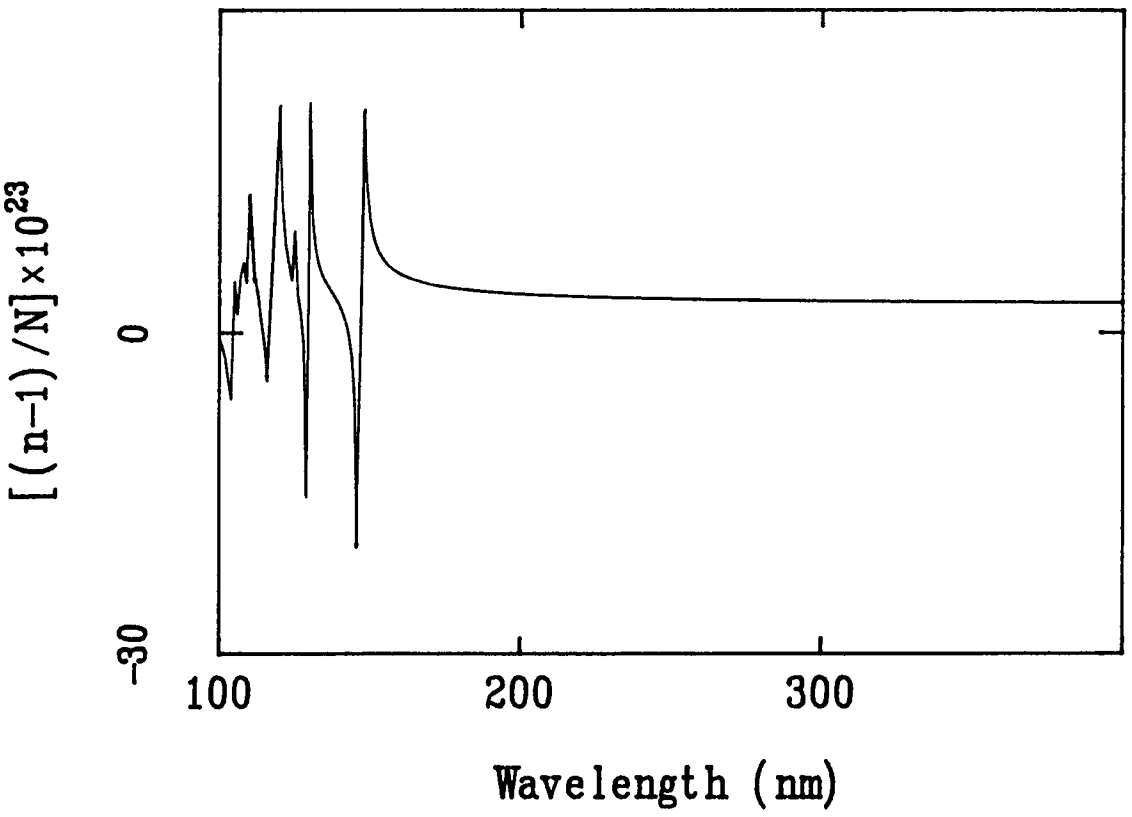

Figure 13. Refractive Index versus λ for Xenon.

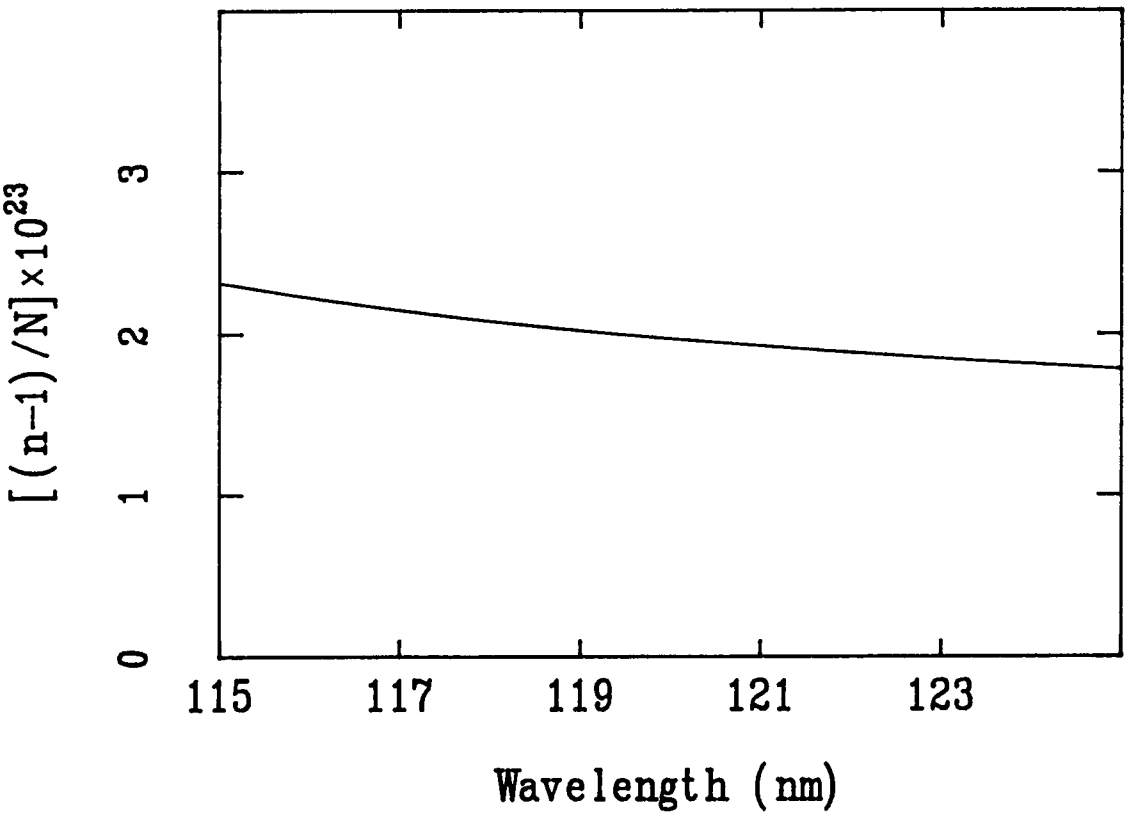

Figure 14. Refractive Index versus λ for Argon.

From Equation 1 and 7

$$N_{Xe}f_{Xe}(118\text{ nm})+N_{Ar}f_{Ar}(118\text{ nm}) - N_{Xe}f_{Xe}(355\text{ nm}) - N_{Ar}f_{Ar}(355\text{ nm}) = 0 \tag{8}$$

$$\frac{N_{Ar}}{N_{Xe}} = \frac{f_{Xe}(355\text{ nm}) - f_{Xe}(118\text{ nm})}{f_{Ar}(118\text{ nm}) - f_{Ar}(355\text{ nm})} \tag{9}$$

where

$$f_{Xe}(118\text{ nm}) = -9.837288 \times 10^{-23}$$

$$f_{Xe}(355\text{ nm}) = 2.758314 \times 10^{-23}$$

$$f_{Ar}(118\text{ nm}) = 2.055206 \times 10^{-23}$$

$$f_{Ar}(355\text{ nm}) = 1.082658 \times 10^{-23}.$$

This yields a N_{Ar}/N_{Xe} ratio of 13 for unfocused geometry. The experimental ratio is 10.25 and the data are shown in Figure 15. The calculated result is off from the experimental result due to the difficulty of calculating the refractive index of xenon at 118 nm which is in between two resonances at 118 nm in xenon. The experimental data might suffer from some inaccuracies if the two gases were not homogeneously mixed. There was no way to stir the gases and if allowed to sit for long periods of time, the gases became contaminated due to leaks in the chamber and the VUV generation efficiency dropped accordingly. The experimental ratio was close to the ratio of 10.5 found in previous work.[28] The same thing was done again except nitrogen was used instead of argon. This was the first instance of a

[28] A. H. Kung, J. F. Young, and S. E. Harris,"Erratum: Generation of 1182-Å radiation in phase-matched mixtures of inert gases [Appl. Phys. Lett. 22, 301 (1973)]," Applied Physics Letters, Volume 28, Number 4, (15 February 1976), pg. 239.

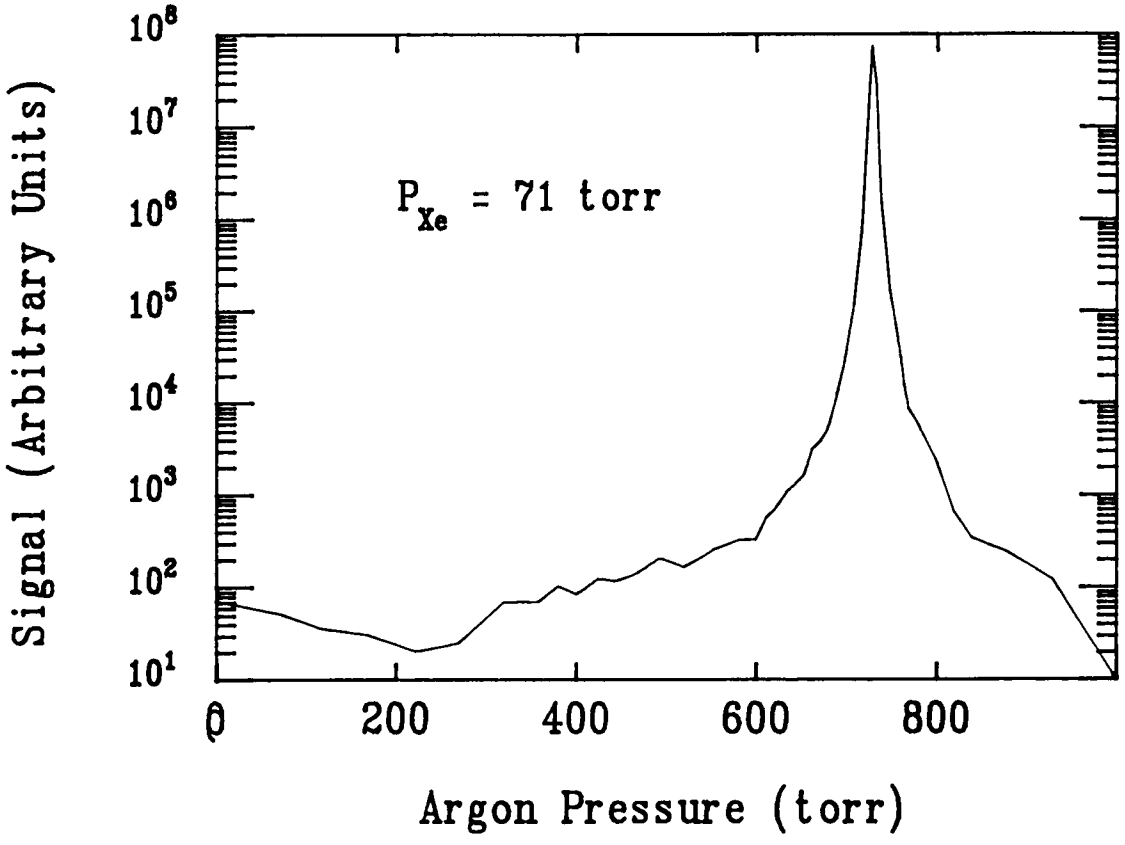

Figure 15. Phase-Matching in Unfocused Geometry with Argon.

molecule being used for phase-matching. As shown in Figure 16, nitrogen didn't work as well as argon. This is to be expected since the oscillator strengths in nitrogen are not as large as in argon. As seen in Figure 17, addition of argon to the generation cell when the UV beam was focused with a 15 cm lens did not produce a great deal of enhancement.

E. Summary

The experimental results presented here were in reasonable agreement with the calculations and previous results. The unfocused data was a little high but this was not surprising considering how sensitive the VUV signal was to inhomogeneities in the beam distribution. The unstable resonator of the Nd:YAG laser tended to produce "hot spots", which were small areas in the beam cross section where the photon flux was higher than it should have been. The focused data were lower than the calculated values. There was some confusion in the literature on the conversion efficiency of VUV in focused geometry. Initial studies gave an experimental conversion efficiency of 2.8% at 13 MW.[29] Due to experimental problems, this value was then changed to 0.14%.[30] The conversion efficiency was then calculated (5.1×10^{-5}) and measured experimentally (2.1×10^{-5}) at 2 MW.[31]

[29] A. H. Kung, J. F. Young, and S. E. Harris, "Generation of 1182-Å radiation in phase-matched mixtures of inert gases," Applied Physics Letters, Volume 22, Number 6, (15 March 1973), pp. 301-302.

[30] A. H. Kung, J. F. Young, and S. E. Harris, "Erratum: Generation of 1182-Å radiation in phase-matched mixtures of inert gases," Applied Physics Letters, Volume 28, Number 4, (15 February 1976), pg. 239

[31] A. H. Kung "Third-harmonic generation in a pulsed supersonic jet of

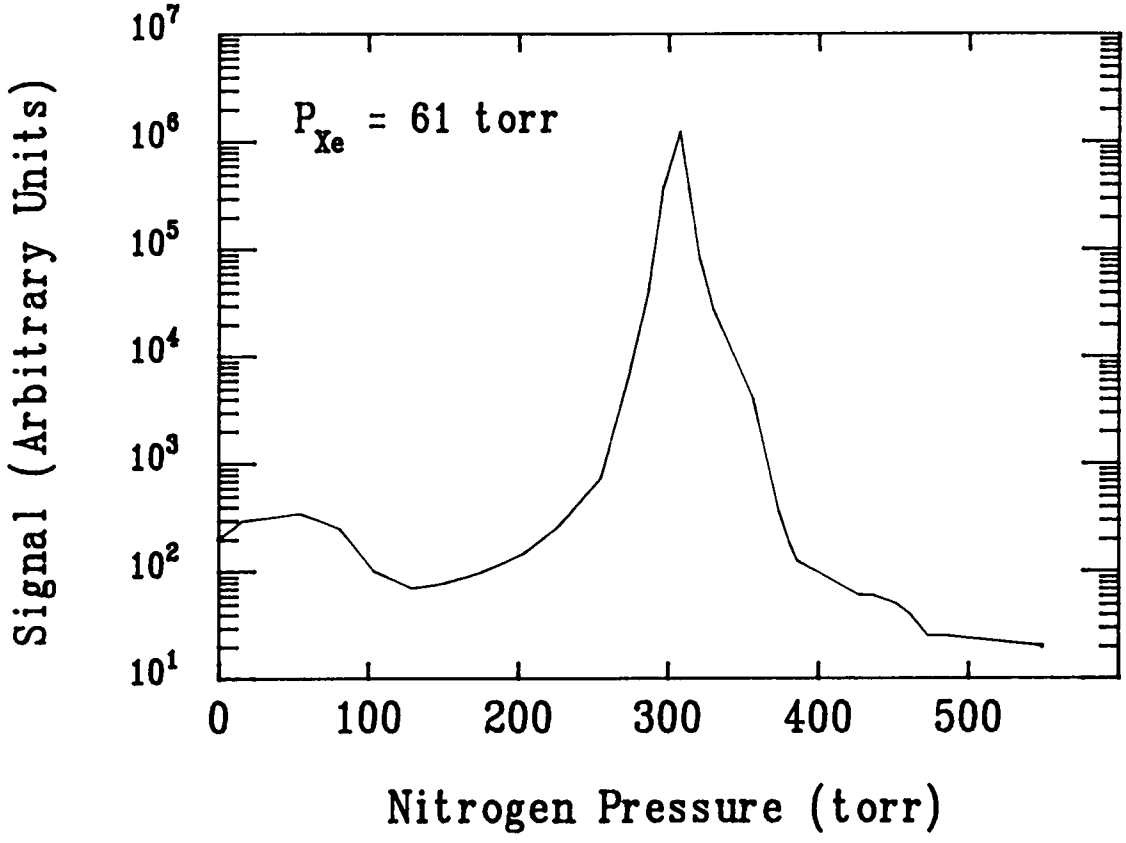

Figure 16. Phase-Matching in Unfocused Geometry with Nitrogen.

xenon,"Optics Letters, Volume 8, Number 1, (January 1983), pp. 24-26.

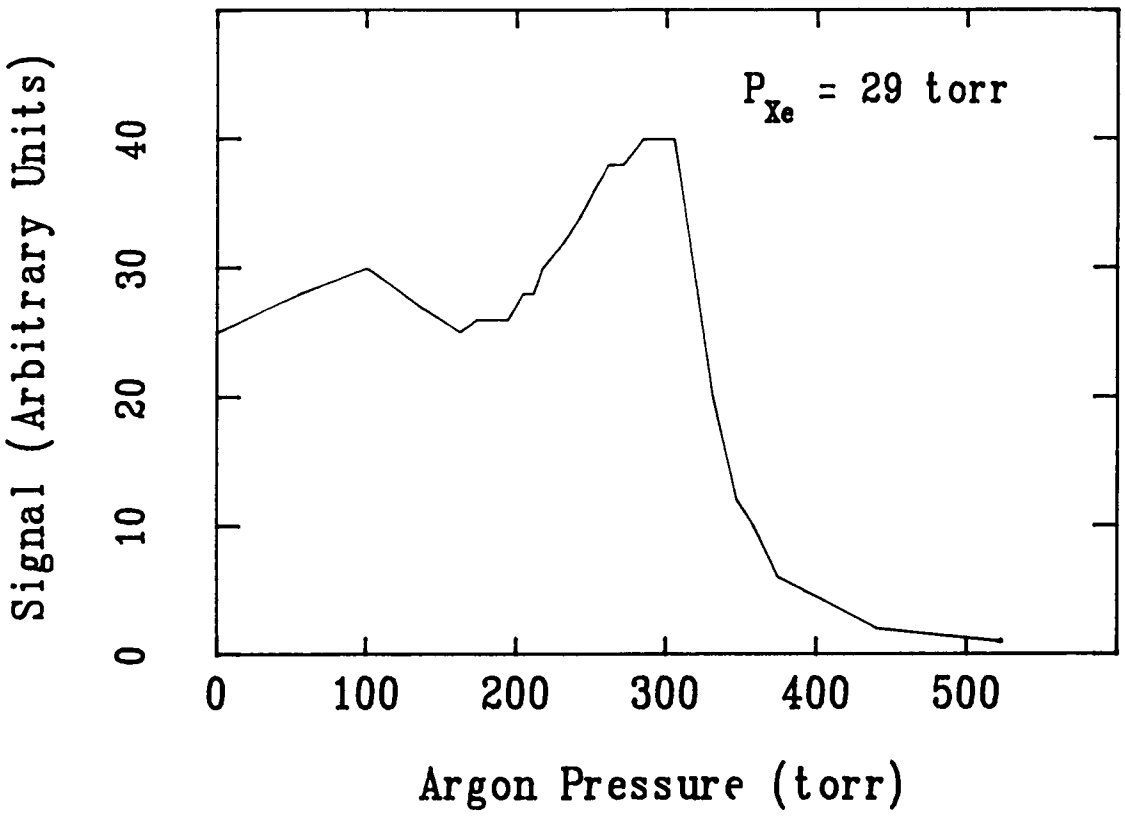

Figure 17. Phase-Matching in Focused Geometry with Argon.

Taking the reduced power into account, these conversion efficiencies were lower than those reported earlier. The trend again was to lower conversion efficiencies and this time for unknown reasons. It showed the difficulties in measuring third-harmonic generation. As the purpose of this work was to utilize coherent VUV light for analytical purposes, great care was taken to carefully control and characterize VUV generation. The measurements that were taken are consistent, and agree with previous experiments and calculations.

CHAPTER IV

TWO-PHOTON SPECTROSCOPY OF ARGON, KRYPTON, AND HYDROGEN

A. Overall Process

Two-photon spectroscopy of Ar, Kr, and H_2 involved the use of a fixed wavelength VUV photon at 118 nm and a tunable visible photon. From the two-photon excited state, the atom or molecule was then ionized by the absorption of an additional UV photon. This photoionization step of the the excited species was saturated so that the signal was a direct measure of the two-photon absorption signal. The target gas was in a cell with pressures of typically <60 torr. The photoelectron was initially detected by a proportional counter and later by a parallel plate detector. Spectra were taken by recording the two-photon signal as the dye laser wavelength was varied. Also the signal could be recorded versus the input laser energy, so that saturation of the photoionization step was insured. Two-photon spectra have been widely reported.[32,33,34] The purpose of this work was

[32]Robin M. Hochstrasser, G. R. Meredith, and H. P. Trommsdorff, "Two-Photon Spectra of Gases by Three-Wave Mixing," Chemical Physics Letters, Volume 53, Number 3, (1 February 1978), pp. 423-428.

[33]Mary J. Wirth, Aaron Koskelo, and Matthew J. Sanders, "Molecular Symmetry and Two-Photon Spectroscopy," Applied Spectroscopy, Volume 35, Number 1, (1981), pp. 14-21.

[34]Robert R. Birge, "An Introduction to Two-Photon Spectroscopy," NATO

to measure two-photon absorption cross sections so that two-photon spectroscopy might be more fully utilized in a quantitative manner.

B. Calculation of the Two-Photon Rate Constant in Argon

It is useful to estimate the size of the VUV-Visible two-photon excitation signal using some of the parameters of the experiment. For this estimate of the signal size, the $Ar(3p^5 4p'\,[3/2]_{J=2}) \leftarrow Ar(3p^6)$ transition has been chosen.

The laser scheme for this transition, as shown in Figure 7, is as follows:

$$\mathrm{Ar}(3p^6) + \omega_1(\lambda = 118\ \mathrm{nm}) + \omega_2(\lambda = 440\ \mathrm{nm}) \rightarrow \mathrm{Ar}(3p^5 4p'\,[3/2]_{J=2}) \qquad (10)$$

$$\mathrm{Ar}(3p^5 4p'\,[3/2]_{J=2}) + \omega_2(\lambda = 440\ \mathrm{nm}) \rightarrow \mathrm{Ar}^+ + e^-. \qquad (11)$$

The VUV and visible photons combine to resonantly excite the argon atom. The remaining visible light (440 nm) from the dye laser is sufficient to ionize the excited argon atom.

The number of argon cations is[35]

$$N_I = N_{Ar} \int_{-L/2}^{L/2} dx \int_0^{\infty} 2\pi P_I(\rho, x) d\rho, \qquad (12)$$

where

N_I = number of argon cations

ASI Series, Series C, (Spectroscopy of Biological Molecules), Volume 139, edited by C. Sandorfy and T. Theophanides, (1984), pp. 457-471.

[35]M. G. Payne, C. H. Chen, G. S. Hurst, and G. W. Foltz, Advances in Atomic and Molecular Physics, Volume 17, edited by D. Bates and B. Bederson, (New York: Academic Press 1981), pp. 229-274.

N_{Ar} = number density of argon atoms in the detection region

$= (1.62 \times 10^{18}$ atoms/cm$^3)$

L = is the distance along the laser beam axis over which argon cations can be detected (2.54 cm)

ρ = radial distance out from the laser beam axis (cm)

x = is the distance along the the laser beam axis from the focal point (cm)

P_I = ionization probability, which is a function of x and ρ.

The ionization probability is given by[36]

$$P_I = 1 - \frac{\Gamma_I R_2}{2J}\left(\frac{e^{-\beta_1 \tau}}{\beta_1} - \frac{e^{-\beta_2 \tau}}{\beta_2}\right) \tag{13}$$

where

Γ_I = ionization rate from the $4p'\,[3/2]_{J=2}$ state

R_2 = two-photon transition rate

$J = \sqrt{R_2^2 + \Gamma_I^2/4}$

$\beta_1 = -J + R_2 + \Gamma_I/2$

$\beta_2 = J + R_2 + \Gamma_I/2$

τ = laser pulse duration $(6 \times 10^{-9}$s).

The ionization rate is[37]

$$\Gamma_I = \frac{\sigma_I I}{\omega} \tag{14}$$

[36]C. H. Chen, G. S. Hurst, and M. G. Payne, "Direct Counting of Xe Atoms," Chemical Physics Letters, Volume 75, Number 3, (1 November 1980), pp. 473-477.

[37]M. G. Payne, C. H. Chen, G. S. Hurst, S. D. Kramer, W. R. Garrett, M. Pindzola "Resonance Ionization Spectroscopy Schemes for Ar, Kr and Xe," Chemical Physics Letters, Volume 79, Number 1, (1 April 1981), pp. 142-148.

where

σ_I = ionization cross section (1.4×10^{-17} cm^2)

I = intensity of the ionizing (visible) laser in the detection region (W/cm^2)

ω = angular frequency of the visible laser light (4.29×10^{15} rad/s).

The ionization cross section is a calculated value.[38] As the ionization process is easily saturated, all that really matters is that the photon fluence exceeds the ionization cross section.

The two-photon transition rate is approximated by[39]

$$R_2 \approx \frac{14 M_2^2 I_1(\rho, x) I_2(\rho, x)}{\sqrt{\Delta_1^2 + \Delta_2^2}} \tag{15}$$

where

M_2 = dimensionless parameter indicative of the radial matrix elements from a Hartree-Fock type calculation (1.7)

I_1 = incident intensity of the coherent VUV light

I_2 = incident intensity of the visible laser light

Δ_1 = full width at half-maximum of the VUV light (1.7×10^{12} rad/s)

Δ_2 = full width at half-maximum of the visible laser light

= (3.77×10^{10} rad/s)

[38]C. Duzy and H. A. Hyman, "Photoionization of excited rare-gas atoms," Physical Review A, Volume 22, Number 5, (November 1980), pp. 1878-1883.

[39]M. G. Payne, C. H. Chen, G. S. Hurst, and G. W. Foltz, Advances in Atomic and Molecular Physics, Volume 17, edited by D. Bates and B. Bederson, (New York: Academic Press 1981), pp. 229-274.

The dimensionless parameter, M_2, yields the response of the atom to the two photons and has been calculated for other transitions in other atoms as well.[40] There can be an enhancement to the two-photon signal when the energy of one of the photons lies close to a one-photon resonance. This is not the case in this transition as the VUV photon lies 1.14 eV from the nearest one-photon allowed transition. The enhancement is proportional to the inverse square of the difference between the photon energy and the resonance energy and so at small detunings the signal can be dramatically increased.

The two-photon excitation rate constant can be defined as

$$K_2 = \frac{14 M_2^2}{\sqrt{\Delta_1^2 + \Delta_2^2}} \tag{16}$$

If the ionization rate is considered to be independent of the laser power then the ionization probability will be the product of the two-photon rate and the shortest laser pulse duration. The number of argon cations produced will be directly proportional to K_2. In the rate formalism, the constant, K_2, can be useful in determining the signal size. The signal would be

$$N_I = N_{Ar} \Delta V K_2 I_1 I_2 \tau \tag{17}$$

where

ΔV = effective ionization volume[41]

[40]M. G. Payne, C. H. Chen, G. S. Hurst, S. D. Kramer, W. R. Garrett, M. Pindzola "Resonance Ionization Spectroscopy Schemes for Ar, Kr and Xe," Chemical Physics Letters, Volume 79, Number 1, (1 April 1981), pp. 142-148.

[41]M. G. Payne, C. H. Chen, G. S. Hurst, S. D. Kramer, W. R. Garrett, M.

All other parameters are as were previously defined. Using the above values for the ground state to $4p'\,[3/2]_{J=2}$ transition in argon, $K_2 = 2.4 \times 10^{-11}\mathrm{s} \cdot \mathrm{cm}^4/\mathrm{J}^2$. Including the photon energies, $K_2 = 1.8 \times 10^{-47}\mathrm{s} \cdot \mathrm{cm}^4$ per VUV and visible photon.

The intensity, assuming a homogeneous Gaussian beam distribution with cylindrical symmetry, is given by[42]

$$I(\rho, x) = \frac{\epsilon}{\tau \pi r^2(x)} \exp\left[\frac{-\rho^2}{r^2(x)}\right] \tag{18}$$

where

ϵ = energy per pulse ($\epsilon_{\mathrm{VUV}} = 1.2 \times 10^{-9}\mathrm{J}, \epsilon_{\mathrm{VIS}} = 6.0 \times 10^{-3}\mathrm{J}$)

τ = pulse duration

$r(x)$ = beam width as a function of distance, x, from the focus

ρ = radial distance from the beam axis.

The beam width is

$$r(x) = \sqrt{(f\theta_{1/2})^2 + (xr_0/f)^2} \tag{19}$$

where

f = lens focal length ($f_{\mathrm{VUV}} = 15$ cm, $f_{\mathrm{VIS}} = 25$ cm)

$\theta_{1/2}$ = half-angle beam divergence of the intial beam before focusing

$= 0.25 \times 10^{-3}\mathrm{rad}$

r_0 = is the half-width to e^{-1} drop in intensity

Pindzola "Resonance Ionization Spectroscopy Schemes for Ar, Kr and Xe," Chemical Physics Letters, Volume 79, Number 1, (1 April 1981), pg. 147.

[42]Ibid.

$= r_{0,\mathrm{VUV}} = 0.33$ cm, $r_{0,\mathrm{VIS}} = 0.15$ cm)

x = distance from the focus (cm).

The visible laser was focused in the center of the detection region, but the coherent VUV beam was focused in the middle of the generation cell. Therefore, the coherent VUV beam was focused 13 cm away from the closest edge of the detection region.

The calculation of the number of argon cations produced by this method can be simplified. As the ionization rate, Γ_I, saturates and is much larger than the two-photon excitation rate, then the following approximation can be made starting with the definition of J in Equation 13.

$$J = \sqrt{\frac{\Gamma_I^2}{4} + R_2^2} = \frac{\Gamma_I}{2}\sqrt{1 - \frac{4R_2^2}{\Gamma_I^2}} \tag{20}$$

Using a binomial series expansion

$$J = \frac{\Gamma_I}{2}\left(1 + \frac{2R_2^2}{\Gamma_I^2} - \ldots\right) \approx \frac{\Gamma_I}{2} \tag{21}$$

$$\beta_1 = R_2 + \frac{\Gamma_I}{2} - J \approx R_2 \tag{22}$$

$$\beta_2 = R_2 + \frac{\Gamma_I}{2} + J \approx \Gamma_I \tag{23}$$

$$P_I = 1 - \frac{\Gamma_I R_2}{2J}\left[\frac{e^{-\beta_1 \tau}}{\beta_1} - \frac{e^{-\beta_2 \tau}}{\beta_2}\right] \tag{24}$$

$$\frac{e^{-\beta_1 \tau}}{\beta_2} \approx 0 \tag{25}$$

$$e^{-\beta_1 \tau} \approx e^{-R_2 \tau} \approx 1 - R_2\tau \tag{26}$$

$$P_I \approx 1 - \frac{\Gamma_I R_2}{2 \cdot \frac{\Gamma_I}{2}}\left[\frac{1 - R_2\tau}{R_2} + 0\right] \tag{27}$$

$$P_I = 1 - (1 - R_2\tau) = R_2\tau. \tag{28}$$

This reduces the overall equation to

$$\begin{aligned} N_I = & \frac{14 N_{Ar} M_2^2 \epsilon_{\mathrm{VUV}} \epsilon_{\mathrm{VIS}}}{\pi\tau\sqrt{\Delta_1^2 + \Delta_2^2}} \int_{-L/2}^{L/2} \frac{-dx}{r_{\mathrm{VUV}}^2(x) + r_{\mathrm{VIS}}^2(x)} \\ & \int_0^{\infty} \frac{-2\rho}{r_{\mathrm{VUV}}^2(x) + r_{\mathrm{VIS}}^2(x)} \exp\left(\frac{-\rho^2}{r_{\mathrm{VUV}}^2(x) + r_{\mathrm{VIS}}^2(x)}\right) d\rho. \end{aligned} \tag{29}$$

The second integral is equal to -1. The overall equation is now

$$N_I = H \int_{-L/2}^{L/2} \frac{dx}{ax^2 + bx + c} \tag{30}$$

where

$$H = \frac{14 N_{Ar} M_2^2 \epsilon_{\mathrm{VUV}} \epsilon_{\mathrm{VIS}}}{\pi\tau\sqrt{\Delta_1^2 + \Delta_2^2}}$$

$$a = \frac{r_{0,\mathrm{VUV}}^2}{f_{\mathrm{VUV}}^2} + \frac{r_{0,\mathrm{VIS}}^2}{f_{\mathrm{VIS}}^2}$$

$$b = \frac{2g r_{0,\mathrm{VUV}}^2}{f_{\mathrm{VUV}}^2}$$

$$c = (f_{\mathrm{VUV}}^2 + f_{\mathrm{VIS}}^2)\theta_{1/2}^2 + \frac{g^2 r_{0,\mathrm{VUV}}^2}{f_{\mathrm{VUV}}^2}$$

g = distance between focus of VUV and visible beams (14.2 cm).

The solution of this integral is

$$N_I = H' \left[\frac{2}{\sqrt{4ac - b^2}} \tan^{-1}\left(\frac{2ax + b}{\sqrt{4ac - b^2}}\right)\right]\Bigg|_{-L/2}^{L/2}. \tag{31}$$

Letting

$$H' = \frac{2H}{\sqrt{4ac - b^2}}$$

the equation becomes

$$N_I = H' \left[\tan^{-1} \left(\frac{aL+b}{\sqrt{4ac-b^2}} \right) - \tan^{-1} \left(\frac{-aL+b}{\sqrt{4ac-b^2}} \right) \right]. \tag{32}$$

Using a convergent series to approximate the arctan function and keeping only one term, the equation becomes

$$N_I = 2H \left(\frac{1}{b-aL} - \frac{1}{b+aL} \right). \tag{33}$$

Using the previously stated values, the above equation yields a value of 3.82×10^5 argon cations. This is sufficiently large to be detected by parallel plates provided that the background, which comes primarily from scattered VUV light, is not too large. Additional laser schemes have been calculated for two-photon excitation, three-photon ionization of argon, krypton, and xenon.[43]

C. Experimental Results

The data for argon and krypton were collected using the proportional counter and the parallel plate detector described in Chapter II. The signal would be found by tuning the dye laser to various wavelengths. Once a peak was found, the signal had to be checked versus various parameters. At an argon pressure of 55 torr the signal began to saturate. Argon pressures below 55 torr were used for the measurement of the two-photon rate constant. If the dye laser was saturating the ionization step, then the signal should be linear with respect to the dye laser

[43]Ibid.

energy. The signal was found to be linear with respect to the dye laser energy at dye laser energies above 1 mJ/pulse. As the VUV energy was very small, it is unlikely that it was saturating its step of the two-photon excitation process. So the VUV was operated under the optimal conditions that were stated in Chapter III. Operating at the above stated conditions, it was assured that the signal was accurately indicative of the two-photon rate constant.

In general it was best to obtain the spectra at the lowest possible laser energies that would still yield a measurable signal. This was so that saturation and space charge effects could be avoided. Space charge problems arise when the electrons were removed from the ionization volume. The cations that remain behind could build up a charge that was sufficient to prevent the removal of additional electrons. The electrons then recombined with the cations and the number of cations that were measured was smaller than the original number of cations that were produced. Space charge problems were most likely to occur at the focus of the laser beam. The numbers of ions that would cause that onset of space charge problems could be estimated.

The diameter, d of the laser beam at the focus is

$$d \approx f\theta_{1/2} \tag{34}$$

where

f = focal length of the lens (0.25 m)

$\theta_{1/2}$ = beam divergence (0.25×10^{-3} rad).

The voltage produced by a charge is

$$V = \frac{q}{4\pi\varepsilon_0 r} \tag{35}$$

where

q = charge (C)

$1/4\pi\varepsilon_0 = 9.0\ \mathrm{N{\cdot}m^2/C^2}$

r = distance between charges (m).

The maximum number of electron-ion pairs that can be produced before space charge problems occur is

$$q = \frac{4\pi\varepsilon_0 V f \theta_0}{1.602 \times 10^{-19}} \tag{36}$$

Using a 25 cm lens and a bias voltage of 100 V the maximum number of electron-ion pairs is 4.3×10^6. Once the signal is this large it will not appear to get any larger with increasing laser power. The signal should be kept below this level in order to get useful information on the two-photon rate.

To measure the two-photon rate constant, the dye laser was tuned to a resonance. The dye laser energy, the UV (355 nm) energy, the argon or krypton pressure and the signal were all recorded for each resonance. The gain of the preamplifier and amplifier were used to convert the signal to the number of cations. The UV energy was converted to the corresponding VUV energy using the data in Figure 12.

The following equation was used to calculate the two-photon rate constant.

$$K_2 = \frac{\pi\tau N_I h\nu_{\mathrm{VUV}} h\nu_{\mathrm{VIS}} \sqrt{4ac - b^2}}{2N\epsilon_{\mathrm{VUV}}\epsilon_{\mathrm{VIS}}\Sigma F} \tag{37}$$

where

K_2 = two-photon rate constant (cm^4 s)

N_I = number ions detected

$h\nu$ = energy of an VUV or visible photon (J)

N = number density of target species (cm^{-3})

ϵ = energy of VUV or visible laser pulse (J)

$$\Sigma F = \tan^{-1}\left(\frac{aL+b}{\sqrt{4ac-b^2}}\right) - \tan^{-1}\left(\frac{-aL+b}{\sqrt{4ac-b^2}}\right)$$

and all other variables were previously defined. Equation 37 was used to tabulate Table 4.

The transition energies are *in vacuo* as determined experimentally and agree with the literature values within the bandwidth of the lasers.[43,44] A spectrum of argon can be seen in Figure 18. The value listed in Table 4 for the $3p^5 4p'\,[3/2]_{J=2} \leftarrow 3p^6$ transition in argon was very close to the value of 1.8×10^{-47} cm^4 s that was calculated using Equation 16 and the previously stated values for the variables in that equation. There was good agreement between the calculated result using

[43]Charlotte E. Moore, Atomic Energy Levels, Volume I, (Washington, D. C.: National Bureau of Standards, December 1971), pg. 212.

[44]Charlotte E. Moore, Atomic Energy Levels, Volume II, (Washington, D. C.: National Bureau of Standards, December 1971), pg. 170.

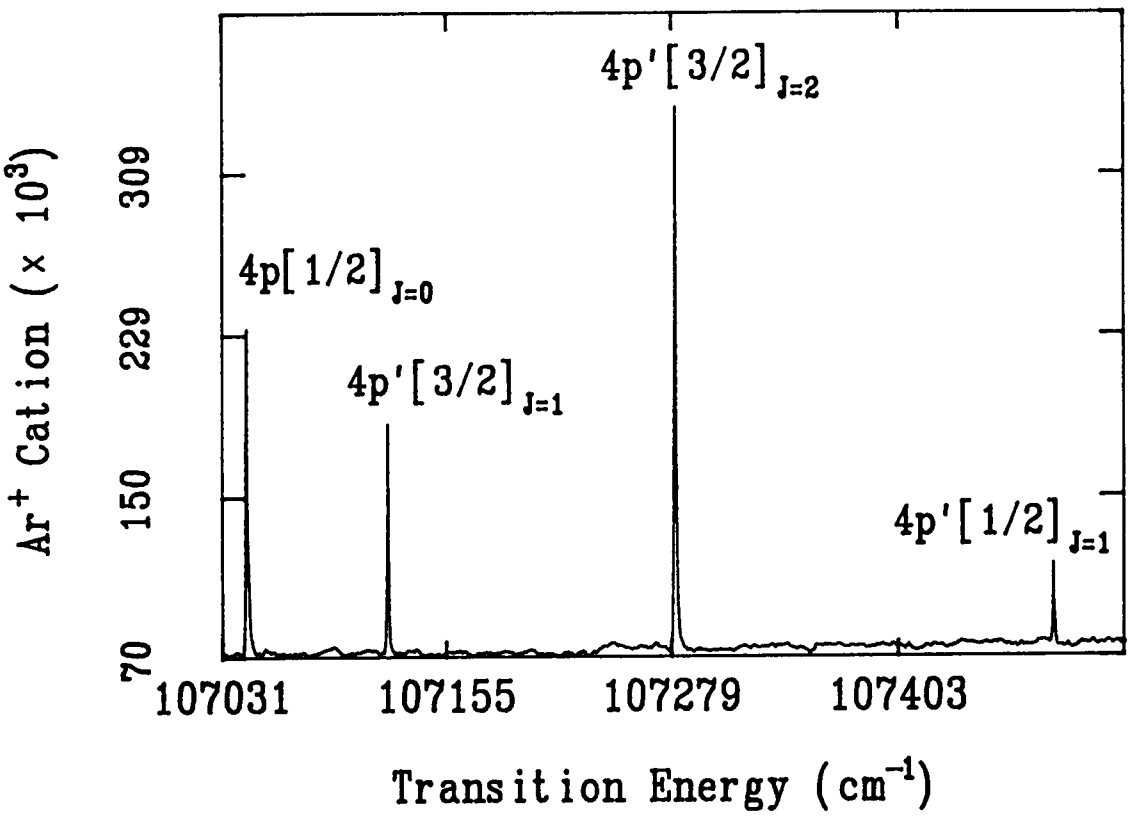

Figure 18. VUV-Visible Spectrum of Argon.

Table 4

Experimental Transition Energies and Two-Photon Rate Constants for Ar and Kr

Transition	Energy (cm^{-1})	K_2 (cm^4 s)
Argon		
$3p^5 4p\,[5/2]_{J=2} \leftarrow 3p^6$	105,611	1.6×10^{-46}
$3p^5 4p\,[3/2]_{J=1} \leftarrow 3p^6$	106,083	2.5×10^{-47}
$3p^5 4p\,[3/2]_{J=2} \leftarrow 3p^6$	106,235	5.8×10^{-47}
$3p^5 4p\,[1/2]_{J=0} \leftarrow 3p^6$	107,051	2.3×10^{-47}
$3p^5 4p'\,[3/2]_{J=1} \leftarrow 3p^6$	107,128	6.2×10^{-48}
$3p^5 4p'\,[3/2]_{J=2} \leftarrow 3p^6$	107,287	1.3×10^{-47}
$3p^5 4p'\,[1/2]_{J=1} \leftarrow 3p^6$	107,495	6.6×10^{-48}
Krypton		
$4p^5 4f\,[3/2]_{J=2} \leftarrow 4p^6$	105,961	3.7×10^{-47}
$4p^5 4f\,[5/2]_{J=2} \leftarrow 4p^6$	106,017	6.2×10^{-48}
$4p^5 4f\,[1/2]_{J=2} \leftarrow 4p^6$	107,410	9.5×10^{-48}

previously calculated atomic wavefunctions[45] and the results that were determined experimentally.

The data for molecular hydrogen were also collected in a high pressure cell. The signal was again checked for inconsistency. A plot of the two-photon signal versus H_2 pressure is shown in Figure 19. The response is linear with respect to H_2 pressure so there is no saturation or space charge effect. The hydrogen signal was smaller than the argon signal so higher pressures were used. Frequently 800 torr of H_2 were used.

[45]M. G. Payne, C. H. Chen, G. S. Hurst, S. D. Kramer, W. R. Garrett, M. Pindzola "Resonance Ionization Spectroscopy Schemes for Ar, Kr and Xe," Chemical Physics Letters, Volume 79, Number 1, (1 April 1981), pg. 145.

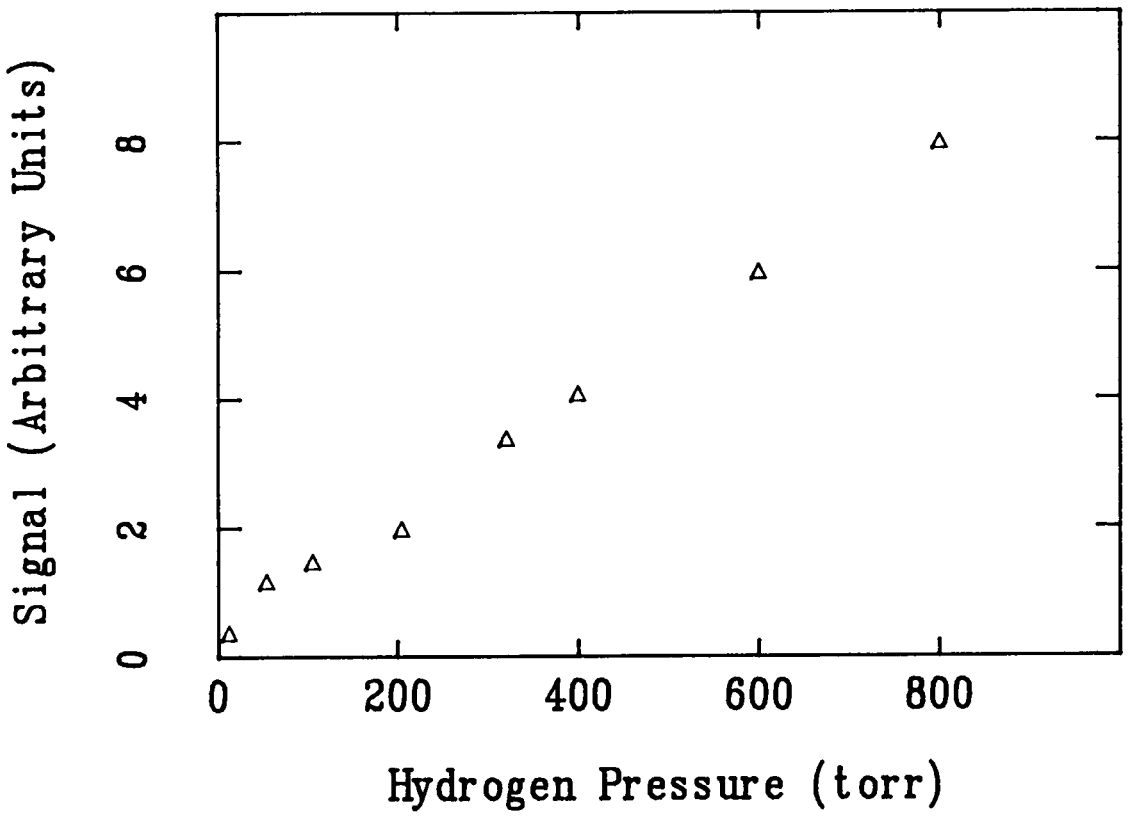

Figure 19. VUV-Visible Signal versus Hydrogen Pressure.

The laser scheme is shown in Figure 20.[46] Since the dye laser beam was present in the ionization volume at much greater fluences than either the UV or the VUV, and the visible photon had sufficient energy to ionize the molecule from the excited state, then it is reasonable to assume that the ionization step was saturated by the dye laser beam. All of the transitions are to the $E,F\ ^1\Sigma_g^+ 2s\sigma + 2p\sigma^2$ state in hydrogen.

The hydrogen spectra are shown in Figures 21-26. The spectra were not corrected for variations in the dye laser intensity at different wavelengths. The spectra were identified with the help of the literature and agree well with previously observed spectra.[47,48]

In general the two-photon selection rules are the same as those for Raman transitions and are as follows. Positive terms combine only with positive terms and negative terms combine only with negative terms. Positive terms do not go to negative terms nor vice versa. Symmetric terms combine only with symmetric terms and antisymmetric terms combine only with antisymmetric terms. Symmetric terms do not combine with antisymmetric terms and vice versa. *Gerade* or even states combine only with *gerade* states and *ungerade* or odd states combine

[46]T. E. Sharp, "Potential-Energy Curves for Molecular Hydrogen and Its Ions," Atomic Data, Volume 2, 1971, pp. 119-169.

[47]L. Wolniewicz and K. Dressler, "The EF and $GK\ ^1\Sigma_g^+$ States os Hydrogen, Adiabatic Calculation of Vibronic States in H_2, HD, and D_2," Journal of Molecular Spectroscopy, Volume 67, (1977), pp. 416-439.

[48]G. H. Dieke, "The Molecular Spectrum of Hydrogen and Its Isotopes," Journal of Molecular Spectroscopy, Volume 2, (1958), pp. 494-517.

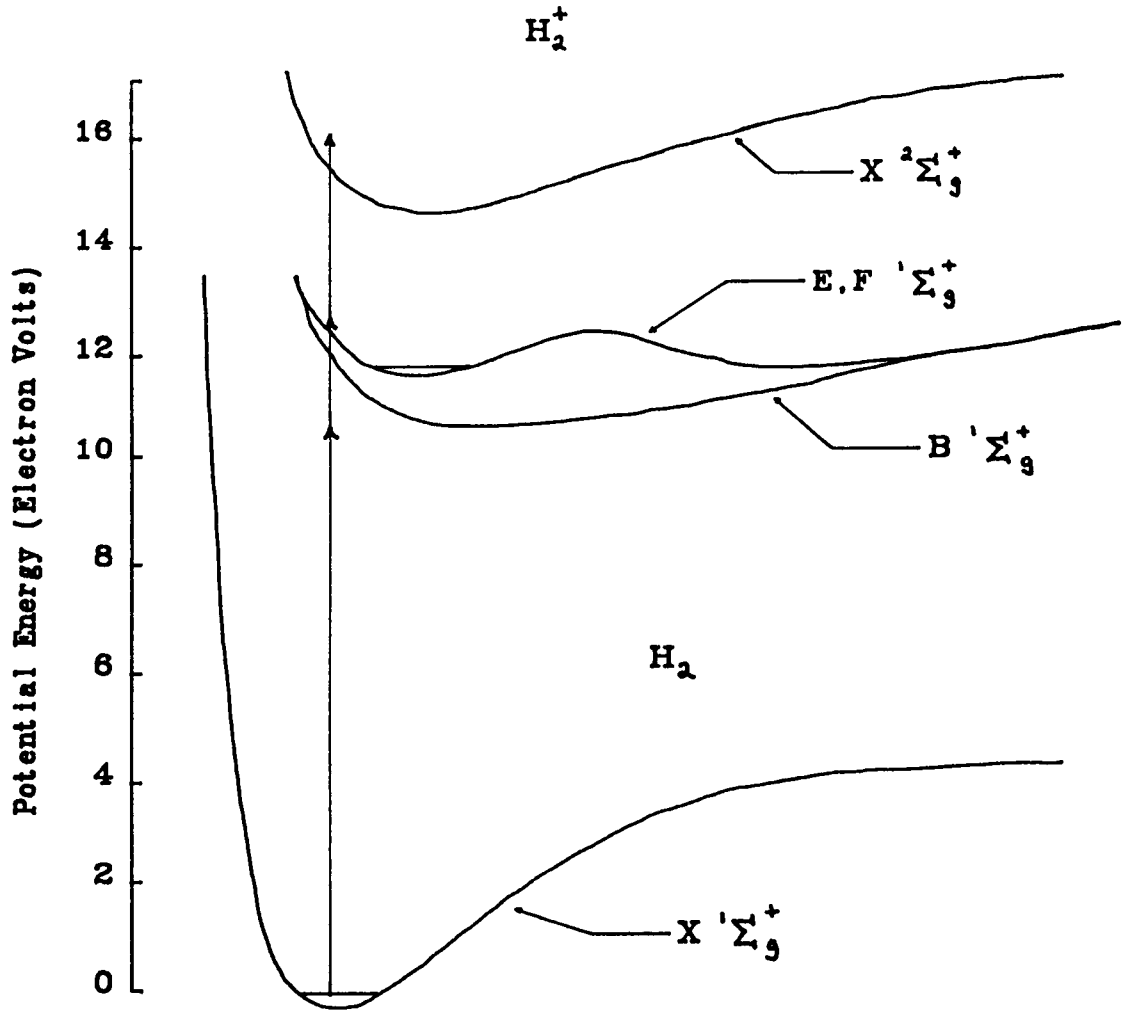

Figure 20. Laser Scheme for Hydrogen.

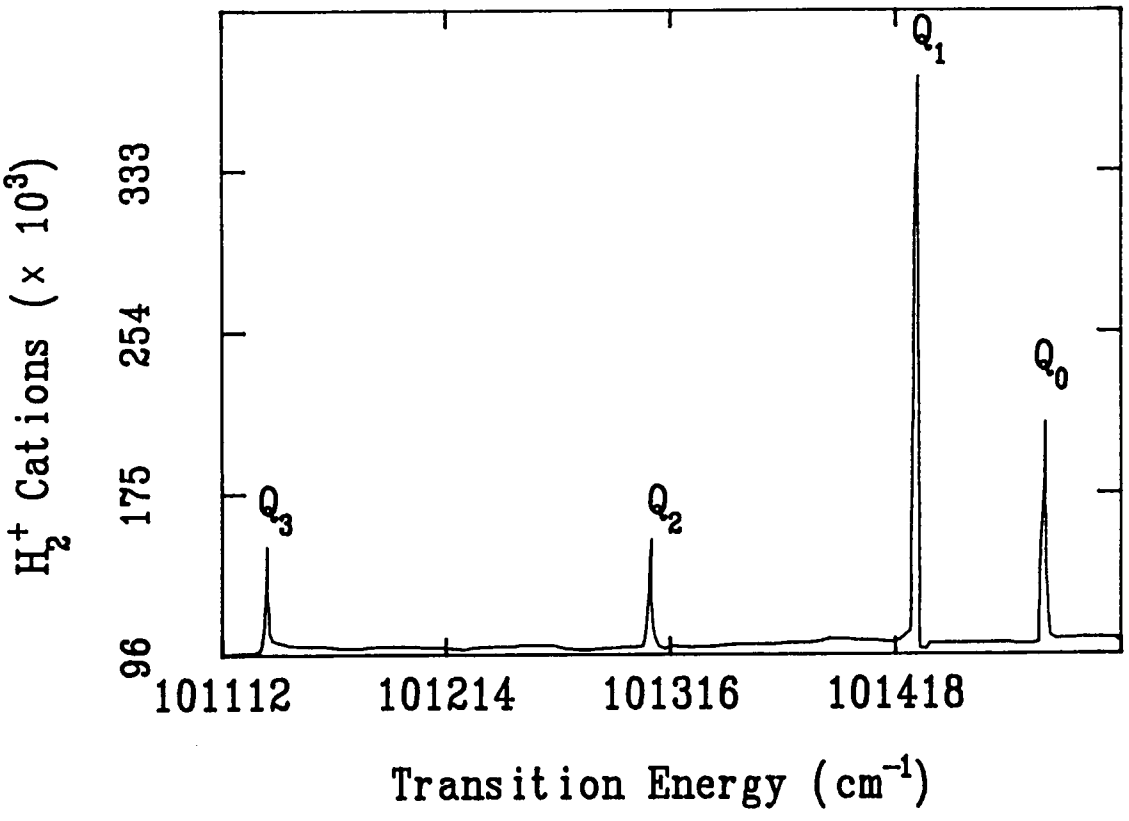

Figure 21. VUV-Visible Spectrum of Hydrogen,
$E, F\ ^1\Sigma_g^+(v' = 3) \leftarrow X\ ^1\Sigma_g^+(v'' = 0)$.

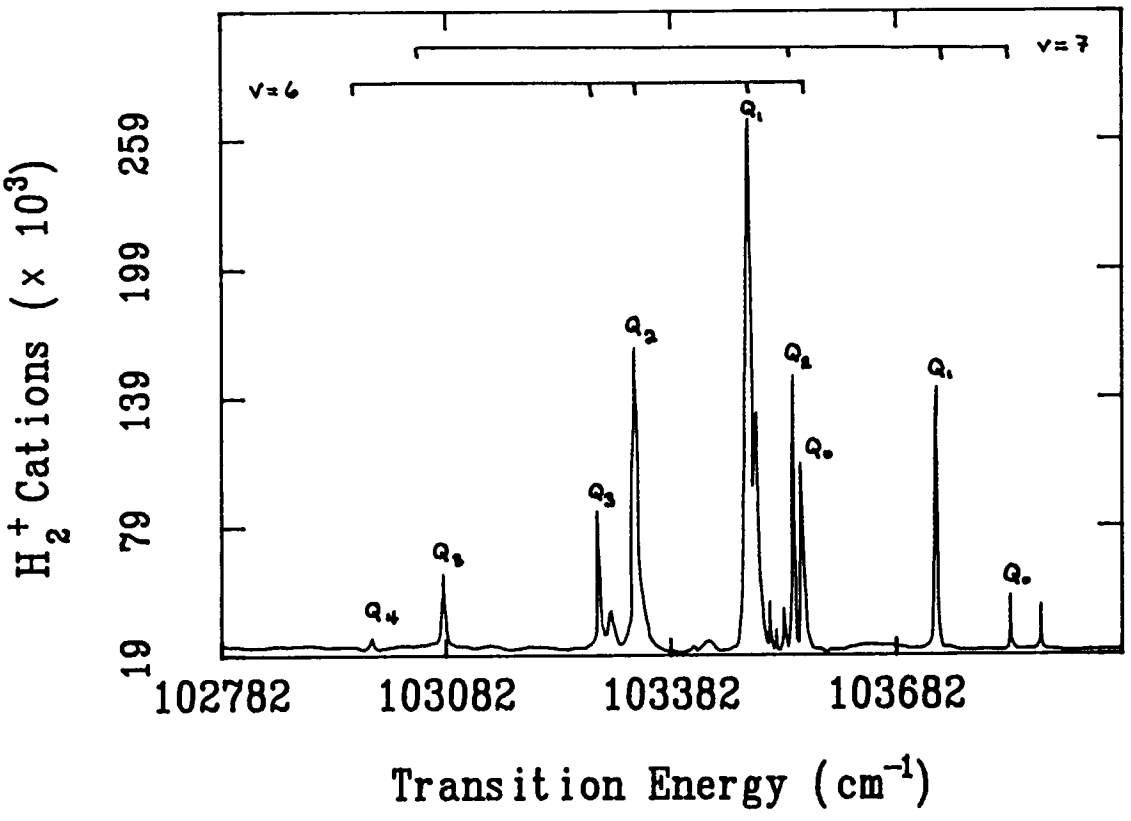

Figure 22. VUV-Visible Spectrum of Hydrogen,
$E, F\ ^1\Sigma_g^+(v' = 6, 7) \leftarrow X\ ^1\Sigma_g^+(v'' = 0)$.

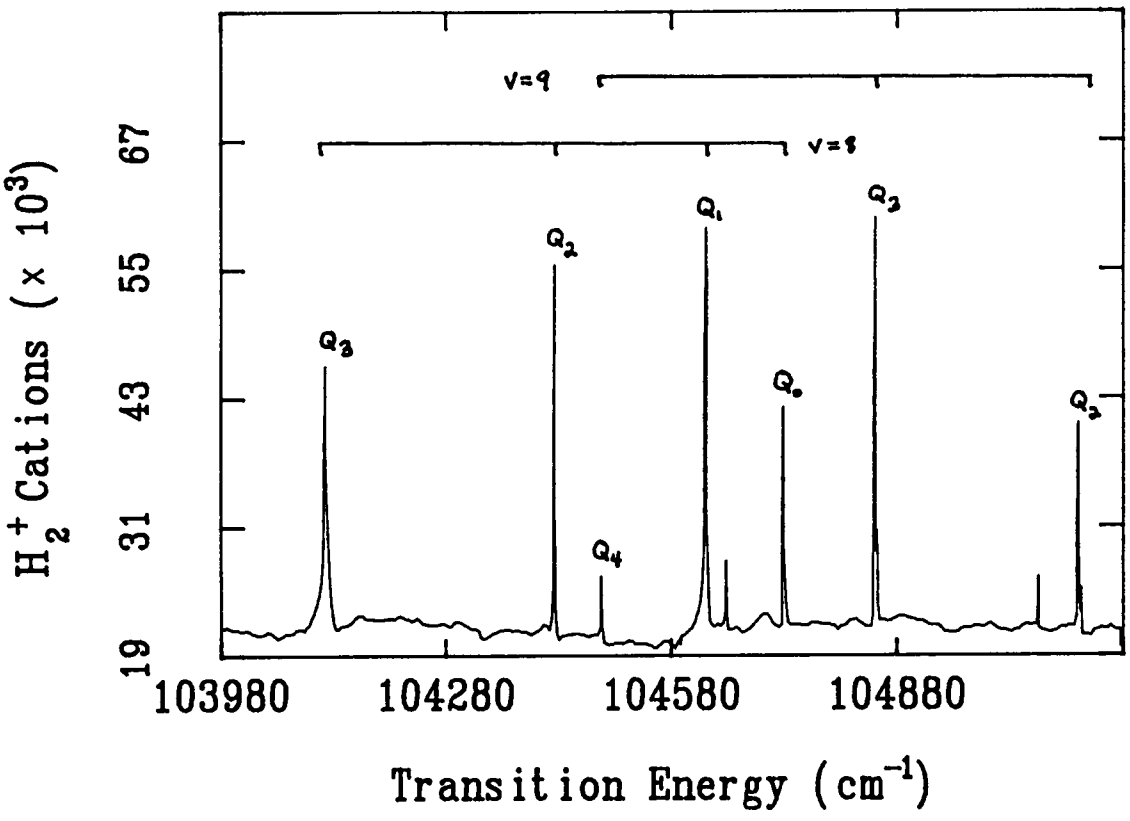

Figure 23. VUV-Visible Spectrum of Hydrogen,
$E, F\ ^1\Sigma_g^+(v' = 8, 9) \leftarrow X\ ^1\Sigma_g^+(v'' = 0)$.

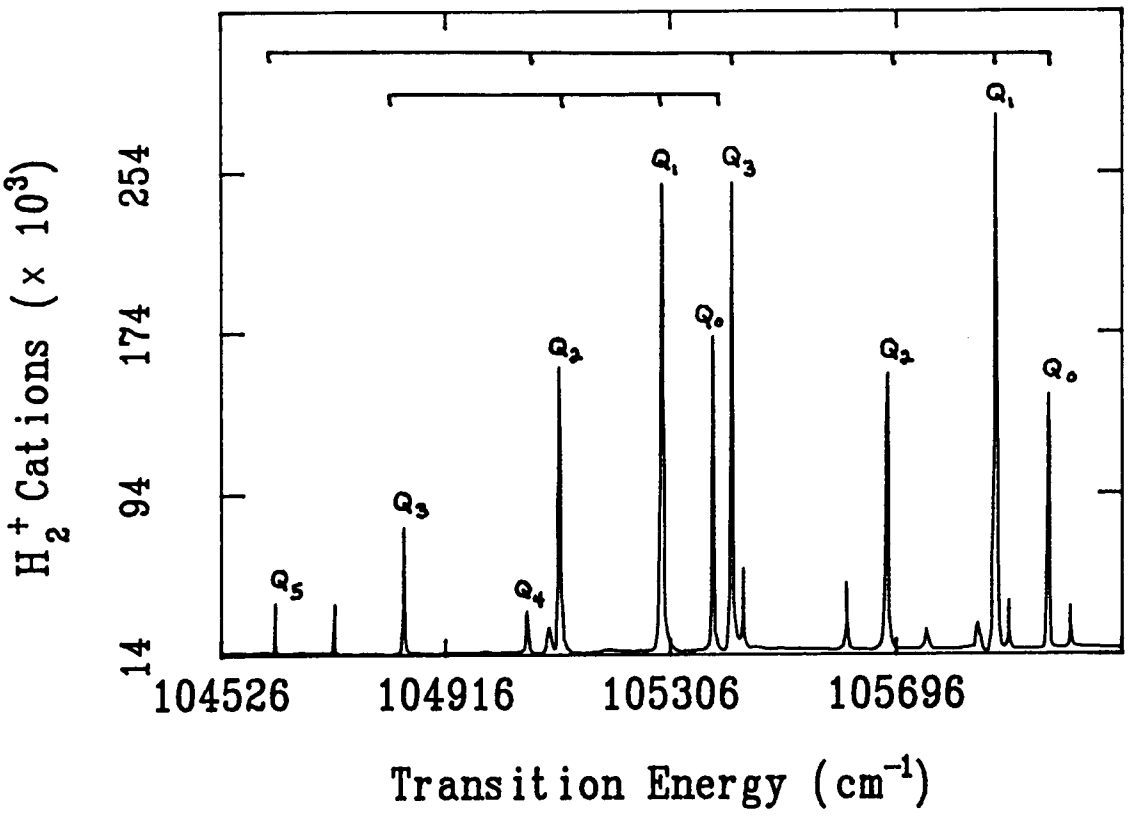

Figure 24. VUV-Visible Spectrum of Hydrogen,
$E, F\ ^1\Sigma_g^+(v' = 9, 10) \leftarrow X\ ^1\Sigma_g^+(v'' = 0)$.

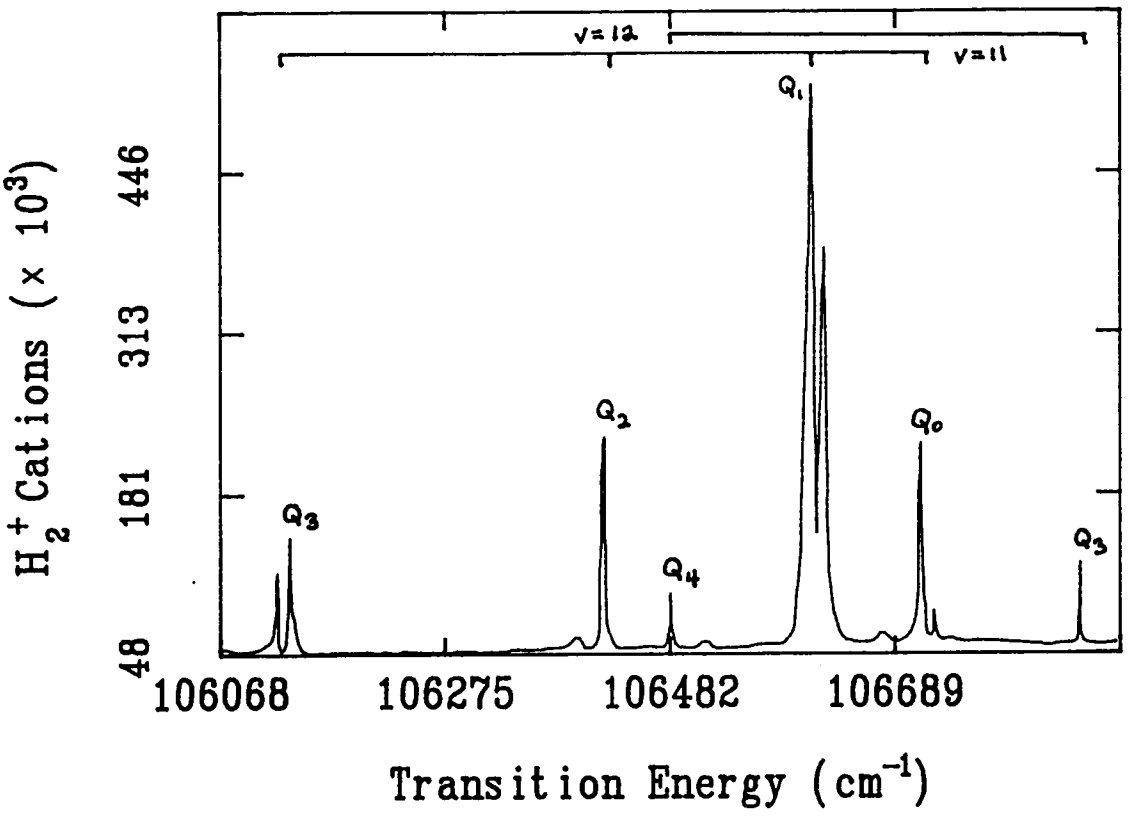

Figure 25. VUV-Visible Spectrum of Hydrogen,
$E, F\ ^1\Sigma_g^+(v' = 11, 12) \leftarrow X\ ^1\Sigma_g^+(v'' = 0)$.

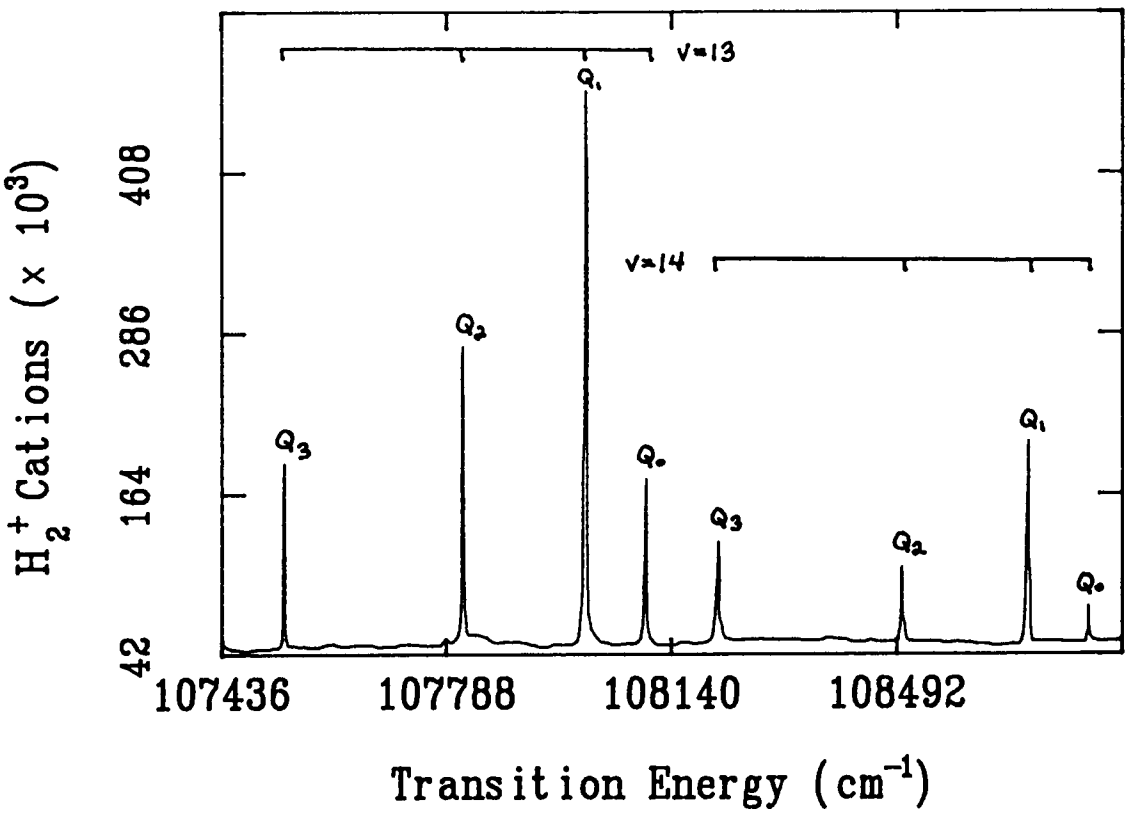

Figure 26. VUV-Visible Spectrum of Hydrogen,
$E, F\ ^1\Sigma_g^+(v' = 13, 14) \leftarrow X\ ^1\Sigma_g^+(v'' = 0)$.

only with *ungerade* states. The rotational-vibrational structure is clearly evident. For transitions from the ground state $X^1\Sigma_g^+$ to the $E,F\ ^1\Sigma_g^+$ state, $\Delta J = 0, \pm 2$.[49] So O,Q, and S branches are allowed with the Q-branches being the dominant feature.[50]

Before the two-photon rate constant could be calculated, the peak heights were corrected for the Boltzmann distribution of rotational states at room temperature. Also the ^{1}H atom had a nuclear spin of $I = \frac{1}{2}$. The total nuclear spin of the molecule was **T**=1,0. Each total nuclear spin state had a statistical weight 2**T**+1. Therefore the antisymmetric rotational levels occurred three times as frequently as the symmetric.[51] The result was the familiar alternation of peaks with a 3 to 1 ratio after the Boltzmann factor had been taken into account. The following equation was used to normalize the peak intensities.

$$N = (2\mathbf{T}+1)(2J''+1)N_0 \exp\left(\frac{-\epsilon(J'')}{kT}\right) \tag{38}$$

where

N = number of molecules in rotational state J''

[49]R. G. Bray and R. M. Hochstrasser, "Two-photon absorption by rotating diatomic molecules," Molecular Physics, Volume 31, Number 4, (1976), pp. 1199-1211.

[50]J. B. Halpern, H. Zacharias, and R. Wallenstein, "Rotational Line Strengths in Two- and Three-Photon Transitions in Diatomic Molecules," Journal of Molecular Spectroscopy, Volume 79, (1980), pp. 1-30.

[51]Gerhard Herzberg, Molecular Spectra and Molecular Structure, I. Spectra of Diatomic Molecules, (New York: Van Nostrand Reinhold Company, 1950), pp. 133-134.

$(2T+1) = 1$ for even J'', 3 for odd J''

N_0 = total number of hydrogen molecules

$\epsilon(J'')$ = energy of J''th rotational state

k = Boltzmann constant = 1.38066×10^{-23} J/K

T = temperature = 298 K

The peaks in each Q-branch were fitted to this distribution and then an average value was taken which was then used to calculate the two-photon rate constant for each vibrational level in the *E,F* state. The data are summarized in Table 5.

Table 5

Transition Energies and Two-Photon Rate Constants for H_2

Transition	Energy (cm^{-1})	K_2 (cm^4 s)
$E,F^1\Sigma_g^+, v' = 3 \leftarrow X^1\Sigma_g^+, v'' = 0$	101,486	2.7×10^{-49}
$E,F^1\Sigma_g^+, v' = 6 \leftarrow X^1\Sigma_g^+, v'' = 0$	103,554	3.1×10^{-49}
$E,F^1\Sigma_g^+, v' = 7 \leftarrow X^1\Sigma_g^+, v'' = 0$	103,833	1.6×10^{-49}
$E,F^1\Sigma_g^+, v' = 9 \leftarrow X^1\Sigma_g^+, v'' = 0$	105,377	4.2×10^{-49}
$E,F^1\Sigma_g^+, v' = 10 \leftarrow X^1\Sigma_g^+, v'' = 0$	105,960	4.1×10^{-49}
$E,F^1\Sigma_g^+, v' = 11 \leftarrow X^1\Sigma_g^+, v'' = 0$	106,709	1.0×10^{-48}
$E,F^1\Sigma_g^+, v' = 12 \leftarrow X^1\Sigma_g^+, v'' = 0$	107,421	6.1×10^{-49}
$E,F^1\Sigma_g^+, v' = 13 \leftarrow X^1\Sigma_g^+, v'' = 0$	108,096	1.3×10^{-48}
$E,F^1\Sigma_g^+, v' = 14 \leftarrow X^1\Sigma_g^+, v'' = 0$	108,790	5.1×10^{-49}

The values listed in the second column were the transitions energies of the Q_0 peaks. The $v' = 0$ peaks of the *E,F* state were not seen because the dye laser could not generate photons at that low an energy. The $v' = 1, 2, 4, 5$ peaks were not seen because they were in the outer minimum (the so called *F* well) of the double minima potential curve, as shown in Figure 27. The unfavorable Frank-

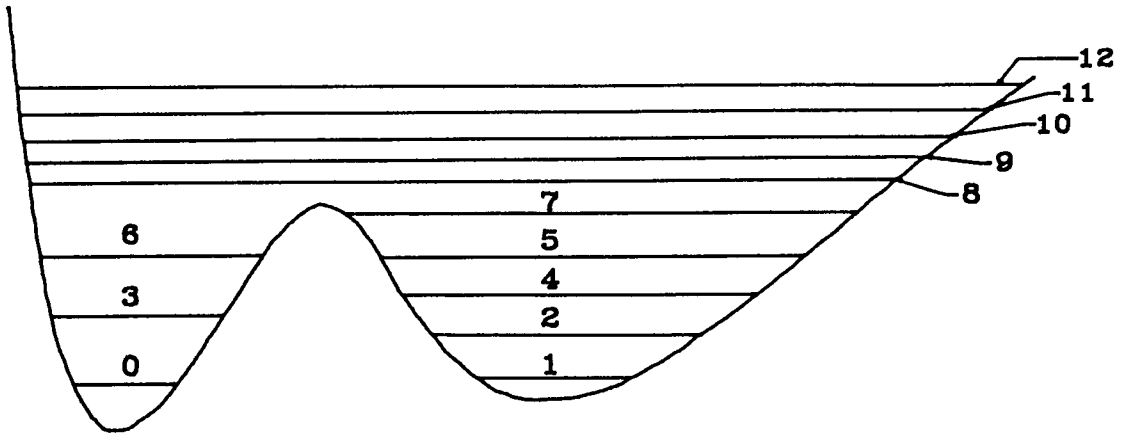

Figure 27. Vibrational Levels in the *E,F* State of Hydrogen.

Condon factors did not allow the observation of these vibrational levels. Quantum mechanical tunneling allowed transitions to the $v' = 7$ vibrational level.

Even averaging the Q peaks into one two-photon rate constant for each vibration yielded a fair amount of scatter in the data. The scatter was large enough to make these data not useful for the calculation of Franck-Condon factors or the determination of the *E,F* potential curve. The data did agree reasonably well with the two-photon absorption cross section given for the $Q_1(0,0)$ peak of 1.5×10^{-30} cm^4 W^{-1} (1.5×10^{-48} cm^4 s) in the literature,[52] though the data in Table 5 tends to be lower. The two photons used in each case were not the same, so that there may have been some enhancement due to an intermediate state as was suggested.[53]

[52]E. E. Marinero, C. T. Rettner, and R. N. Zare, "Quantum-State-Specific Detection of Molecular Hydrogen by Three-Photon Ionization," Physical Review Letters, Volume 48, Number 19, (10 May 1982), pp. 1323-1326.

[53]Ibid.

CHAPTER V

TWO-PHOTON SPECTROSCOPY OF NITRIC OXIDE AND RELATED WORK

A. Experimental Method

For two-photon spectroscopy to become more useful it must be applicable to molecules. Hydrogen was studied in a high pressure (~1 atmosphere) cell because the rotational spacing was large enough for a spectrum to be resolved. For other molecules this was not the case. The rotational spacing was much smaller and therefore the levels overlap with each other and many more levels became populated at room temperature. One solution to this problem was to use a supersonic jet expansion into a vacuum.

During the formation of a supersonic nozzle beam, a great deal of translational and internal relaxation occurs.[54] The dynamics of a supersonic jet can be quite complicated.[55] Ignoring shock waves, shear forces, heat sources, heat sinks, heat conductivity and assuming an isentropic expansion, the temperature in the beam

[54]Bruce D. Kay, T. D. Raymond, and J. K. Rice, "Time-of-flight characterization of pulsed supersonic helium free- jet expansions," Review of Scientific Instruments, Volume 57, Number 9, (September 1986), pp. 2266-2273.

[55]Ul'yan G. Pirumov and Gennadi S. Roslyakov, Gas Flow in Nozzles, (Heidelberg: Springer-Verlag, 1986).

is given by[56]

$$\frac{T}{T_0} = \frac{1}{1 + \frac{1}{2}(\gamma - 1) M^2} \tag{39}$$

where

γ = heat-capacity ratio, C_p/C_v

M = Mach number = $A(X/D)^{\gamma-1}$

A = constant which depends on γ

= 3.26 for a monoatomic gas

X = distance from the nozzle (cm)

D = nozzle diameter (cm)

There is a point downstream from the nozzle where density drops to a point where the two-body collision rate is insignificant. At this point, the terminal Mach number, M_T, for argon is given by[57]

$$M_T = 133 (P_0 D)^{0.4} \tag{40}$$

where

P_0 = pressure in the reservoir (atm)

An argon jet can be cooled to about 2 K.[58]

---

[56]Richard E. Smalley, Lennard Wharton, and Donald H. Levy, "Molecular Optical Spectroscopy with Supersonic Beams and Jets," Accounts of Chemical Research, Volume 10, Number 4 (4 April 1977), pp. 139-145.

[57]R. A. Oman, A. Bogan, C. H. Weiser, and C. H. Li, Research Department, Grumman Aircraft Engineering Co., Report RE-166, 1963.

[58]P. Andersen, M. Faubel, D. Haeusler, G. Kraft, H.-W. Luelf, and J. G. Skofronick, "Characteristics of a piezoelectric pulsed nozzle beam," Review of Scientific Instruments, Volume 56, Number 11, (November 1985), pp. 2038-2042.

When the molecules are seeded into the cooled beams, the molecule will be in the lowest electronic and vibrational level and, depending on the rotational spacing, only the lowest rotational levels will be occupied. This will make the spectra much easier to resolve and interpret.

Equation 12 can no longer be used because the species to be ionized is no longer homogeneously distributed. The number density of the species of interest is a function of x and ρ. The particle density as a function of position must be determined. The nozzle hole had a diameter of 0.1 mm. The beam divergence was 20°. A simple approach is taken to the particle density. It is assumed that all of the jet is completely enclosed by a spherical sector circumscribed by the 20° angle of divegence. Also it is assumed that the particle density is equal for any distance, r, from the nozzle. The number of particles emitted from the nozzle in one pulse is

$$N = N_0 A v t \tag{41}$$

where

N = number of particles per pulse

N_0 = particle density in the reservoir (cm^{-3})

A = area of nozzle hole = $\pi(0.01\ \mathrm{cm}/2)^2$

v = velocity of particles out of supersonic nozzle

$= \sqrt{3\gamma kT/m}$

γ = heat-capacity ratio, C_p/C_v

k = Boltzmann constant

T = temperature (K)

m = mass of particles (argon = 6.634×10^{-26} kg).

t = pulse duration (s)

The length, r, of the gas pulse from the nozzle is

$$r = vt. \tag{42}$$

The volume, V, of a spherical sector is

$$V = \frac{2}{3}\pi r^3 \sin\theta \tag{43}$$

where

r = length of the spherical sector (cm)

θ = half-angle of spherical sector (10°).

The number of particles with respect to time is

$$\frac{dN}{dt} = N_0 A v. \tag{44}$$

Making the substitution that $r = vt$, the volume of the spherical sector with respect to time is

$$\frac{dV}{dt} = 2\pi v^3 t^2 \sin\theta. \tag{45}$$

The density is just

$$D = \frac{dN/dt}{dV/dt} = \frac{N_0 A}{2\pi v^2 t^2 \sin\theta}. \tag{46}$$

Again using the substitution that $r = vt$ the density as a function of distance from the nozzle is

$$D = \frac{N_0 A}{2\pi r^2 \sin\theta} \tag{47}$$

Using Equation 44, the variation of the particle density can be examined over the detection region. The hole of the mass spectrometer is 0.38 cm and the center of the mass spectrometer is 3.18 cm away from the pulsed nozzle. The variation of particle density from the top of the mass spectrometer entrance hole to the bottom of the hole is 2.5%. Within the accuracy of this experiment, the particle density can be considered uniform in the region of the mass spectrometer entrance hole. An alternative solution to the problem would be to do a numerical integration of Equation 12. More complicated and realistic laser beam profiles and particle distributions could be employed in a numerical integration but with the experimental uncertainty the resultant two-photon rate constant would not be improved. So a homogeneous particle distribution will be assumed in the region of the mass spectrometer entrance hole with a value that results from being 3.18 cm away from the nozzle.

For the work with nitric oxide the ultraviolet laser beam was focused in front of the mass spectrometer. The dye laser beam was not focused at all. The same method that was used to derive Equation 34 is employed again. This results in the following expression for the two-photon rate constant

$$K_2 = \frac{\pi\tau N_I h\nu_{UV} h\nu_{VIS}\sqrt{ac}}{N\epsilon_{UV}\epsilon_{VIS}\Sigma F} \tag{48}$$

where

$$a = \frac{r_{0,UV}^2}{f_{UV}^2}$$

$$c = f_{UV}^2 + r_{VIS}^2$$

$$\Sigma F = \tan^{-1}\left(\frac{L}{2}\sqrt{\frac{a}{c}}\right) - \tan^{-1}\left(\frac{-L}{2}\sqrt{\frac{a}{c}}\right)$$

and $L = 0.38$ cm and all other variables have been previously defined.

The potential energy curves for nitric oxide are shown in Figure 28.[59] The observed transitions were from the ground $X^2\Pi_{1/2}$ state to the $A^2\Sigma^+$ and $C^2\Pi$ excited states. From the excited state, the molecule was ionized by the absorption of an additional ultraviolet photon. The $A^2\Sigma^+(\upsilon = 0, 1) \leftarrow X^2\Pi_{1/2}$ two-photon transitions were exclusively with visible photons from the dye laser. The remaining two-photon transitions were observed with a visible photon from the dye laser and a UV photon from the third harmonic of the Nd:YAG laser (355 nm). The hyperfine structure could not be resolved due to the bandwidth of the lasers. The ground state $X^2\Pi$ belonged to Hund's case (a) but went to case (b) with increasing rotation.[60] The upper states $A^2\Sigma^+$ and $C^2\Pi$ were almost pure Hund's case (b).

[59]Forrest R. Gilmore, "Potential Energy Curves for N_2, NO, O_2 and Corresponding Ions," Journal of Quantitative Spectroscopy & Radiative Transfer, Volume 5, (1965), pp. 369- 390.

[60]Gerhard Herzberg, op. cit. pp. 218-224.

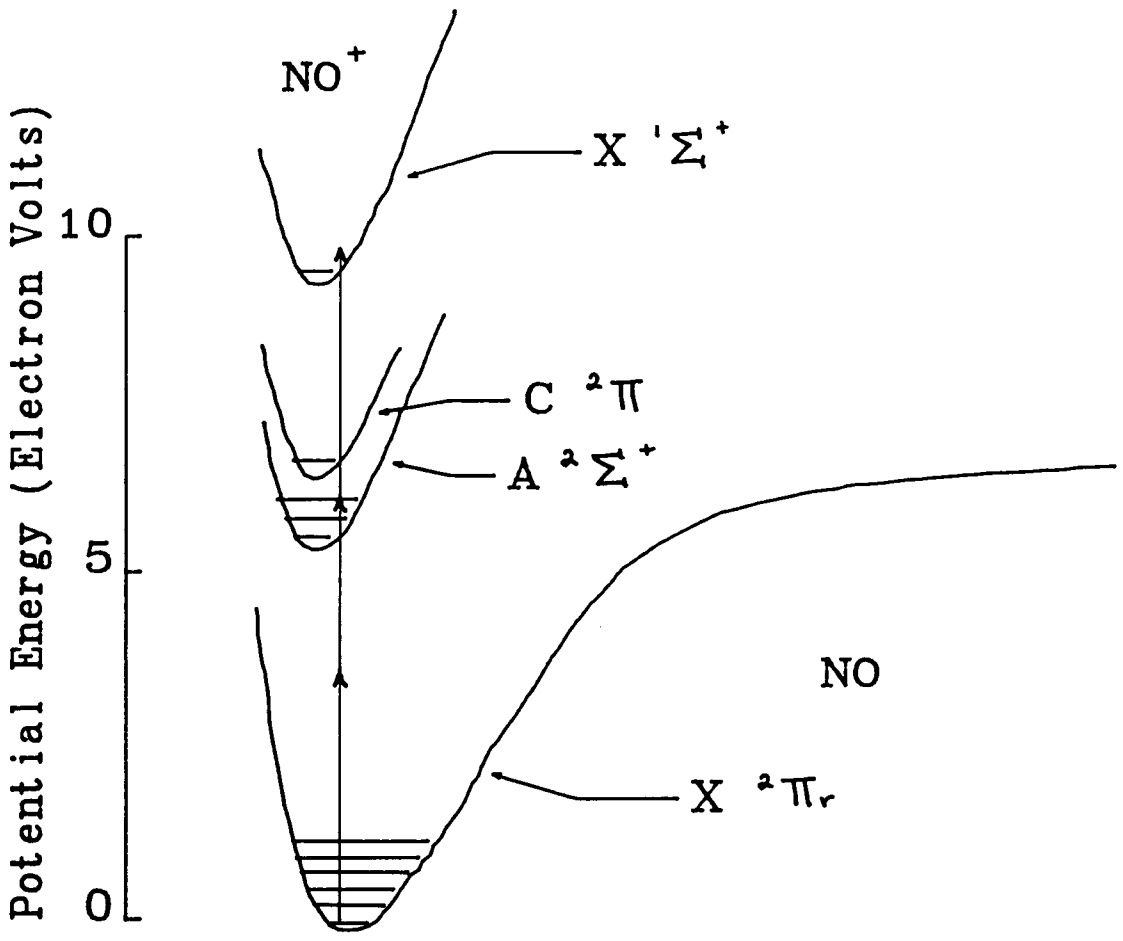

Figure 28. Potential Energy Diagram of Nitric Oxide.

The result was that the $A^2\Sigma^+ \leftarrow X^2\Pi$ tended to have weak Q transitons[61] while the $C^2\Pi \leftarrow X^2\Pi$ were dominated by Q transitions.[62]

B. Experimental Results

The NO spectra are shown in Figures 29-33. The peaks were identified using the literature.[63] [64,65] [66,67,68] Based on the peaks in Figure 30 that originated from the $J'' = \frac{1}{2}$ and the $J'' = \frac{3}{2}$ rotational levels, the rotational temperature was between 1 and 3 degrees Kelvin. The other spectra appeared to have comparable temperatures. When the laser fluence was too high, as in Figure 34, the peaks

---

[61] J. B. Halpern et. al. op. cit. pg. 11.

[62] Phillip A. Freedman, "The two photon absorption spectrum of NO $C^2\Pi(v = 0) \leftarrow X^2\Pi(v = 0)$," Canadian Journal of Physics, Volume 55, (1977), pp. 1387-1392.

[63] Ibid. pp. 1390-1391.

[64] Irén Deézsi, "A Recent Rotational Analysis of the γ Bands of the *NO* Molecule," Acta Physica, Volume 9, (1958), pp. 125-150.

[65] A. Lagerqvist and E. Miescher, "Absorptionsspektrum des NO-Moleküls Feinstruktur-Analyse der δ- and β-Banden und homogene Störung $C^2\Pi$–$B^2\Pi$," Helvetica Physica Acta, Volume 31, (1958), pp. 221-262.

[66] F. Ackermann and E. Miescher, "High Resolution Study of the $C^2\Pi$—$X^2\Pi$ Emission Bands of the NO Molecule," Journal of Molecular Spectroscopy, Volume 31, (1969), pp. 400-405.

[67] R. Engleman, Jr., P. E. Rouse, H. M. Peek, and V. D. Baiamonte, "Beta and Gamma Band Systems of Nitric Oxide," Los Alamos Scientific Laboratory Report LA-4364, (July 1970).

[68] E. Miescher and K. P. Huber, "Electronic Spectrum of the NO Molecule," International Review of Science, Physical Chemistry, Series Two, Volume I, edited by A. D. Buckingham, (Butterworth, London, 1975), pp. 37-73.

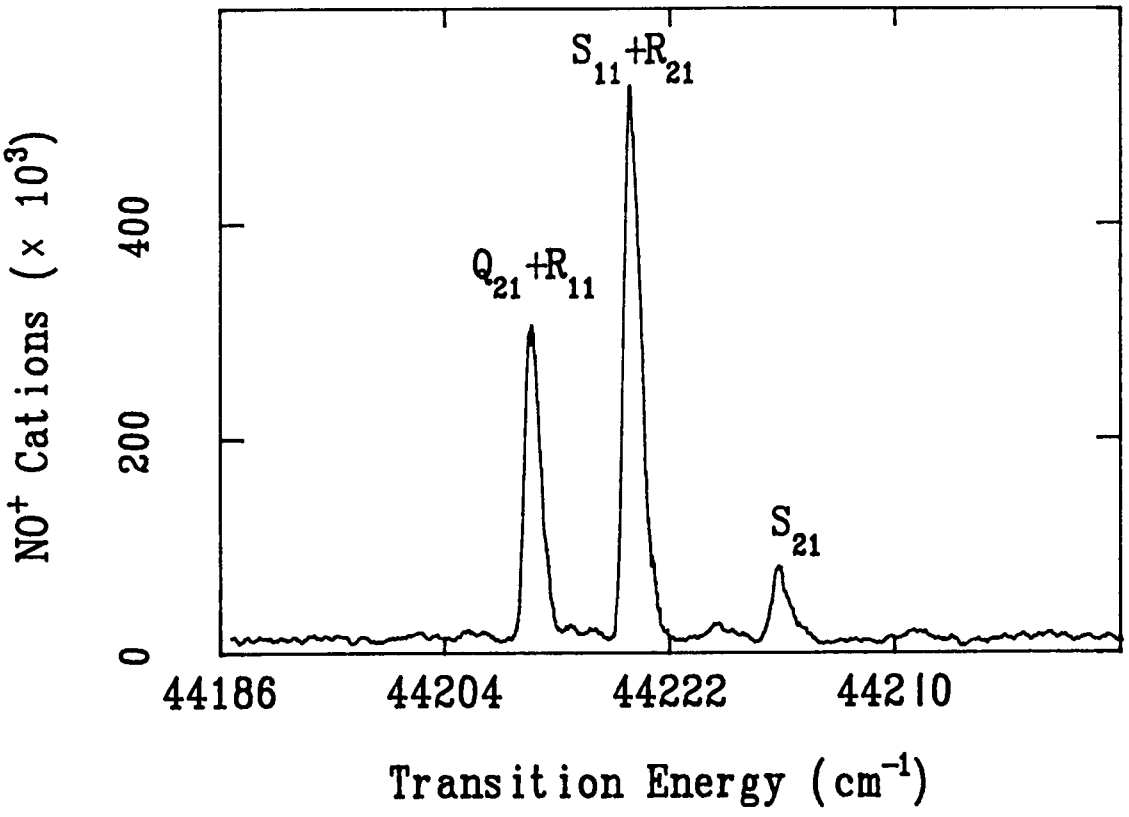

Figure 29. Two-Photon Spectrum of Nitric Oxide,
$A\ ^2\Sigma^+(v'=0) \leftarrow X\ ^2\Pi_{1/2}(v''=0)$.

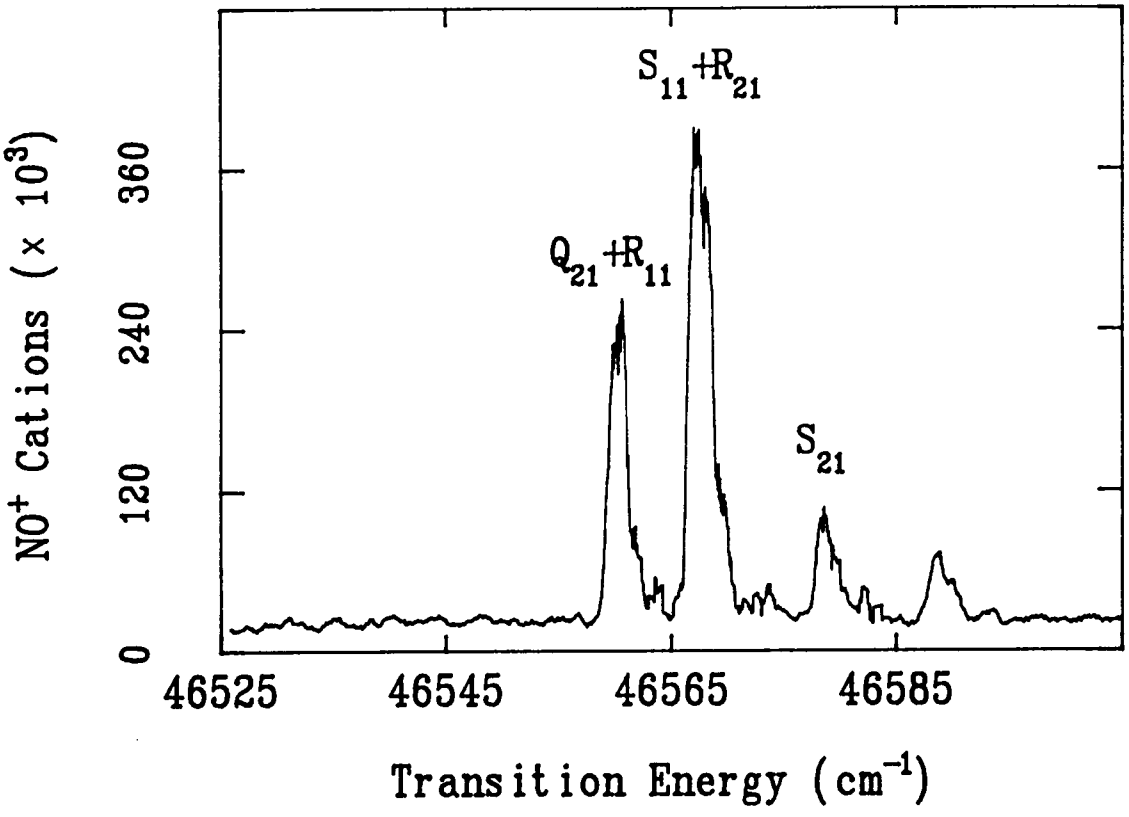

Figure 30. Two-Photon Spectrum of Nitric Oxide,
$A\ ^2\Sigma^+(v' = 1) \leftarrow X\ ^2\Pi_{1/2}(v'' = 0)$.

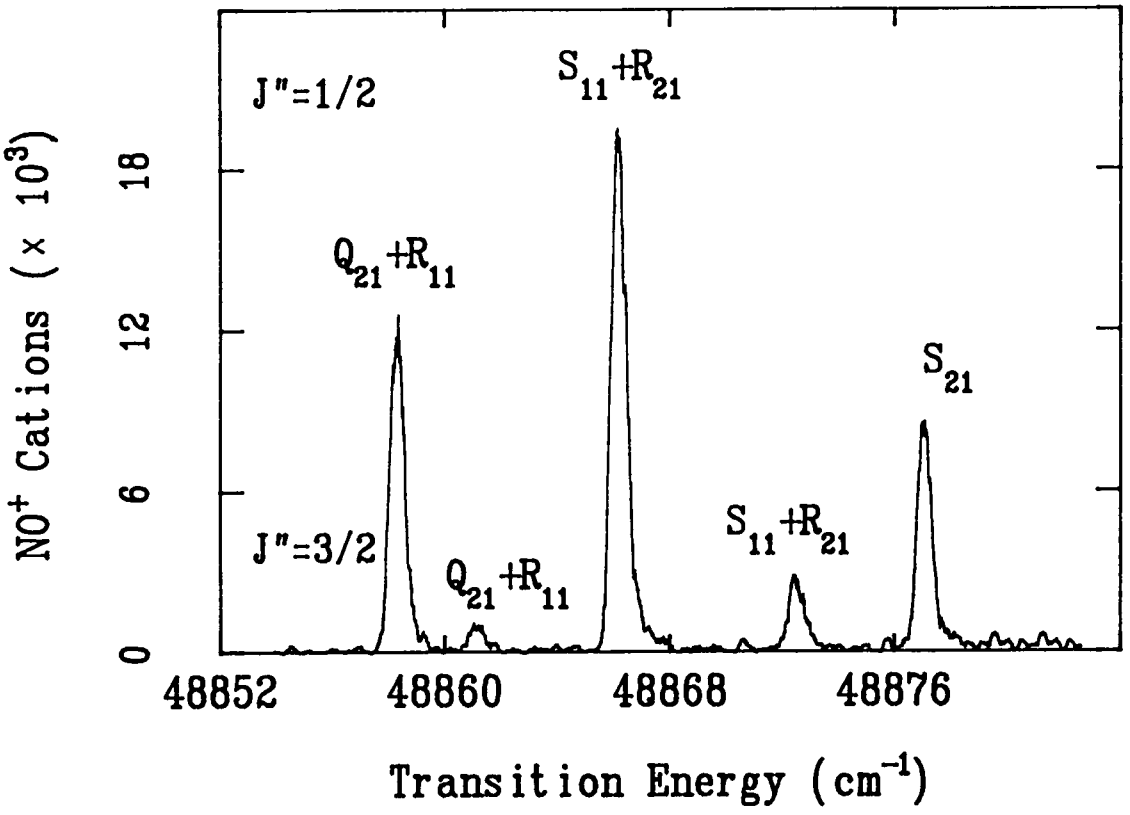

Figure 31. UV-Visible Spectrum of Nitric Oxide,
$A\ ^2\Sigma^+(v' = 2) \leftarrow X\ ^2\Pi_{1/2}(v'' = 0)$.

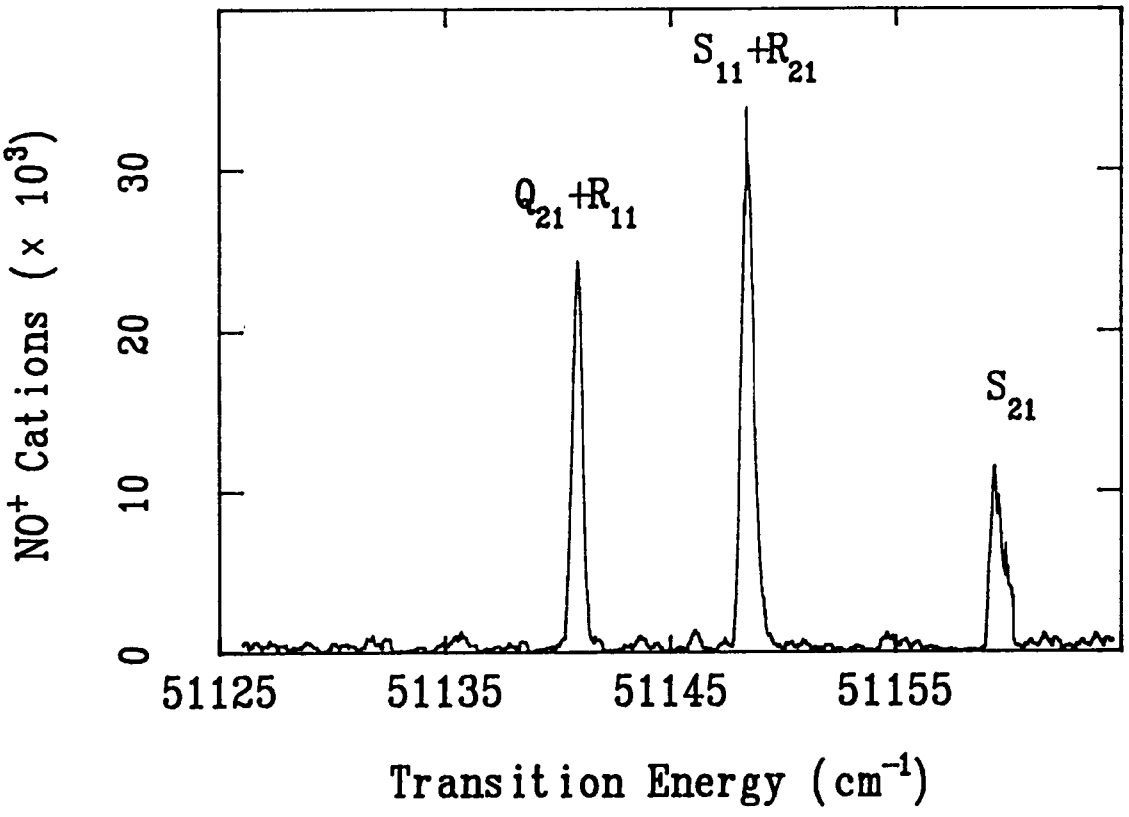

Figure 32. UV-Visible Spectrum of Nitric Oxide,
$A\ ^2\Sigma^+(v' = 3) \leftarrow X\ ^2\Pi_{1/2}(v'' = 0)$.

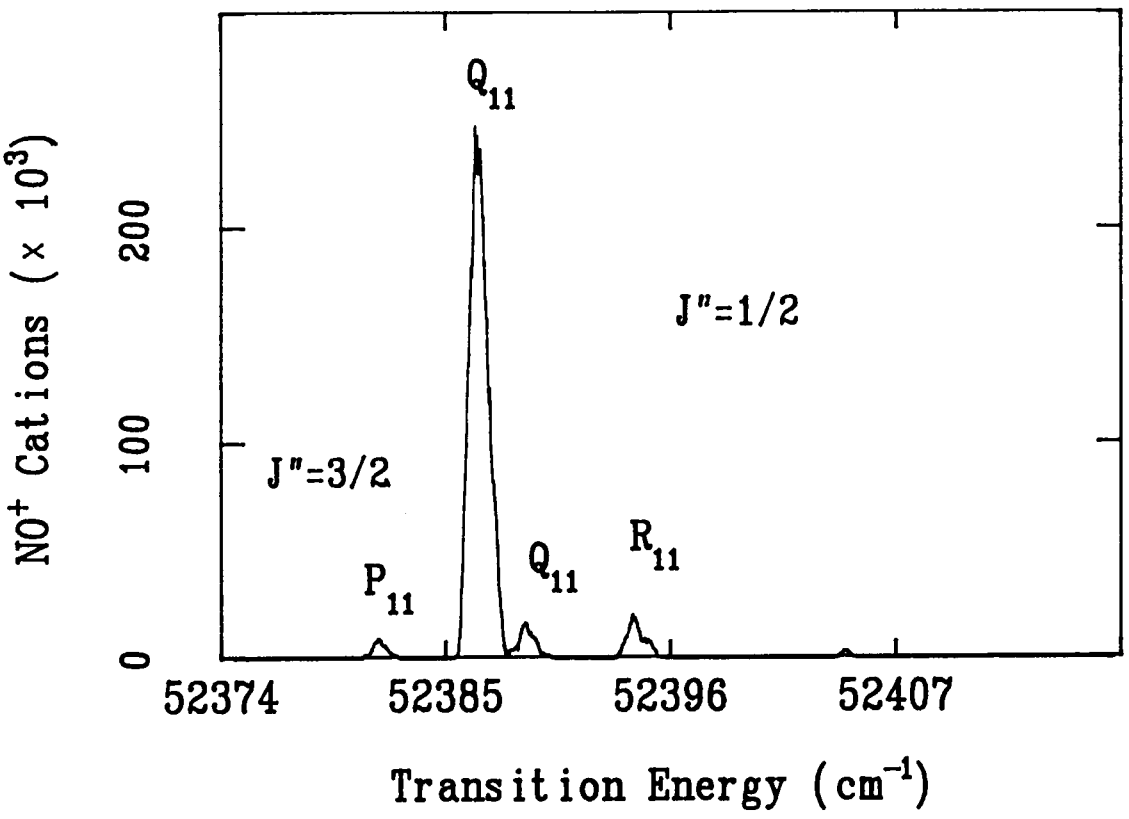

Figure 33. UV-Visible Spectrum of Nitric Oxide,
$C\ ^2\Pi^+(v' = 0) \leftarrow X\ ^2\Pi_{1/2}(v'' = 0)$.

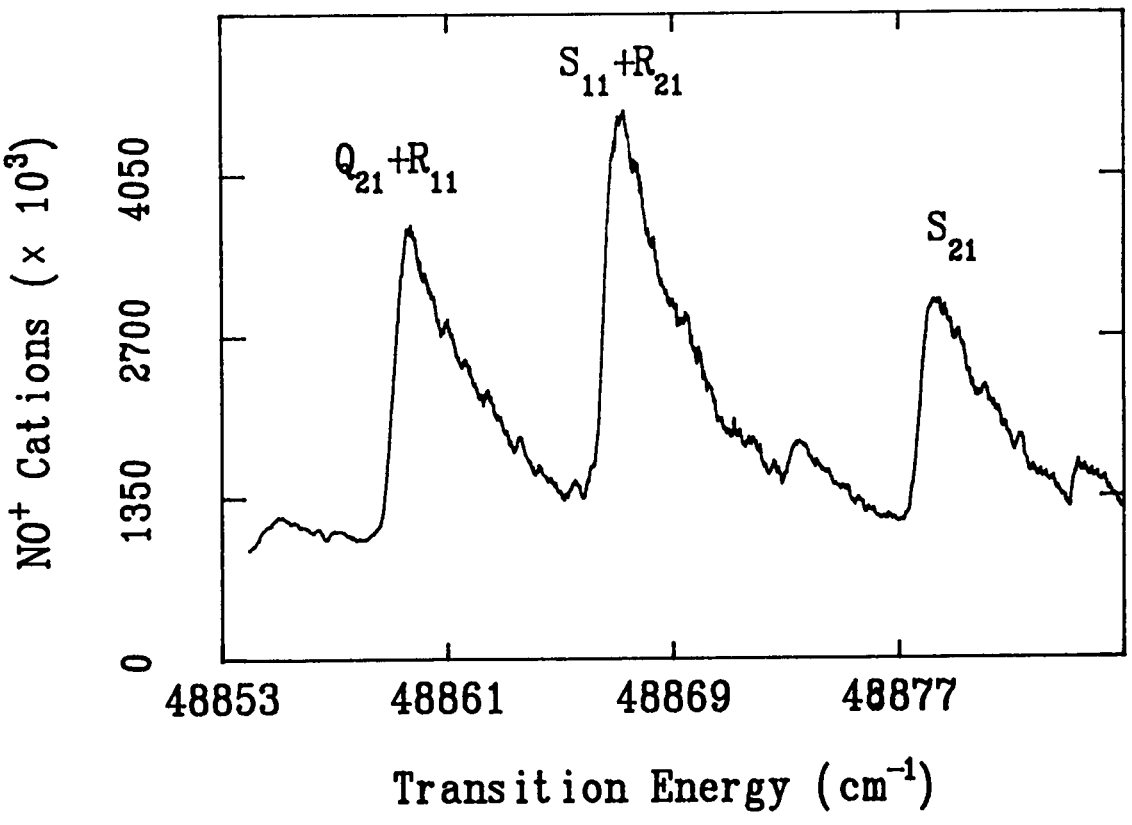

Figure 34. Asymmetrically Broadened Peaks in Nitric Oxide Spectrum, $A\ ^2\Sigma^+(v' = 2) \leftarrow X\ ^2\Pi_{1/2}(v'' = 0)$.

became asymmetrically broadened due to ac Stark shifts, power broadening, saturation effects and space charge problems as has been well documented.[69] In Figure 35, the signal was measured at various laser energies. This was done to find the appropriate energy for measuring the two-photon rate and to make certain that the signal was not saturated. In Figures 29 and 30, the excitation was done with two photons from the same focused dye laser beam. In Figures 31-33 the excitation was done with a tunable photon from an unfocused dye laser beam and a fixed wavelength photon from a beam of the third harmonic (355 nm) of the Nd:YAG laser that was focused with a 25 cm lens. The spectra in Figures 29 and 30 could not be produced using UV-visible excitation. Using only one color, the ionization scheme involves two photons for excitation and two photons for ionizing the excited molecule. Therefore it was a four-photon ionization scheme overall using the two lowest vibrational levels of the $A\ ^2\Sigma^+$ state as an intermediate resonant step. Since the four-photon ionization signal was comparable with the three-photon signal there must have been an accidental intermediate resonance between the $A\ ^2\Sigma^+$ state and the ionization continuum when one color was used. When two colors were used to ionize NO employing the same intermediate resonant step the process again involved four photons. Since the UV photons were present in much greater concentration than the visible photons, then the UV photons dominate the ioniza-

[69]R. Ernest Demaray, Charles Otis, Kenneth Aron, and Philip Johnson, "Laser enhanced collisional effects in the multiphoton ionization of molecules in supersonic expansions," Journal of Chemical Physics, Volume 72, Number 10, (15 May 1980), pp. 5772-5773.

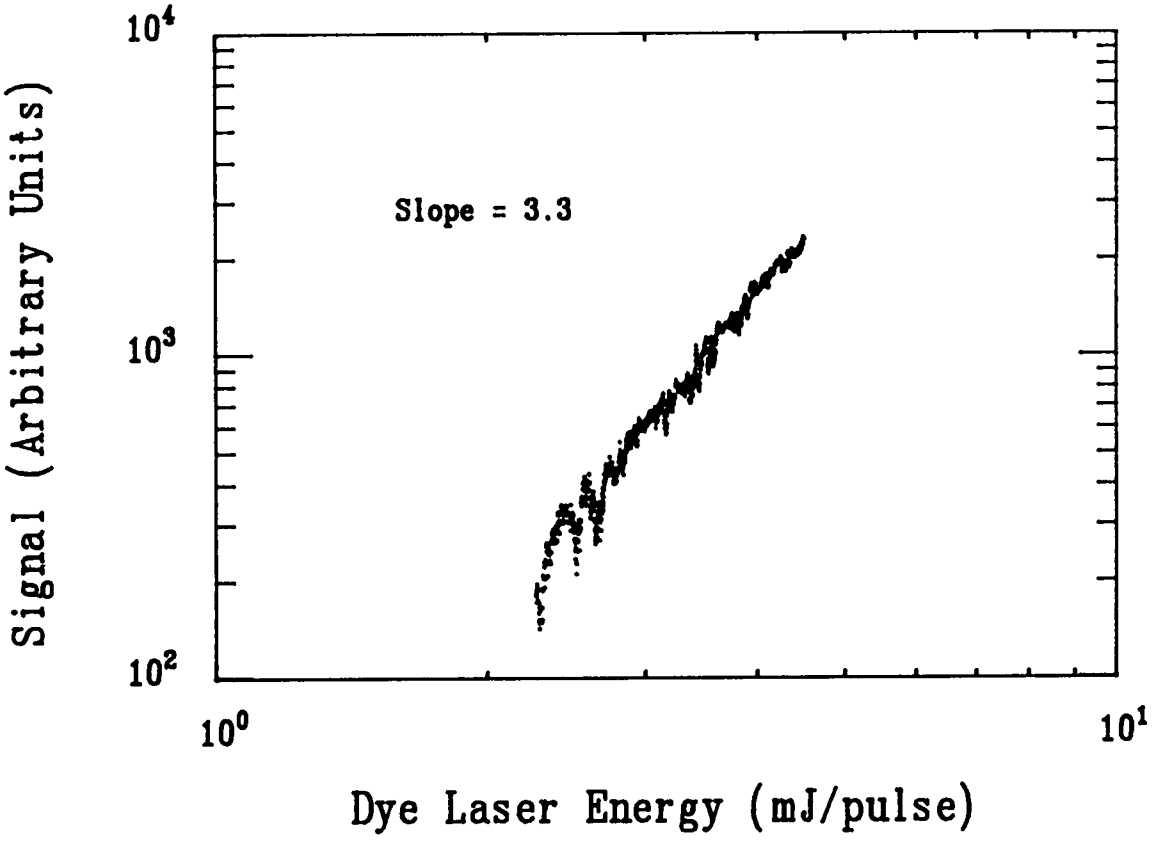

Figure 35. Four-Photon Ionization Signal versus Laser Energy in NO at 46568 cm^{-1}.

tion process. With the UV photons, there was not any intermediate resonance to enhance the ionization process. This would explain why the two-photon spectra to the $A^2\Sigma^+(v = 0, 1)$ were seen using only the dye laser but the spectra could not be observed when the UV laser was used in conjunction with the dye laser. When the resonant intermediate step was $v = 2$ of the $A^2\Sigma^+$ state or higher, then one UV photon was sufficient to ionize excited state nitric oxide. The overall ionization scheme in this case was a three-photon process. Equation 48 was used to tabulate the two-photon rate constants in Table 6. These two-photon rate constants for $A \leftarrow X$ transitions agree well with previous determinations, when the corresponding bandwidths are taken into account.[70,71]

Table 6

Transition Energies and Two-Photon Rate Constants for NO

Transition	Energy (cm^{-1})	K_2 (cm^4 s)
$A^2\Sigma^+, v' = 2 \leftarrow X^2\Pi_{1/2}, v'' = 0, J'' = \frac{1}{2}$		
$Q_{21}(J' = \frac{1}{2}), R_{11}(J' = \frac{3}{2})$	48,858	2.2×10^{-50}
$S_{11}(J' = \frac{5}{2}), R_{21}(J' = \frac{3}{2})$	48,866	3.6×10^{-50}
$S_{21}(J' = \frac{5}{2})$	48,877	1.4×10^{-50}
$A^2\Sigma^+, v' = 3 \leftarrow X^2\Pi_{1/2}, v'' = 0, J'' = \frac{1}{2}$		
$Q_{21}(J' = \frac{1}{2}), R_{11}(J' = \frac{3}{2})$	51,141	3.9×10^{-50}
$S_{11}(J' = \frac{5}{2}), R_{21}(J' = \frac{3}{2})$	51,148	5.5×10^{-50}
$S_{21}(J' = \frac{5}{2})$	51,160	1.9×10^{-50}
$C^2\Pi, v' = 0 \leftarrow X^2\Pi_{1/2}, v'' = 0, J'' = \frac{1}{2}$		
$Q_{11}(J' = \frac{1}{2})$	52,385	3.1×10^{-49}
$R_{11}(J' = \frac{3}{2})$	52,393	2.3×10^{-50}

[70]K. P. Gross and R. L. McKenzie, "The two-photon absorptivity of rotational transitions in the $A\ ^2\Sigma^+(v' = 0) - -X\ ^2\Pi(v'' = 0)$ gamma band of nitric oxide," Journal of Chemical Physics, Volume 76, Number 11, (1 June 1982), pp. 5260-5266.

[71]J. Burris, T. J. McGee and T. J. McIlrath, "A Two-Photon Absorption Cross Section Measurement in Nitric Oxide," Chemical Physics Letters, Volume 101, Number 6, (4 November 1983), pp. 588-592.

C. The van der Waals Molecule, ArNO

Spectra were obtained for the van der Waals molecule, ArNO. The electronic states of NO were only slightly perturbed (1%) by the van der Waals interaction with Ar.[72] So it was convenient to describe the ArNO molecule in terms of the NO molecule. The only accessible transitions were those in the region of $\mathrm{ArNO}(C^2\Pi, v' = 0) \leftarrow \mathrm{ArNO}(X^2\Pi_{1/2}, v'' = 0)$.[73] There were four Ar–NO vibrations observed as seen in Figure 36.

It was hoped that the two-photon rate constant could be measured for a van der Waals molecule. The trouble was measuring how many van der Waals molecules were produced in the supersonic nozzle jet expansion. Van der Waals molecules were very weakly bound and many techniques that were used to measure the number of van der Waals molecules dissociate the molecule. It was very difficult to measure the amount of dissociation since the dissociation products were already present in large concentrations. Measurement of the ArNO/NO ratio using the electron impact ionizer of a quadrapole mass spectrometer indicated a ratio of 0.32%. Using the lasers to ionize the molecules gave an ArNO/NO ratio of 0.01%. There was no way of knowing which if either method was correct. Without the initial ArNO number density the two-photon rate constant could not be measured.

---

[72]B. J. Howard, C. M. Western and P. D. Mills, "Van der Waals Molecules," Faraday Discussions of the Chemical Society, Number 73, (1982), pp. 129-130.

[73]John C. Miller and Wu-Chieh Cheng, "Multiphoton Ionization of NO-Rare Gas van der Waals Species," The Journal of Physical Chemistry, Volume 89, Number 9, (1985), pp. 1647-1653

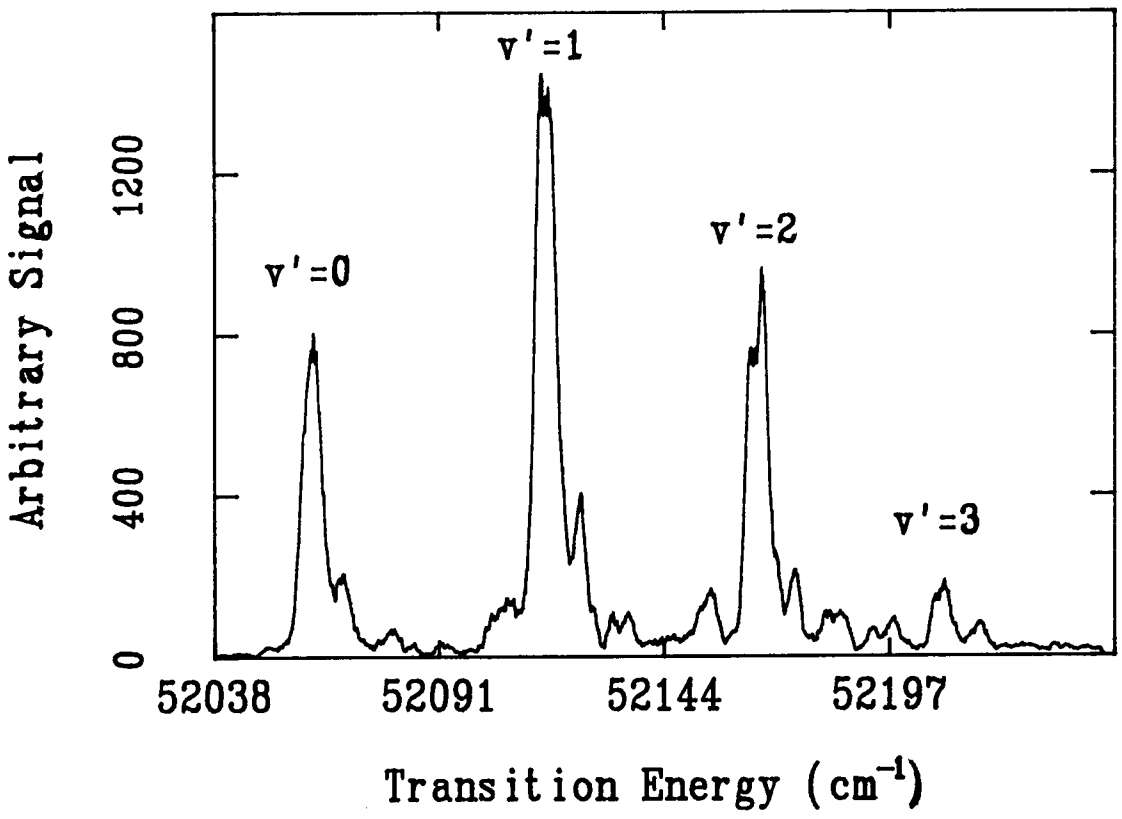

Figure 36. UV-Visible Spectrum of ArNO,
$C\ ^2\Pi^+(v = 0, 1, 2, 3) \leftarrow X\ ^2\Pi_{1/2}(v'' = 0)$.

A slower scan of the Ar–NO $v = 1$ peak, as shown in Figure 37, revealed some structure. Splitting has been observed in the ArNO peaks,[74] but the cause of the splitting was not clear. The splitting between peaks in Figure 37 was ~ 0.8 cm^{-1}. This was nearly equivalent to the bandwidth of the lasers. So the spectrum may be a convolution of some finer structure which was not revealed by the broadband lasers that were used. The splitting could be indicative of some rotational structure. Using an Ar–NO bond length of 3.65 Å,[75] the rotational constant could be calculated. The rotational constant was ~ 0.07 cm^{-1}. This value agrees with the rotational constant that was found by scattering experiments.[76] This was smaller than the bandwidth of the lasers and the rotational structure should not be revealed in the spectrum of Figure 37. There has been some explanation on this splitting.[77]

---

[74]Kenji Sato, Yohji Achiba, and Katsumi Kimura, "The Ar-NO van der Waals complex studied by resonant multiphoton ionization spectroscopy involving photoion and photoelectron measurements," The Journal of Chemical Physics, Volume 81, Number 1, (1 July 1984), pp. 57-62.

[75]H. H. W. Thuis, S. Stolte, J. Reuss, J. J. H. Van den Biesen, and C. J. N. Van den Meijdenberg, "Angle Dependent Interaction Potentials for NO-Ar, NO-Kr and NO-Xe Derived from Various Total Collision Cross Section Data," Chemical Physics, Volume 52, (1980), pp. 211-225.

[76]P. Casavecchia, A. Lagana and G. G. Volpi, "Anisotropic Intermolecular Potentials for NO-Ar and NO-Kr from Total Differential Cross Section Measurements," Chemical Physics Letters, Volume 112, Number 5, (21 December 1984), pp. 445-451.

[77]John C. Miller and Wu-Chieh Cheng, op. cit. pg. 1651.

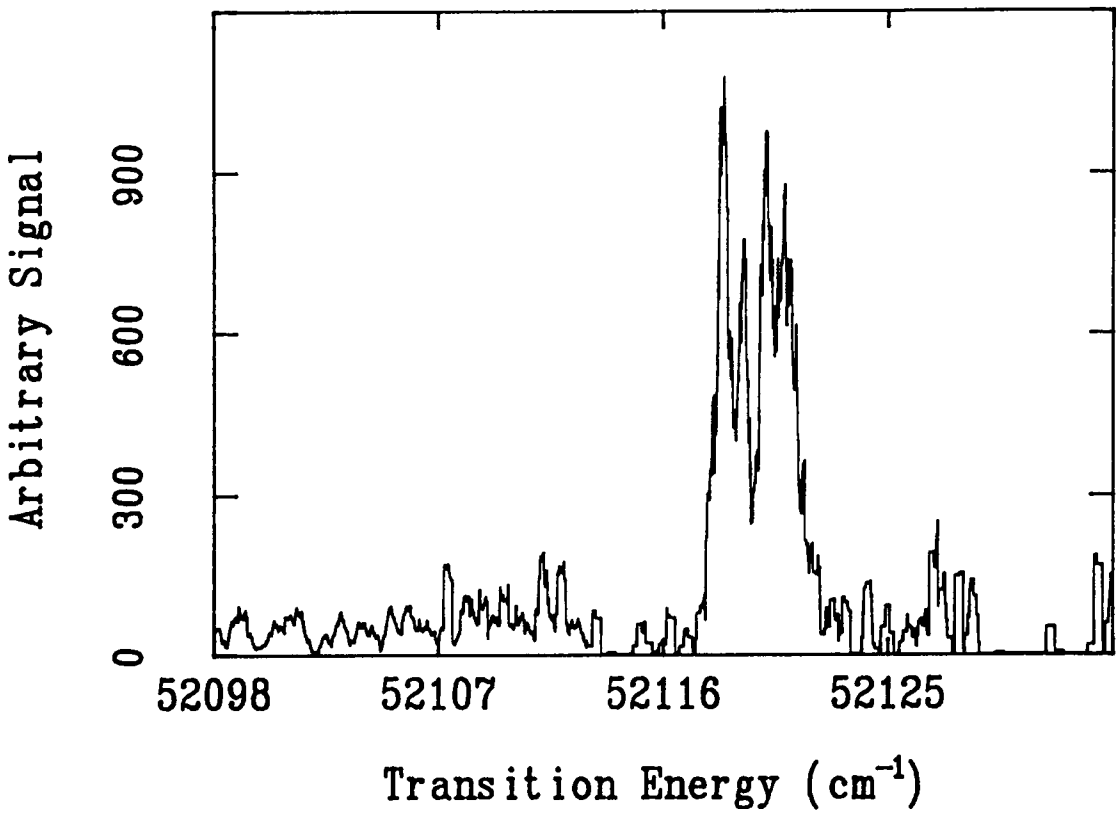

Figure 37. UV-Visible Spectrum of ArNO,
$C\ ^2\Pi^+(v=1) \leftarrow X\ ^2\Pi_{1/2}(v''=0)$.

CHAPTER VI

CONCLUSION

A. Usefullness of Two-Photon Spectroscopy

Two-photon absorption is the simplest nonlinear spectroscopic technique. There are already many uses and applications of two-photon spectroscopy.[78] The future looks bright for new uses and applications of two-photon spectroscopy.

This work demonstrated two-photon spectroscopy of atoms and molecules and also showed that these measurements can be quantitative. This is important for future applications. Those who are interested in using two-photon spectroscopy will need quantitative information in order to determine if the two-photon signal will be useful for them. Some more fundamental information can be gathered once the two-photon rate constant is known, such as the ionization rate from the various two-photon allowed excited states. Two-photon spectroscopy can also be done on minority components such as van der Waals molecules.

There were some difficulties with this method. Signal fluctuations were greater than with one photon spectroscopy, as was evident in the hydrogen data. Also the

[78]M. P. McCann, C. H. Chen and M. G. Payne, "Vacuum Ultraviolet Generation and Use in Two-Photon Resonance Spectroscopy," Chemical Physics Letters, Volume 138, Number 2,3 (17 July 1987), pp. 250-256.

calculations which were used to produce the two-photon rate constants assumed several conditions which may not have been valid. A Gaussian beam profile was assumed. This most certainly was not true but this assumption yielded reasonable results and made the calculations much easier. It was assumed that the ionization step was saturated. This was true in most cases but was not true for the NO spectra in Figures 29 and 30. Perfect overlap of the two beams was assumed. The laser beams were aligned very carefully and overlapped over a long distance. The overlap could also be optimized by moving the beams and observing the signal but neither of these techniques guarantees the overlap that was assumed in the calculation. If the overlap was not ideal then the two-photon rate constants would be lower than expected.

B. Future Improvements and Directions

There are some exciting future applications of two-photon spectroscopy. Some of the more obvious are as follows. The wavelength tuning range could be extended. This could be done with a system of doubling and mixing crystals. This would broaden the range of two-photon transitions that could be examined. The laser bandwidth could be narrowed. With narrower bandwidths, additional rotational structure or even hyperfine structure could be resolved. The peaks listed in Table 6 could be distinguished from each other. A laser that produces a Gaussian beam would tend to have fewer intensity fluctuations in the beam and would be more

accurately described in the calculation. A diode pumped Nd:YAG laser would have a more easily characterized beam.

A container could be installed which would introduce liquid vapor into the pulsed nozzle. Larger molecules could be examined in this way, such as benzene. It is also hoped that some filaments could be used close the pulsed nozzle. The filaments could then be used to bombard the supersonic jet with electrons. This electron bombardment would induce the production of various excited and radical species. A lot of interesting information could come out of those studies.

Finally some word on the quantity that was measured. A better quantity could be found that would reflect an atom's or molecule's response to a two-photon absorption. The two-photon rate constant (or the two-photon absorption cross section) are a function of the laser bandwidth. So for the two-photon rate constants to be useful quantities, the spectral bandwidth of the lasers that are used to obtain them must be known. The two-photon Rabi rate is not a function of the spectral bandwidth of the lasers but it is a function of the laser intensity. So for the two-photon Rabi rate to be used, the intensity of the two lasers must be known. The simplest solution would be to use something such as M_2 as defined in Equation 15. This would add an additional step to the calculation of the signal magnitude from the above quantity but this quantity would be more universal since it is not dependent on the bandwidth of the laser that is used to measure it.

REFERENCES

REFERENCES

Yohji Achiba, Kenji Sato, and Katsumi Kimura, "Multiphoton ionization photoelectron spectroscopic study on NO: Autoionization pathway through dissociative superexcited valence states," The Journal of Chemical Physics, Volume 82, Number 9, (1 May 1985), pp.3959-3967.

F. Ackermann and E. Miescher, "Spin-Orbit Coupling in Molecular Rydberg States of the Nitric Oxide Molecule," Chemical Physics Letters, Volume 2, Number 6, (October 1968), pp. 351-352.

G. S. Agarwal and Surya P. Tewari, "Theory of four-photon resonant vacuum-ultraviolet generation with reabsorption via resonant two-photon process," Journal of the Optical Society of America, B, Volume 2, Number 9, (September 1985), pp. 1409-1416.

Scott L. Anderson, Glenn D. Kubiak and Richard N. Zare, "Resonant-Enhanced Multiphoton Ionization of Molecular Hydrogen via the $E, F^1\Sigma_g^+$ State: Photoelectron Energy and Angular Distributions," Chemical Physics Letters, Volume 105, Number 1, (2 March 1984), pp. 22-27.

Yoshikazu Anezaki, Takayuki Ebata, Naohiko Mikami and Mitsuo Ito, "Two-Color Multiphoton Ionization and Fluorescence Dip Spectra of NO in a Supersonic Free Jet. Highly Excited ns, np, nf Rydberg States," Chemical Physics, Volume 97, (1985), pp. 153-163.

M. A. Baig and J. P. Connerade, "New high-resolution photoabsorption study of the Lyman bands of H_2," Journal of Physics B: Atomic and Molecular Physics, Volume 18, (1985), pp. L809-L813.

R. F. Barrow and E. Miescher, "Fine Structure Analysis of NO Absorption Bands in the Schumann Region," Proceedings of the Physical Society, Volume 70, Section A, (1957), pp. 219-222.

William K. Bischel, Jeffrey Bokor, Daniel J. Klinger, and Charles K. Rhodes, "Nonlinear Optical Processes in Atoms and Molecules Using Rare-Gas Halide Lasers," IEEE Journal of Quantum Electronics, Volume QE-15, Number 5, (May 1979), pp. 380-392.

N. Bjerre, R. Kachru, and H. Helm, "Three-photon double-resonance spectroscopy of autoionizing Rydberg states in H_2," Physical Review A, Volume 31, Number 2, (February 1985), pp. 1206-1208.

J. Bokor, R. R. Freeman, R. L. Panock, and J. C. White, "Generation of high-brightness coherent radiation in the vacuum ultraviolet by four-wave parametric oscillation in mercury vapor," Optics Letters, Volume 6, Number 4, (April 1981), pp. 182-184.

Keith D. Bonin, T. J. McIlrath, and Kouichi Yoshino, "High-resolution laser and classical spectroscopy of xenon autoionization," Journal of the Optical Society of America, B, Volume 2, Number 8, (August 1985), pp. 1275-1283.

J. H. M. Bonnie, P. J. Eenshuistra, J. Los and H. J. Hopman, "Influence of the Vibrational Quantum Number of the Resonant State in Resonant Multiphoton Ionization/Dissociation of Hydrogen Molecules," Chemical Physics Letters, Volume 125, Number 1, (21 March 1986), pp. 27-32.

R. G. Bray, R. M. Hochstrasser and J. E. Wessel, "Continuously Tunable Two-Photon Excitation of Individual Rotational Levels of the $A^2\Sigma^+$ State of Nitric Oxide," Chemical Physics Letters, Volume 27, Number 2, (15 July 1974), pp. 167-171.

R. G. Bray, Robin M. Hochstrasser and H. N. Sung, "Two-Photon Excitation Spectra of Molecular Gases: New Results for Benzene and Nitric Oxide," Chemical Physics Letters, Volume 33, Number 1, (15 May 1975), pp. 1-4.

J. Burris and T. J. McIlrath, "Experimental methods for the determination of two-photon cross sections using four-wave mixing," Journal of the Optical Society of America, B, Volume 2, Number 8, (August 1985), pp. 1307-1312.

J. Burris and T. J. McIlrath, "Theoretical study relating the two-photon absorption cross section to the susceptibility controlling four-wave mixing,"Journal of the Optical Society of America, B, Volume 2, Number 8, (August 1985), pp. 1313-1317.

David W. Chandler and L. R. Thorne, "Measured radiative lifetimes for H_2 and HD in the $E, F^1\Sigma_g^+$ electronic state," The Journal of Chemical Physics, Volume 85, Number 4, (15 August 1986), pp. 1733-1737.

G. R. Cook and P. H. Metzger, "Photoionization and Absorption Cross Sections of H_2 and D_2 in the Vacuum Ultraviolet Region," Journal of the Optical Society of America, Volume 54, Number 8, (August 1964), pp. 968-972.

C. Cornaggia, J. Morellec and D. Normand, "Resonant multiphoton ionisation-dissociation of H_2," Journal of Physics B: Atomic and Molecular Physics, Volume 18, (1985), pp. L501-L506.

C. Cornaggia, D. Normant, J. Morellec, G. Mainfray, and C. Manus, "Resonant multiphoton ionization of H_2 via the $E, F^1\Sigma_g^+$ state: Absorption of photons in the ionization continuum," Physical Review A, Volume 34, Number 1, (July 1986), pp. 207-215.

Jon B. Cross and James J. Valentini, "High repetition rate pulsed nozzle beam source," Review of Scientific Instruments, Volume 53, Number 1, (January 1982), pp. 38-42.

H. M. Crosswhite, The Hydrogen Molecule Wavelength Tables of Gerhard Heinrich Dieke, (New York: Wiley-Inerscience, 1972), pp. E1-E13.

I. Dabrowski, "The Lyman and Werner bands of H_2," Canadian Journal of Physics, Volume 62, (1984), pp. 1639-1664.

H. Egger, R. T. Hawkins, J. Bokor, H. Pummer, M. Rothschild, and C. K. Rhodes, "Generation of high-spectral-brightness tunable XUV radiation at 83 nm," Optics Letters, Volume 5, Number 7, (July 1980), pp. 282-284.

R. Engleman, Jr., and P. Rouse, "The β and γ Bands of Nitric Oxide Observed During the Flash Photolysis of Nitrosyl Chloride," Journal of Molecular Spectroscopy, Volume 37, (1971), pp. 240-251.

E. E. Eyler and F. M. Pipkin, "Observation of the $4s^3\Sigma_g^+$ state of H_2," The Journal of Chemical Physics, Volume 77, Number 11, (1 December 1982), pp. 5315-5318.

R. Gallusser and K. Dressler, "Multistate vibronic coupling between the excited $^2\Pi$ states of the NO molecule," The Journal of Chemical Physics, Volume 76, Number 9, (1 May 1982), pp. 4311-4327.

W. R. Garrett, W. R. Ferrell, M. G. Payne, and John C. Miller, "Influence of third-harmonic fields on multiphoton ionization of noble gases in unfocused laser beams," Physical Review A, Volume 34, Number 2, (August 1986), pp. 1165-1177.

L. Gerö and R. Schmid, "Dissociation Energy of the NO Molecule," Proceedings of the Physical Society, Volume 60, Part 6, Number 342, (1 June 1948), pp. 533-540.

G. Herzberg and L. L. Howe, "The Lyman Bands of Molecular Hydrogen," Canadian Journal of Physics, Volume 37, (1959), pp. 636-659.

R. Hilbig, G. Hilber, A. Timmermann, and R. Wallenstein, "Generation of Coherent Tunable VUV Radiation," Laser Spectroscopy VI: Proceedings of the Sixth International Conference, Interlaken, Switzerland, June 27-July 1, 1983, Editors H. P. Weber and W. Luthy, (Berlin; New York: Springer-Verlag, 1983), pp. 387-391.

R. Hilbig, A. Lago and R. Wallenstein, "Tunable XUV Radiation Generated by Nonresonant Frequency Tripling in Neon," Optics Communications, Volume 49, Number 4, (15 March 1984), pp. 297-301.

R. Hilbig and R. Wallenstein, "Enhanced Production of Tunable VUV Radiation by Phase-Matched Frequency Tripling in Krypton and Xenon," IEEE Journal of Quantum Electronics, Volume QE-17, Number 8, (August 1981), pp. 1566-1573.

R. Hilbig and R. Wallenstein, "Narrowband tunable VUV radiation generated by nonresonant sum- and difference-frequency mixing in xenon and krypton," Applied Optics, Volume 21, Number 5, (1 March 1982), pp. 913-917.

R. Hilbig and R. Wallenstein, "Resonant Sum and Difference Frequency Mixing in Hg," IEEE Journal of Quantum Electronics, Volume QE-19, Number 12, (December 1983), pp. 1759-1770.

Robin M. Hochstrasser, G. R. Meredith and H. P. Trommsdorff, "Two-Photon Spectra of Gases by Three-Wave Mixing," Chemical Physics Letters, Volume 53, Number 3, (1 February 1978), pp. 423-428.

D. C. Jacobs, R. J. Madix, and R. N. Zare, "Reduction of 1+1 resonance enhanced MPI spectra to population distributions: Application to the NO $A^2\Sigma^+$–$X^2\Pi$ System," The Journal of Chemical Physics, Volume 85, Number 10, (15 November 1986), pp. 5469-5479

Ch. Jungen and O. Atabek, "Rovibronic interactions in the photoabsorption spectrum of molecular hydrogen and deuterium: An application of multichannel quantum defect methods," The Journal of Chemical Physics, Volume 66, Number 12, (15 June 1977), pp. 5584-5609.

Danield J. Kligler and Charles K. Rhoades, "Observation of Two-Photon Excitation of the H_2 $E, F^1\Sigma_g^+$ State," Physical Review Letters, Volume 40, Number 5, (30 January 1978), pp. 309-313.

A. Lagerqvist and E. Miescher, "Absorption Spectrum of the NO Molecule, II. New Fine-Structure Analysis Below 1600 Å," Canadian Journal of Physics, Volume 40, (1962), pp. 352-357.

A. Lagerqvist and E. Miescher, "Absorption Spectrum of the NO Molecule, VI. Band Structures Below 1600 Å, Rydberg States $C^2\Pi, D^2\Sigma^+, K^2\Pi, M^2\Sigma^+$, $S^2\Sigma^+$, Non-Rydberg States $B^2\Pi, L^2\Pi$ and their Interactions," Canadian Journal of Physics, Volume 44, (1966), pp. 1525-1539.

David M. Lubman and Russ M. Jordan, "Design for improved resolution in a time-of-flight mass spectrometer using a supersonic beam and laser ionization source," Review of Scientific Instruments, Volume 56, Number 3, (March 1985), pp. 373-376.

E. E. Marinaro, C. T. Rettner, R. N. Zare and A. H. Kung, "Excitation of H_2 Using Continuously Tunable Coherent XUV Radiation (97.3-102.3 nm)," Chemical Physics Letters, Volume 95, Number 6, (18 March 1983), pp. 486-491.

Richard B. Miles and Stephen E. Harris, "Optical Third-Harmonic Generation in Alkali Metal Vapors," IEEE Journal of Quantum Electronics, Volume QE-9, Number 4, (April 1973), pp. 470-483.

John C. Miller, "Ultrasensitive, Isotopically Selective Detection of Nitric Oxide by Multiphoton Ionization in a Supersonic Beam," Analytical Chemistry, Volume 58, Number 8, (July 1986), pp. 1702-1705.

John C. Miller, "Multiphoton spectroscopy of X-NO (X=Kr,Xe,Ch_4) van der Waals molecules," The Journal of Chemical Physics, Volume 86, Number 6, (15 March 1987), pp. 3166-3171.

Paul J. Miller, Peter Chen, and William A. Chupka, "High-Resolution One-Photon Ionization Spectrum of NO Using Third-Harmonic Generation," Chemical Physics Letters, Volume 120, Number 2, (4 October 1985), pp. 217-222.

T. Namioka, "Absorption Spectra of H_2 in the Vacuum-Ultraviolet Region. I. The Lyman and the Werner Bands," The Journal of Chemical Physics, Volume 40, Number 11, (1 June 1964), pp. 3154-3165.

M. G. Payne and W. R. Garrett, "Cooperative effects on multiphoton ionization and third-harmonic generation in the region near three-photon resonance," Physical Review A, Volume 26, Number 1, (July 1982), pp. 356-371.

M. G. Payne, "Vaccum ultraviolet light generation applications to resonance ionization spectroscopy," Resonance Ionization Spectroscopy, Edited by G. S.

Hurst and C. Grey Morgan (Bristol, UK: Adam Hilger, Ltd., 1987), pp. 59-66.

S. T. Pratt, P. M. Dehmer, and J. L. Dehmer, "Resonant multiphoton ionization of H_2 via the $B^1\Sigma_u^+, v = 7, J =$ 2and4 levels with photoelectron energy analysis," The Journal of Chemical Physics, Volume 78, Number 7, (1 April 1983), pp. 4315-4320.

S. T. Pratt, P. M. Dehmer, and J. L. Dehmer, "Photoionization of Excited Molecular States. $H_2C^1\Pi_u$," Chemical Physics Letters, Volume 105, Number 1, (2 March 1984), pp. 28-33.

M. Rothschild, H. Egger, R. T. Hawkins, J. Bokor, H. Pummer, and C. K. Rhodes, "High-resolution spectroscopy of molecular hydrogen in the extreme ultraviolet region," Physical Review A, Volume 23, Number 1, (January 1981), pp. 206-213.

H. Rottke and H. Zacharias, "Generation of nuclear-spin-polarized protons by resonant ionization of hydrogen atoms," Physical Review A, Volume 33, Number 1, (January 1986), pp. 736-738.

H. Schomburg, H. F. Döbele, and B. Rückle, "Generation of Tunable Narrow-Bandwidth VUV Radiation by Anti-Stokes SRS in H_2," Applied Physics B, Volume 30, (1983), pp. 131-134.

Y. R. Shen, The Principles of Nonlinear Optics, (New York: J. Wiley & Sons, 1984).

Triveni Srinivasan, Hans Egger, Herbert Pummer, and Charles K. Rhodes, "Generation of Extreme Ultraviolet Radiation at 79 nm by Sum Frequency Mixing," IEEE Journal of Quantum Electronics, Volume QE-19, Number 8, (August 1983), pp. 1270-1276.

Surya P. Tewari and G. S. Agarwal, "Control of Phase Matching and Nonlinear Generation in Dense Media by Resonant Fields," Physical Review Letters, Volume 56, Number 17, (28 April 1986), pp. 1811-1814.

Frank S. Tomkins and Rita Mahon, "High-efficiency four-wave sum and difference mixing in Hg vapor," Optics Letters, Volume 6, Number 4, (April 1981), pp. 179-181.

C. R. Vidal, "Advances in Vacuum Ultraviolet Spectroscopy," Proceedings of the International Conference on Lasers, 1984, Published in 1985, pp. 1-11.

Stephen C. Wallace, "Nonlinear Optics and Laser Spectroscopy in the Vacuum Ultraviolet," Photophysics and Photochemistry in the Vacuum Ultraviolet, NATO Advanced Study Institute Series, Series C, 142, Edited by S. P. McGlynn et. al., (D. Reidel Publishing Company, 1985), pp. 105-131.

R. Wallenstein and H. Zacharias, "Λ-Type Doubling and Spin-Rotation Splitting of NO, Measured in Simultaneous One- and Two-Photon Laser Spectroscopy," Optics Communications, Volume 25, Number 3, (June 1978), pp. 363-367.

K. H. Welge, "VUV Laser Spectroscopy of Atomic and Molecular Hydrogen," Laser Applications in Chemistry, NATO Advanced Study Institute Series, Series B, 105, (1984), pp. 103-115.

M. G. White, W. A. Chupka, M. Seaver, A. Woodward, and S. D. Colson, "Resonant multiphoton ionization of NO via the $A^2\Sigma^+$ state: Photoelectron spectra and angular distributions," The Journal of Chemical Physics, Volume 80, Number 2, (15 January 1984), pp. 678-686.

P. G. Wilkinson, "The electronic isotope shift in the Lyman bands of H_2 and D_2," Canadian Journal of Physics, Volume 46, (1968), pp. 1225-1235.

I. C. Winkler, R. Stachnik, J. I. Steinfeld and S. Miller, "Evaluation of 2-photon ionization spectroscopy as a proble of NO ground state population distributions," Spectrochimica Acta, Volume 42A, Number 2/3, pp. 339-342.

L. Wolniewicz and K. Dressler, "The EF, GK, and $H\bar{H}^1\Sigma_g^+$ states of hydrogen. Improved *ab initio* calculation of vibrational states in the adiabatic approximation," The Journal of Chemical Physics, Volume 82, Number 7, (1 April 1985), pp. 3292-3299.

Yun Mui Yiu, Thomas J. McIlrath, and Rita Mahon, "Effects of spacial modes on third-harmonic generation," Physical Review A, Volume 20, Number 6, (December 1979), pp. 2470-2485.

Yun-Mui Yiu, Keith D. Bonnin, and T. J. McIlrath, "Two-Photon resonant upconversion in xenon," Optics Letters, Volume 7, Number 6, (June 1982), pp. 268-270.

K. Yoshino and D. E. Freeman, "Absorption spectrum of xenon in the vacuum-ultraviolet region," Journal of the Optical Society of America, B, Volume 2, Number 8, (August 1985), pp. 1268-1274.

David Zakheim and Philip Johnson, "Two- and three-photon resonances in the four-photon ionization spectrum of nitric oxide at low temperature," The Journal of Chemical Physics, Volume 68, Number 8, (15 April 1978), pp. 3644-3653.

C. W. Zucker and E. E. Eyler, "Photodissociation cross sections from the *E,F* state of H_2," The Journal of Physical Chemistry, Volume 85, Number 12, (15 December 1986), pp. 7180-7183.

VITA

Michael Paul McCann was born in Teaneck, New Jersey on June 30, 1955. He attended various grammer schools in New Jersey, Ohio, and Maryland. He graduated from St. Elizabeth's School in Bernardsville, New Jersey in June 1969. The following September he entered Delbarton School in Morristown, New Jersey and graduated in June 1973. In the fall of 1973 he enrolled at Dickinson College in Carlisle, Pennsylvania. In September of 1977 he graduated with a Bachelor of Science degree with a major in Chemistry.

After working a short while, he entered Western Kentucky University in Bowling Green, Kentucky in January 1978. He received a Master of Science degree with a major in Physical Chemistry in June 1981.

After working at Oak Ridge National Laboratory for a short while, he accepted a teaching assistantship at the University of Tennessee, Knoxville in September 1981. He received the Doctor of Philosophy degree with a major in Physical Chemistry in December 1987.

The author is a member of the American Physical Society and the Optical Society of America. Mr. McCann will be employed in a post-doctoral position at Oak Ridge National Laboratory through the University of Tennessee, Knoxville after graduation.